

000 001 002 003 004 005 A CONVERGENCE ANALYSIS OF ADAPTIVE OPTIMIZ- 006 ERS UNDER FLOATING-POINT QUANTIZATION 007 008 009

010 **Anonymous authors**
011

012 Paper under double-blind review
013
014
015
016
017
018
019
020
021
022
023
024
025
026
027

ABSTRACT

028 The rapid scaling of large language models (LLMs) has made low-precision training
029 essential for reducing memory, improving efficiency, and enabling larger models and datasets.
030 Existing convergence theories for adaptive optimizers, however, assume all components are exact and neglect hardware-aware quantization, leaving open the question of why low-precision training remains effective. We introduce the first theoretical framework for analyzing the convergence of adaptive optimizers, including Adam and Muon, under floating-point quantization of gradients, weights, and optimizer states (e.g., moment estimates). Within this framework, we derive convergence rates on smooth non-convex objectives under standard stochastic gradient assumptions, explicitly characterizing how quantization errors from different components affect convergence. We show that both algorithms retain rates close to their full-precision counterparts provided mantissa length scales only logarithmically with the number of iterations. Our analysis further reveals that Adam is highly sensitive to weights and second-moment quantization due to its reliance on $\beta_2 \rightarrow 1$, while Muon requires weaker error control and is thus potentially more robust. These results narrow the gap between empirical success and theoretical understanding of low-precision training methods. Numerical experiments on synthetic and real-world data corroborate our theory.
031

1 INTRODUCTION

032 The rapid scaling of large language models (LLMs) has made low-precision training indispensable
033 for modern deep learning. By reducing memory usage and improving computational efficiency,
034 low-precision formats such as bfloat16 (BF16) and FP8 enable training with larger models and
035 datasets on contemporary hardware accelerators (Peng et al., 2023; Fishman et al., 2025). The
036 introduction of FP8 in Nvidia’s Hopper GPU architecture (NVIDIA, 2022; Micikevicius et al., 2022)
037 further cements its role as a practical datatype for the next generation of LLM training. In practice,
038 numerous frameworks now leverage mixed- or low-precision formats to quantize gradients, weights,
039 and optimizer states (Liu et al., 2024; 2025), showing that aggressively quantized training can scale
040 to trillion-token workloads without loss of accuracy.

041 Despite its empirical success, a rigorous theoretical understanding of quantization, particularly for
042 adaptive optimizers like Adam (Kingma, 2014) with decoupled weight decay (Loshchilov & Hutter,
043 2019) and Muon (Jordan et al., 2024), which are widely used in practice, remain largely under-
044 developed. Existing theoretical work on the non-convex optimization analysis under quantization
045 has primarily focused on Stochastic Gradient Descent with quantized gradients (QSGD) (Alistarh
046 et al., 2017). For example, Jiang & Agrawal (2018) established $\mathcal{O}(1/T^{1/4})$ convergence under un-
047 biased quantization, while error-feedback mechanisms (Karimireddy et al., 2019) were later intro-
048 duced to handle biased quantization with the same guarantees. Extensions to QSGD and Quantized
049 SGDM with error feedback have been analyzed in various settings (Tang et al., 2019; Zheng et al.,
050 2019; Koloskova et al., 2020), again achieving $\mathcal{O}(1/T^{1/4})$ rates. **More recent efforts target Quantized**
051 **Adam (Chen et al., 2021; Modoranu et al., 2024; Ozkara et al., 2025).** Chen et al. (2021)
052 proved convergence of Adam with quantized gradients and weights under error feedback achieves
053 $\mathcal{O}(1/T^{1/4})$, but the method requires storing error terms for every parameter, which is memory-
054 intensive and impractical for modern low-precision LLM training. Modoranu et al. (2024) reduced
055 this cost by compressing error feedback with unbiased compression, proving $\mathcal{O}(1/T^{1/4})$ conver-

gence for Adam with quantized gradients. Ozkara et al. (2025) further explored stochastic rounding (SR) as a mechanism for mitigating numerical errors in low-precision training, providing analyses of implicit regularization and convergence of Adam under SR; however, their analysis omits optimizer state quantization or practical floating-point formats, which are increasingly central to low-bit LLM optimization (Dettmers et al., 2021; Xi et al., 2025; Fishman et al., 2025). This leaves a critical gap: practical low-bit training crucially involves the quantization of optimizer states (e.g., momentum and second-moment estimates), a component these analyses omit. Furthermore, these studies often rely on assumptions like unbiased quantization or error-feedback mechanisms that are not consistent with modern large-scale LLM training. Consequently, the community lacks a theoretical framework to explain the robust convergence observed when adaptive optimizers are quantized in all components during LLM training.

This paper. The objective of this work is to develop the convergence analysis of adaptive optimization algorithms with a more practical quantization configuration. In particular, we develop the first analytical framework for quantized adaptive optimizers under floating-point quantization. More importantly, following the practical configuration (Liu et al., 2024), our framework explicitly models the quantization of all key components: gradients, weights, momentum, and second moments. We then establish convergence guarantees for both Adam and Muon optimizers, expressing the results as a function of the quantization errors in these components. This clearly reveals how each type of error individually affects convergence. Crucially, rather than relying on unbiased quantization assumptions or storing per-parameter error feedback, we require only relative error control, which aligns with the behavior of standard floating-point formats (FP32 \rightarrow BF16 or FP8; Section 3, Figure 5, 6, 10, 11; see also (Kuzmin et al., 2022)).

We then summarize the main contributions of this work as follows:

- We introduce a rigorous analytical framework for adaptive optimizers under hardware-aware low-precision training, explicitly modeling the quantization of weights, gradients, and optimizer states (Section 3). Unlike prior works that rely on unbiased quantization assumptions or error-feedback mechanisms, which are impractical in large-scale LLM training, we adopt a relative error model (Assumption 3.1) that faithfully captures the behavior of floating-point quantization. This facilitates a formal and rigorous convergence analysis for quantized adaptive optimization algorithms that closely align with real-world implementations.
- We provide the first convergence guarantees for quantized Adam (Theorem 4.5) and Muon (Theorem 4.6) on smooth non-convex objectives under the relative error quantization model (Assumption 3.1), which closely reflects the behavior of floating-point quantization. Our analysis shows that both methods attain the same convergence rates as their full-precision counterparts (Défossez et al., 2022; Shen et al., 2025), provided the mantissa length increases only logarithmically with the number of iterations, which is consistent with practical hardware precision.
- Our analysis in Theorems 4.5 and 4.6 precisely characterizes how quantization errors in different components impact convergence. Notably, we show that Adam is particularly sensitive to quantization of weights and second moments due to their dependence on β_2 , which is typically set close to 1 for convergence in practice and theory (Figure 7). **This aligns with empirical observations from Peng et al. (2023); Yu et al. (2024), where weights and second moments require slightly higher precision than gradients or the momentum.** Our experiments (Figures 3, 4, 8, 9, 12) corroborate this, demonstrating graceful degradation with reduced precision and near full-precision performance at moderate mantissa lengths. In contrast, Theorem 4.6 reveals that Muon is more tolerant to quantization, requiring weaker relative error conditions (e.g., $1/T^{1/2}$ versus $1/T^2$ for Adam). This robustness stems from the SVD-based sign operator in Muon, which avoids the amplification of quantization errors by the inverse square root of historical gradient variances. This theoretical insight also explains empirical findings in Liu et al. (2025) that Muon exhibits superior robustness to low-precision training compared to Adam (Figure 13).

Overall, our results narrow the gap between the empirical success of quantized adaptive training and its theoretical understanding, providing a foundation for analyzing and designing future low-precision optimization algorithms.

Notations. Scalars are denoted by lowercase letters (x, \dots), vectors by bold lowercase (\mathbf{x}, \dots), and matrices by bold uppercase (\mathbf{X}, \dots). The i -th entry of \mathbf{x} is x_i , and the (i, j) -th entry of \mathbf{X} is

108 X_{ij} . The ℓ_2 norm of \mathbf{x} is $\|\mathbf{x}\|_2 = \sqrt{\sum_i x_i^2}$, the Frobenius norm of \mathbf{X} is $\|\mathbf{X}\|_F = \sqrt{\sum_{i,j} X_{ij}^2}$,
 109 and the nuclear norm of \mathbf{X} is $\|\mathbf{X}\|_* = \sum_i \sigma_i(\mathbf{X})$, where $\sigma_i(\mathbf{X})$ denotes the i -th singular value. For
 110 $d \in \mathbb{N}^+$, let $[d] = \{1, 2, \dots, d\}$. For real sequences $\{a_t\}$ and $\{b_t\}$, we write $a_t = O(b_t)$ if there
 111 exist constants $C, N > 0$ such that $a_t \leq Cb_t$ for all $t \geq N$; $a_t = \Omega(b_t)$ if $b_t = O(a_t)$; $a_t = \Theta(b_t)$
 112 if both $a_t = O(b_t)$ and $a_t = \Omega(b_t)$; and we use $\tilde{O}(\cdot)$ and $\tilde{\Omega}(\cdot)$ to suppress logarithmic factors. The
 113 quantization operator is $\mathcal{Q}(\cdot)$, with x^Q denoting the quantized version of x .
 114

115

116 2 RELATED WORK

117

118 **Adaptive Optimization.** Adaptive optimizers are a key part of deep learning because they can
 119 automatically respond to changes in the data. The progression of modern adaptive optimizers began
 120 with Adagrad (Duchi et al., 2011), which scales learning rates based on the accumulated sum of past
 121 squared gradients. Despite extensive convergence analysis (Zou et al., 2019; Chen et al., 2018; Shi
 122 et al., 2020; Li & Orabona, 2019; Faw et al., 2022), its aggressive learning rate decay often leads to
 123 premature stalling. RMSProp (Hinton et al., 2012) addressed this issue by using an exponentially
 124 decaying average of squared gradients instead, a method whose convergence has also been well-
 125 studied (Zaheer et al., 2018; De et al., 2018; Shi et al., 2020; Li et al., 2025). Adam (Kingma, 2014)
 126 then synthesized these ideas by incorporating momentum, effectively combining the adaptive learning
 127 rates of RMSProp with first-moment estimates. Its widespread success has motivated a vast body
 128 of theoretical work analyzing its convergence and implicit bias generalization under various settings
 129 (Reddi et al., 2018; Défossez et al., 2022; Zou et al., 2019; Chen et al., 2018; Zhang et al., 2022;
 130 Wang et al., 2022; Guo et al., 2021; Hong & Lin, 2023; Li et al., 2023; Wang et al., 2023; Zhang
 131 et al., 2025; 2024; Zou et al., 2023; Cattaneo et al., 2024). More recently, the Muon optimizer (Jordan
 132 et al., 2024) was proposed, which leverages a matrix-based perspective for optimization, with
 133 its convergence guarantees established by concurrent works (Shen et al., 2025; Sato et al., 2025).
 134 While convergence guarantees for these methods have been established in high-precision settings,
 135 their behavior under the low-precision quantization common in modern large model training is not
 136 well understood, a gap that this paper aims to address.

137

138 **Low-bit Training.** As the field of deep learning continues to advance rapidly, the scale of mod-
 139 els, particularly Large Language Models (LLMs), has grown exponentially. Low precision train-
 140 ing (Wang et al., 2018; Wortsman et al., 2023; Liu et al., 2023; Xi et al., 2024; Liu et al., 2024)
 141 has become a prominent technique in modern deep learning, offering reductions in both computa-
 142 tional costs and memory requirements. Mixed-precision training typically performs forward and
 143 backward passes in low-precision formats like FP16 (Micikevicius et al., 2017) or the more stable,
 144 wider-range BF16 (Kalamkar et al., 2019), while maintaining master weights and optimizer states in
 145 FP32. The advent of hardware like NVIDIA’s Hopper GPU architecture (NVIDIA, 2022) has made
 146 8-bit floating-point (FP8) training a practical reality for further efficiency gains (Micikevicius et al.,
 147 2022; Peng et al., 2023; Xi et al., 2025; Fishman et al., 2025). Even more aggressive approaches
 148 now extend to 4-bit (FP4) training (Wang et al., 2025; Zhou et al., 2025). Especially in adaptive op-
 149 timization, the optimizer states can consume as much memory as the model parameters themselves.
 150 This has motivated a class of methods that specifically compresses these states, decompressing them
 151 to a higher precision just-in-time for the weight update to save memory (Dettmers et al., 2021; Peng
 152 et al., 2023; Li et al., 2024; Fishman et al., 2025; Xi et al., 2025). Despite the empirical success
 153 of these techniques, a comprehensive theory explaining their convergence behavior remains absent.
 154 Our work addresses this gap by establishing an analytical framework that formally incorporates
 155 quantization errors from all parts of a realistic low-bit training pipeline, from gradients and weights
 156 to the crucial optimizer states themselves.

157

158 **Quantization Convergence.** Most convergence guarantees for optimizers assume ideal, high-
 159 precision arithmetic, failing to account for the quantization effects inherent in modern large-scale
 160 training. Much of the existing theoretical work in this area has therefore focused on the convergence
 161 of Quantized Stochastic Gradient Descent (SGD). Early analyses established convergence rates for
 SGD with quantized gradients, often relying on the strong assumption of an unbiased quantizer
 (Alistarh et al., 2017; Jiang & Agrawal, 2018; Wen et al., 2017). To handle more practical, biased
 quantization schemes, subsequent work introduced error-feedback mechanisms to compensate for
 the quantization bias and still guarantee convergence (Karimireddy et al., 2019; Zheng et al., 2019;

Tang et al., 2019; Koloskova et al., 2020). Complementing these efforts on gradient compression, another line of research has analyzed the convergence of SGD when the model weights themselves are also quantized (Markov et al., 2023). Beyond SGD, analyzing quantized adaptive optimizers is a more recent challenge. Early work in this direction includes Hou et al. (2019), which studies Adam with $\beta_1 = 0$, analyzing joint quantization of both gradients and weights in convex settings. Other studies have applied error-feedback to ensure the convergence of Adam under quantized weights and gradients in non-convex settings (Chen et al., 2021; Modoranu et al., 2024; Robert et al., 2025). However, these existing analyses for adaptive methods rely heavily on error-feedback mechanisms, which are often impractical in state-of-the-art LLM training pipelines (Xi et al., 2025; Fishman et al., 2025). Complementary work on stochastic rounding (SR) (Ozkara et al., 2025) studies a different quantization regime: SR is approximately unbiased but introduces variance, and their Adam analysis quantizes only the final weight update while assuming full-precision gradients and optimizer states (with $\beta_1 = 0$). Such an additive-noise formulation and simplification avoid the recursive and interaction-heavy quantization error propagation that arises in adaptive optimization under realistic floating-point rounding. In contrast, our work addresses this critical gap by providing the first convergence framework for adaptive optimizers under a realistic floating-point error model that covers all components of the training process, without resorting to error-feedback or unbiasedness assumptions.

3 PRELIMINARIES AND PROBLEM SETUP

3.1 PRELIMINARIES

We begin by formalizing the quantization operator and its error properties. Our focus is on floating-point quantization, which is widely adopted in practice. Compared to integer quantization, floating-point formats achieve strictly smaller reconstruction errors due to their exponent scaling (Kuzmin et al., 2022). This explains why most large-scale low-precision training frameworks rely on floating-point representations, including recent FP8 and mixed-precision systems (Peng et al., 2023; Liu et al., 2024; Fishman et al., 2025).

Floating-point quantization. Let $\mathcal{Q} : \mathbb{R} \rightarrow \mathbb{R}$ be a scalar quantization operator applied elementwise to vectors and matrices. We illustrate \mathcal{Q} through the common case of quantizing from single precision (fp32) to brain floating-point (bf16). The fp32 format uses 1 sign bit, 8 exponent bits, and 23 mantissa bits (total 32 bits) (IEEE, 2019), while bf16 keeps the same sign and exponent layout but truncates the mantissa to 7 bits (Wang & Kanwar, 2019). Thus, FP32 can be written as

$$x_{\text{fp32}} = (-1)^S \times 2^{E-127} \times (1.M_{0:22}),$$

where S is the sign bit, E the exponent, and $M_{0:22}$ the mantissa bits. Quantization discards the low-order 16 mantissa bits $M_{7:22}$, possibly with rounding or truncation. The BF16 number becomes

$$x_{\text{bf16}} = (-1)^S \times 2^{E-127} \times (1.M_{0:6} + C \cdot 2^{-7}),$$

where $C \in \{0, 1\}$ is a carry bit from rounding. Dequantization pads the truncated mantissa with zeros to recover an fp32 value. Figure 1 visualizes this process.

Relative error. The above construction implies that the quantization error satisfies

$$|x_{\text{bf16}} - x_{\text{fp32}}| = |C \cdot 2^{-7} - 0.M_{7:22} \cdot 2^{-7}| \cdot 2^{E-127} \leq 2^{-7} \cdot 2^{E-127} \leq q|x_{\text{fp32}}|,$$

where $q = \Theta(2^{-M})$ and M is the mantissa length of the target format (here $M = 7$ for bf16). More generally, we assume the absence of underflow and overflow, so that the sign and exponent remain unchanged after quantization. This prevents large quantization errors and guarantees convergence of the quantization process. In practice, this assumption is well justified: low-precision LLM training commonly employs engineering techniques such as per-tensor or per-channel scaling, which ensure that post-quantization values remain within the representable range (Peng et al., 2023; Fishman et al., 2025). Under this condition, the relative quantization error decays exponentially with the number of mantissa bits—a property that is intrinsic to floating-point representations. This observation motivates the following assumption.

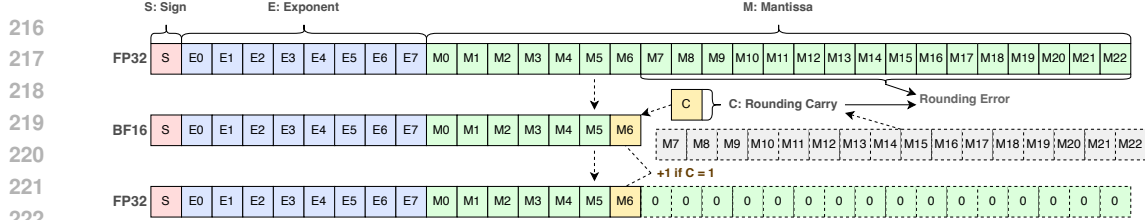


Figure 1: Floating-point quantization from fp32 to bf16. Only the mantissa is truncated, while sign and exponent remain unchanged.

Assumption 3.1 (Quantization Error). Let $\mathcal{Q} : \mathbb{R} \rightarrow \mathbb{R}$ be a scalar quantization operator applied elementwise. Then, for any $x \in \mathbb{R}$, the quantization error is relatively bounded:

$$|x^Q - x| \leq q|x|,$$

where $q = \Theta(2^{-M})$, and M is the mantissa length of the target floating-point format.

3.2 PROBLEM SETUP

We study stochastic optimization (3.1) with low-precision training under an analytical quantization framework shown in Figure 2. Formally, the goal is to minimize the loss:

$$\min_{\mathbf{W} \in \mathbb{R}^{m \times n}} F(\mathbf{W}) = \mathbb{E}_{\xi}[f(\mathbf{W}; \xi)], \quad (3.1)$$

where \mathbf{W} denotes the model parameters, ξ is a random variable representing the data, and $f(\mathbf{W}; \xi)$ is the sample loss. We denote $F^* = \inf_{\mathbf{W}} F(\mathbf{W}) > -\infty$ as the optimal objective value.

Low-precision training framework. During training, both computation and communication are constrained by memory and bandwidth. Modern practice therefore quantizes weights, gradients, and optimizer states into lower-precision formats (e.g., BF16, FP8) to accelerate training (Peng et al., 2023; Liu et al., 2024; Fishman et al., 2025). We model this process with the analytical framework shown in Figure 2. The key steps are:

1. The master maintains full-precision weights \mathbf{W}_t but transmits their quantized version \mathbf{W}_t^Q to workers.
2. Workers perform forward and backward passes with \mathbf{W}_t^Q , compute gradients $\nabla f(\mathbf{W}_t^Q; \xi)$, quantize them, and send quantized gradients back.
3. The master dequantizes gradients, updates quantized optimizer states (e.g., momentum, second moment), and applies the optimizer update. Updated states are re-quantized for storage.

The first two steps can be illustrated by Algorithm 1, while the third step depends on the choice of optimizer (e.g., Adam in Algorithm 2 or Muon in Algorithm 3). The dashed arrows in Figure 2 highlight the quantization operations applied to weights, gradients, and optimizer states within the proposed framework.

Relative errors. We denote the relative errors q of different components after applying \mathcal{Q} as

$$q_W \quad (\text{weights}), \quad q_G \quad (\text{gradients}), \quad q_M \quad (\text{first moment}), \quad q_V \quad (\text{second moment}).$$

Each error term arises from applying a floating-point quantization operator \mathcal{Q} that satisfies Assumption 3.1. Formally, for any quantized quantity \mathbf{X}_t (e.g., \mathbf{W}_t , \mathbf{G}_t , \mathbf{M}_t , \mathbf{V}_t) at iteration t , its relative quantization error is defined as the smallest constant $q \geq 0$ such that

$$|\mathbf{X}_t^Q|_{ij} - |\mathbf{X}_t|_{ij}| \leq q_X ||\mathbf{X}_t|_{ij}|, \quad \forall t \in 0, \dots, T-1.$$

In particular, we have

$$q_W := \inf \{q \geq 0 : ||\mathbf{W}_t^Q|_{ij} - |\mathbf{W}_t|_{ij}| \leq q ||\mathbf{W}_t|_{ij}|, \forall t\},$$

$$q_G := \inf \{q \geq 0 : ||\mathbf{G}_t^Q|_{ij} - |\mathbf{G}_t|_{ij}| \leq q ||\mathbf{G}_t|_{ij}|, \forall t\},$$

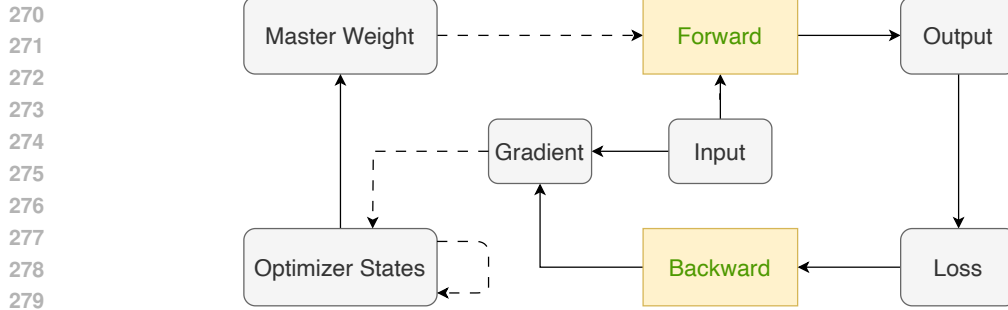


Figure 2: An analytical low-precision training framework

Algorithm 1 Analytical Adaptive Method Quantization Training Framework

```

1: Input 1: Algorithm  $\mathcal{A} \in \{\text{Adam, Muon}\}$  and its parameters set  $\Theta \in \{\{\beta_1, \beta_2, \epsilon\}, \{\beta\}\}$ , initial
2: weights  $\mathbf{W}_0$ , learning rate schedule  $\{\eta_t\}$ , batch size  $B$ , quantization operator  $\mathcal{Q}$ 
3: for  $t = 0, \dots, T - 1$  do
4:   Sample batch  $\{\xi_{t,i}\}_{i=1}^B$  uniformly ▷  $B$  workers
5:    $\mathbf{G}_t = \frac{1}{B} \sum_{i=1}^B \nabla^Q f(\mathbf{W}_t^Q; \xi_{t,i})$  ▷ Master receives  $B$  quantized gradients
6:    $\mathbf{W}_{t+1} = \mathcal{A}(\mathbf{W}_t, \mathbf{G}_t, \Theta, t)$  ▷ Update by Adam or Muon
7: end for

```

Algorithm 2 Adam($\mathbf{W}_t, \mathbf{G}_t, \Theta, t$)

```

1:  $\{\beta_1, \beta_2, \epsilon\} \leftarrow \Theta$ 
2:  $\mathbf{M}_t \leftarrow \beta_1 \mathbf{M}_{t-1}^Q + \mathbf{G}_t$  if  $t > 0$  else  $\mathbf{M}_0 = \mathbf{G}_0$ 
3:  $\mathbf{V}_t \leftarrow \beta_2 \mathbf{V}_{t-1}^Q + \mathbf{G}_t^2$  if  $t > 0$  else  $\mathbf{V}_0 = \mathbf{G}_0^2$ 
4: return  $\mathbf{W}_t - \eta_t \mathbf{M}_t / \sqrt{\mathbf{V}_t + \epsilon \mathbf{1}}$ 

```

Algorithm 3 Muon($\mathbf{W}_t, \mathbf{G}_t, \Theta, t$)

```

1:  $\{\beta\} \leftarrow \Theta$ 
2:  $\mathbf{M}_t = \beta \mathbf{M}_{t-1}^Q + (1 - \beta) \mathbf{G}_t$  if  $t > 0$  else  $\mathbf{M}_0 = \mathbf{G}_0$ 
3:  $(\mathbf{U}_t, \mathbf{S}_t, \mathbf{V}_t) = \text{SVD}(\mathbf{M}_t)$ 
4: return  $\mathbf{W}_t - \eta_t \mathbf{U}_t \mathbf{V}_t^\top$ 

```

$$q_M := \inf \{q \geq 0 : |[\mathbf{M}_t^Q]_{ij} - [\mathbf{M}_t]_{ij}| \leq q |[\mathbf{M}_t]_{ij}|, \forall t\},$$

$$q_V := \inf \{q \geq 0 : |[\mathbf{V}_t^Q]_{ij} - [\mathbf{V}_t]_{ij}| \leq q |[\mathbf{V}_t]_{ij}|, \forall t\}.$$

This framework is more general than most prior theoretical analyses, which typically consider quantization of only a subset of components (e.g., gradients).

Optimizers. We focus on two adaptive optimizers: Adam (Kingma, 2014) and Muon (Jordan et al., 2024). Algorithm 1 outlines the general quantized training loop, while Algorithms 2 and 3 detail the specific update rules for Adam¹ and Muon, respectively. Note that the quantization operator \mathcal{Q} can represent any floating-point quantization (e.g., fp32 \rightarrow bf16 or fp8) satisfying Assumption 3.1.

In the following sections, we will analyze the convergence of quantized Adam and Muon under this framework with relative quantization errors (q_W, q_G, q_M, q_V).

4 MAIN RESULTS

We now present our main theoretical results on the convergence of quantized Adam and Muon under the analytical framework in Section 3. We begin by stating the assumptions required for our analysis, followed by the convergence theorems for each optimizer.

Assumption 4.1 (Unbiased Stochastic Gradient). The stochastic gradient $\nabla f(\mathbf{W}; \xi)$ is an unbiased estimator of the true gradient $\nabla F(\mathbf{W})$, i.e., $\mathbb{E}[\nabla f(\mathbf{W}; \xi)] = \nabla F(\mathbf{W})$.

Assumption 4.2 (Stochastic Gradient Bounds). The stochastic gradient $\nabla f(\mathbf{W}; \xi)$ satisfies the following bounds depending on the algorithm:

¹Our Algorithm slightly differs from the standard Adam, but will not affect the proof. We provide a detailed discussion in Appendix A.1.

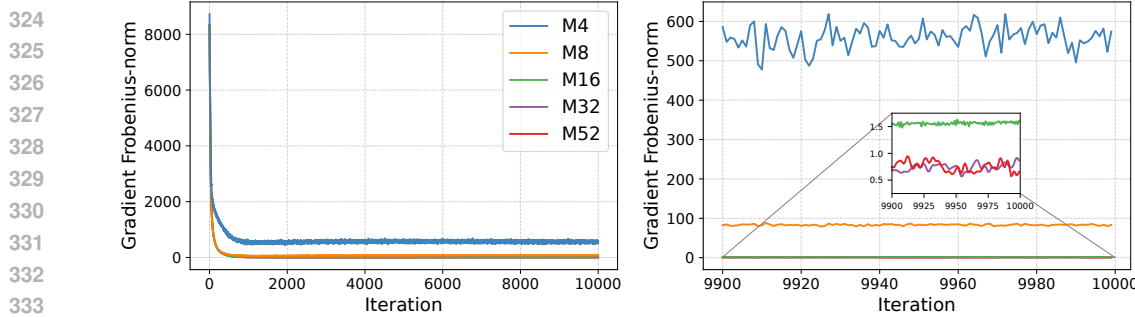


Figure 3: Rosenbrock: Adam gradient norms under different mantissa precisions M (left: full 10,000 iterations; right: last 100 iterations). Larger mantissa bit-lengths yield smaller converged gradient norms. Together with Figure 5, this shows that higher precision reduces quantization error and improves convergence, consistent with Theorem 4.5.

- **Adam:** The stochastic gradient is ℓ_∞ uniformly almost surely bounded, i.e., there exists a constant $R > \sqrt{\epsilon}$ (where $\epsilon > 0$ is the stability constant used to simplify the final bounds) such that

$$\|\nabla f(\mathbf{W}; \xi)\|_\infty = \max_{i,j} |[\nabla f(\mathbf{W}; \xi)]_{ij}| \leq R - \sqrt{\epsilon}, \quad \text{a.s.}.$$

- **Muon:** The stochastic gradient has bounded variance, i.e., there exists a constant $\sigma > 0$ such that

$$\mathbb{E}[\|\nabla f(\mathbf{W}; \xi) - \nabla F(\mathbf{W})\|_F^2] \leq \sigma^2.$$

Assumption 4.3 (Smoothness). The objective function $F : \mathbb{R}^{m \times n} \rightarrow \mathbb{R}$ is L -smooth, i.e., for any $\mathbf{X}, \mathbf{Y} \in \mathbb{R}^{m \times n}$, we have

$$\|\nabla F(\mathbf{X}) - \nabla F(\mathbf{Y})\|_F \leq L\|\mathbf{X} - \mathbf{Y}\|_F.$$

Assumptions 4.1, 4.2 and 4.3 are standard in the analysis of smooth non-convex stochastic optimization (Zaheer et al., 2018; Chen et al., 2019; Zou et al., 2019; Défossez et al., 2022; Chen et al., 2022; Zhang et al., 2022; Wang et al., 2023). They are usually employed to control the stochastic gradient noise and the local geometry of the objective function.

We remark that a more general (L_0, L_1) -smoothness condition (Zhang et al., 2020), which has been adopted in recent analyses of Adam (Li et al., 2023; Wang et al., 2024; Hong & Lin, 2024), allows the smoothness constant to depend on the gradient norm: $\|\nabla F(\mathbf{X}) - \nabla F(\mathbf{Y})\|_F \leq (L_0 + L_1\|\nabla F(\mathbf{Y})\|_F)\|\mathbf{X} - \mathbf{Y}\|_F$. While this condition can better capture practical deep learning scenarios, since our focus is on characterizing how quantization errors influence the convergence behavior of Adam and Muon, we adopt the standard L -smoothness assumption for simplicity. Extending our results to (L_0, L_1) -smoothness remains an interesting direction for future work.

Finally, we assume the optimization begins from a controlled initialization:

Assumption 4.4 (Bounded Initialization). The initial parameter matrix \mathbf{W}_0 and its gradient are bounded in Frobenius norm, i.e., $\|\mathbf{W}_0\|_F \leq D$, $\|\nabla F(\mathbf{W}_0)\|_F \leq G$, for some constants $D, G > 0$.

Bounding the initialization ensures that quantization errors remain controlled and their propagation through the optimization iterations can be rigorously analyzed, which is crucial for establishing convergence guarantees under low-precision training.

4.1 THEORETICAL RESULTS OF ADAM

We first present the convergence result of Adam under FP quantization in the following theorem.

Theorem 4.5 (Convergence of Quantized Adam). Suppose Assumptions 3.1, 4.1–4.4 hold. Let $d = mn$ be the number of trainable parameters, consider the Quantized Adam algorithm defined in 1 run for T iterations with $\eta_t = (1 - \beta_1)\Omega_t\eta$, where $\Omega_t = \sqrt{\sum_{j=0}^{t-1} \beta_2^j}$. Suppose $\beta_1^2(1 + q_M)^2 < \beta_2(1 - q_V)$, $\beta_1(1 + q_M) < \beta_2(1 - q_V)$, and $2\beta_1/(1 - \beta_1) \leq T$, then for an iteration index τ chosen

378 randomly from $\{0, \dots, T-1\}$ with $P(\tau=j) \propto (1-\beta_1^{T-j})$, we have:

$$\begin{aligned} 380 \mathbb{E} [\|\nabla F(\mathbf{W}_\tau)\|_F^2] &\leq 4(1+q_G)R \frac{F_0 - F_*}{\eta T} + \frac{\tilde{Q}(T)}{T} + \frac{2q_W T \eta \cdot (1-\beta_1) d^{\frac{3}{2}} \eta L (1+q_G) R^2}{\sqrt{\epsilon} (1-\beta_2) \sqrt{1 - \frac{\beta_1^2 (1+q_M)^2}{\beta_2 (1-q_V)}}} \\ 381 &+ \frac{4(1+q_G)d}{\sqrt{\epsilon} (1-\beta_2)} (q_G R^3 + L q_W R^2 D) + \frac{C}{T} \left(\ln \left(1 + \frac{(1+q_G)R)^2}{\epsilon (1-\beta_2) (1-q_V)} \right) - T \ln(\beta_2 (1-q_V)) \right), \\ 382 \end{aligned}$$

386 where C is a constant depending on the problem hyperparameters, and $\tilde{Q}(T)$ is a function with
387 respect to T , q_V , q_G , and q_M , which approaches zero when $q_V, q_M \rightarrow 0$ (please refer to Eq A.43
388 for their detailed formula).

389 Moreover, by setting $\eta = \Theta(1/\sqrt{T})$, $1-\beta_2 = \Theta(1/T)$, $q_G = \mathcal{O}(1/T)$, $q_M = \mathcal{O}(1/T)$, $q_V =$
390 $\mathcal{O}(1/T^2)$, $q_W = \mathcal{O}(1/T^2)$, then $\tilde{Q}(T)/T = \mathcal{O}(T^{-1/2})$ (refer to Eq. A.44 for calculation details)
391 and

$$\mathbb{E}[\|\nabla F(\mathbf{W}_\tau)\|_F] = \tilde{\mathcal{O}}(T^{-1/4}).$$

395 Theorem 4.5 provides the first convergence guarantee for Adam under a practical floating-point
396 quantization model (Peng et al., 2023; Liu et al., 2024; Fishman et al., 2025), in contrast to prior
397 works that assume unbiased quantization or error-feedback mechanisms (Jiang & Agrawal, 2018;
398 Chen et al., 2021; Modoranu et al., 2024). The most similar prior theoretical work is Ozkara
399 et al. (2025), whose analysis also builds on Défossez et al. (2022); however, they consider only
400 quantization of the final weight update, assuming full-precision gradients and optimizer states with
401 $\beta_1 = 0$, and thus do not capture the recursive error propagation arising from fully quantized Adam
402 under realistic floating-point rounding. Our analysis demonstrates that by setting the hyperparameters
403 as $\eta = \Theta(1/\sqrt{T})$ and $1-\beta_2 = \Theta(1/T)$, and ensuring the relative quantization errors sat-
404 isfy $q_G, q_M = \mathcal{O}(1/T)$ and $q_W, q_V = \mathcal{O}(1/T^2)$, Quantized Adam achieves a convergence rate
405 of $\tilde{\mathcal{O}}(T^{-1/4})$, which successfully matches the established one for its full-precision counterpart in
406 smooth non-convex optimization (Guo et al., 2021; Défossez et al., 2022; Wang et al., 2023; Hong
407 & Lin, 2024).

408 Our theorem further reveals a nuanced sensitivity to different types of quantization error. The re-
409 quired precision for the second moment (q_V) is stricter than for the first moment (q_M). This sensitiv-
410 ity arises because accumulated errors in the second-moment estimate \mathbf{V}_t are non-linearly amplified
411 by the update step's inverse square root. This theoretical finding provides a rigorous explanation for
412 the empirical observation that the second moment often require higher precision than the first mo-
413 ment in low-bit training setups (Peng et al., 2023; Yu et al., 2024; Fishman et al., 2025). Similarly,
414 the stricter precision requirement for weights ($q_W = \mathcal{O}(1/T^2)$) is necessary to control error accu-
415 mulation over the entire training trajectory. Our analysis must account for the potential growth of
416 weight magnitudes throughout training, which acts as an amplification factor for the relative quanti-
417 zation error. To guarantee convergence under this worst-case scenario of unbounded weight growth,
418 the proof requires q_W to decay rapidly to counteract this amplification. However, this strict condition
419 is a consequence of the proof's generality. In practice, where weight norms often remain bounded,
420 this error amplification is less severe, and the precision requirement for q_W could be relaxed to
 $\mathcal{O}(1/T)$.

4.2 THEORETICAL RESULTS OF MUON

423 Then, we present the convergence result of quantized Muon in the following theorem.

424 **Theorem 4.6** (Convergence of Quantized Muon). Suppose Assumptions 3.1, 4.1–4.4 hold. Con-
425 sider the Quantized Muon algorithm in 1 and 3 run for T iterations with $\eta_t = \eta, \beta(1+q_M) < 1$,
426 then

$$\begin{aligned} 428 \frac{1}{T} \sum_{t=0}^{T-1} \mathbb{E}[\|\nabla F(\mathbf{W}_t)\|_F] &\leq \frac{\mathbb{E}[F(\mathbf{W}_0) - F(\mathbf{W}_T)]}{\eta T} + \frac{2\beta L \eta r}{1-\beta} + \frac{6\sigma\sqrt{r}}{T(1-\beta)\sqrt{B}} + \sqrt{\frac{1-\beta}{1+\beta} \frac{6\sigma\sqrt{r}}{\sqrt{B}}} + \\ 429 &\frac{L \eta r}{2} + C_2 \cdot \left(q_G + q_W + q_G T \eta + q_W T \eta + \frac{q_M \beta}{1-\beta(1+q_M)} (1+T\eta) \right), \\ 430 \end{aligned}$$

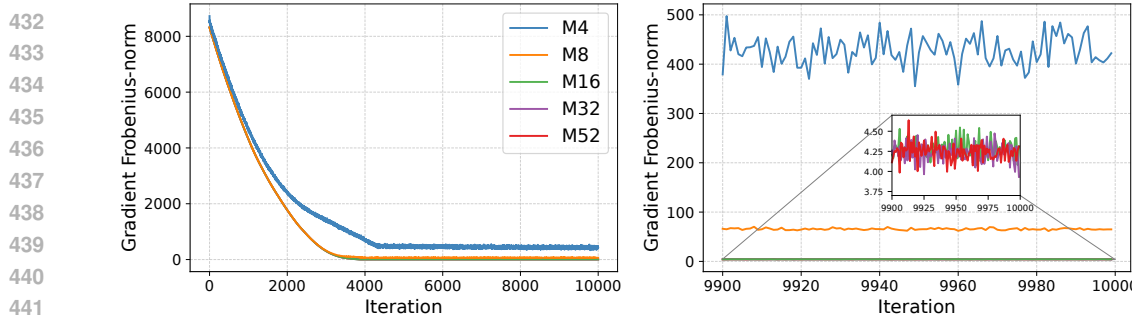


Figure 4: Rosenbrock: Muon gradient norms under different mantissa precisions M (left: full 10,000 iterations; right: last 100 iterations). Larger mantissa bit-lengths yield smaller converged gradient norms. Together with Figure 6, this shows that higher precision reduces quantization error and improves convergence, consistent with Theorem 4.6.

where C_2 is absolute constant, $r = \min\{m, n\}$. Moreover, suppose $F(\mathbf{W}_0) - F^* \leq \Delta$ for constant $\Delta > 0$, set $1 - \beta = \Theta(T^{-1/2})$, $\eta = \Theta(T^{-3/4})$, and $B = 1$, if $q_G = q_W = q_M = \mathcal{O}(T^{-1/2})$, then

$$\frac{1}{T} \sum_{t=0}^{T-1} \mathbb{E}[\|\nabla F(\mathbf{W}_t)\|_F] = \mathcal{O}(T^{-1/4}).$$

Theorem 4.6 establishes the convergence of Quantized Muon under relative quantization errors (q_W, q_G, q_M) for weights, gradients, and momentum, respectively—a practical setting for low-precision training (Peng et al., 2023; Liu et al., 2024; Fishman et al., 2025), in contrast to prior works that assume unbiased quantization or error-feedback mechanisms (Jiang & Agrawal, 2018; Chen et al., 2021; Modoranu et al., 2024). As a sanity check, when $q_W = q_G = q_M = 0$, our result recovers the exact convergence rate $\mathcal{O}(1/T^{1/4})$ of Shen et al. (2025) up to constant factors. More importantly, as long as the mantissa length of the floating-point format scales logarithmically with T , i.e., $M = \Omega(\log T)$, the quantization errors decay as $q_W = q_G = q_M = \mathcal{O}(T^{-1/2})$. With appropriate choices of η and β (as in Theorem 4.6), the full-precision convergence rate $\mathcal{O}(T^{-1/4})$ is preserved.

Finally, we highlight a sharp contrast with quantized Adam. Theorem 4.6 requires only relative errors on the order of $q = \mathcal{O}(T^{-1/2})$, whereas Theorem 4.5 demands stricter conditions, at least $q = \mathcal{O}(T^{-1})$ and in some cases $q = \mathcal{O}(T^{-2})$. This theoretical distinction explains why Muon adapts more efficiently to low-precision settings than Adam, corroborating the empirical observations of Liu et al. (2025).

Experiments. We evaluate our theory on synthetic, image, and LLM benchmarks.

Synthetic setup. For the synthetic benchmark, we adopt the classical Rosenbrock function (Rosenbrock, 1960). Let $\mathbf{W} \in \mathbb{R}^{m \times n}$, and define $F(\mathbf{W}) = \sum_{j=1}^{n-1} \left(100\|\mathbf{W}_{j+1} - \mathbf{W}_j^2\|_F^2 + \|\mathbf{1}_m - \mathbf{W}_j\|_F^2 \right)$, where \mathbf{W}_j denotes the j -th column of \mathbf{W} and $\mathbf{1}_m$ is the m -dimensional all-ones vector. We set $m = 50$, $n = 100$, and run $T = 10,000$ iterations with learning rate $\eta = 5 \times 10^{-4}$. Mantissa bit-lengths are selected from $M = 4, 8, 16, 24, 32, 52$ to quantize gradients, weights, and optimizer states. For Adam, we use $\beta_1 = 0.9$, $\beta_2 = 0.999$, and $\epsilon = 10^{-8}$; for Muon, we set $\beta = 0.9$ and employ $n_s = 10$ power iterations, following Jordan et al. (2024).

CIFAR-10 setup. We train a 4-layer fully connected network [FC(512) – ReLU – FC(256) – ReLU – FC(64) – ReLU – FC(10)] on CIFAR-10 using Adam and Muon. Additional implementation details are provided in Appendix C.

nanoGPT setup. We train nanoGPT on OpenWebText ($\sim 26M$ parameters, 4 layers, 4 heads, embedding 384, batch size 128, block size 512). Both AdamW and Muon are tested under varying mantissa lengths M , with Muon applied to 2D parameters in transformer blocks and AdamW applied to all 1D parameters (embedding, lm_head, layernorm).

486 **Empirical Validation of Theory.** Across all benchmarks, our results empirically validate Theorems 4.5 and 4.6. We observe a direct link between quantization error and convergence. As shown
 487 across the Rosenbrock, CIFAR-10, and nanoGPT experiments (Figures 3, 4, 8, 9, 12, 13), very
 488 low mantissa lengths (M) lead to significant convergence degradation. This degradation correlates
 489 directly with high relative quantization errors (detailed in Appendix Figures 5, 6, 10, 11), which
 490 stall the optimization. Conversely, moderate M values yield sufficiently small errors, enabling con-
 491 vergence nearly identical to the full-precision baseline. Furthermore, our experiment in Figure 7
 492 explicitly confirms our analysis of Adam, showing that optimizer sensitivity to quantization error
 493 increases significantly as $\beta_2 \rightarrow 1$. The language modeling results in Figure 13 suggest that Muon is
 494 more robust than AdamW under low-precision training, consistent with Theorems 4.5 and 4.6. We
 495 provide full experimental details and results in Appendix C.
 496

497 5 CONCLUSION AND LIMITATIONS

500 We introduced the first theoretical framework for analyzing adaptive optimizers under realistic
 501 floating-point quantization, jointly modeling the quantization of gradients, parameters, and opti-
 502 mizer states. Unlike prior work, our analysis does not rely on unbiased quantization or error feed-
 503 back—assumptions that are impractical in modern large-scale low-precision training. Within this
 504 framework, we derived the first convergence guarantees for Adam and Muon, with rates expressed
 505 explicitly in terms of component-wise quantization errors. Our results highlight that Adam is highly
 506 sensitive to parameter and second-moment quantization due to its reliance on $\beta_2 \rightarrow 1$, whereas
 507 Muon requires weaker error control and is therefore more robust. These findings explain empirical
 508 observations in large-scale LLM training and narrow the gap between practice and theory.
 509

510 **Limitations and Future Directions.** Several challenges remain. First, our analysis focuses on
 511 smooth unconstrained non-convex objectives, leaving open extensions to broader settings, including
 512 (L_0, L_1) -smooth functions (Zhang et al., 2020), non-smooth convex objectives (Mishchenko & De-
 513 fazio, 2023; Defazio et al., 2024), constrained or composite problems (Kovalev, 2025; Pethick et al.,
 514 2025), and structured scenarios studied in recent works (Shen et al., 2025). Second, our theoreti-
 515 cal guarantees assume an increasing-bit regime, $M = \Omega(\log T)$, to control cumulative quantization
 516 error. In practice, bit-width is typically fixed (e.g., FP8 or BF16), which means convergence is
 517 guaranteed only to a neighborhood of a stationary point; understanding why moderate fixed preci-
 518 sion suffices empirically remains an open question. Third, we focus primarily on fully quantized
 519 Adam/Muon and have not yet extended the framework to other popular optimizers benchmarked
 520 in LLM training (Vlassis et al., 2025; Semenov et al., 2025; Wen et al., 2025). Finally, our anal-
 521 ysis models quantized states under exact arithmetic and does not account for practical consider-
 522 ations such as low-precision operations (e.g., FP8 matrix multiplications) or communication-efficient
 523 distributed training, which are critical for large-scale training. Incorporating these aspects would
 524 provide a more complete theoretical account of large-scale low-precision optimization.
 525

526 524 ETHICS STATEMENT

527 We have carefully reviewed the ICLR Code of Ethics and affirm that our work does not raise any
 528 significant ethical concerns. Our research is purely theoretical and experimental within the scope
 529 of optimization and quantization. It does not involve human subjects, personally identifiable or
 530 sensitive data, or applications that may pose harm. All experiments are conducted on synthetically
 531 generated datasets and standard benchmark datasets (e.g., CIFAR-10) and are intended solely to
 532 validate the theoretical analysis. We believe our methodology and contributions adhere to principles
 533 of fairness, transparency, and research integrity.
 534

535 534 REPRODUCIBILITY STATEMENT

536 We have made significant efforts to ensure the reproducibility of our work. All theoretical results
 537 are fully detailed, with complete proofs provided in Appendix A and Appendix B. The experimental
 538 setup, including training protocols, hyperparameters, and evaluation details, is comprehensively
 539 documented in Appendix C. Experiments are conducted on both synthetically generated datasets and
 the CIFAR-10 benchmark dataset; for synthetic datasets, precise generation procedures are included

540 to eliminate ambiguity. Together, these details allow independent researchers to reproduce both the
 541 theoretical and experimental results that support the main conclusions of the paper.
 542

543 **REFERENCES**
 544

545 Dan Alistarh, Demjan Grubic, Jerry Li, Ryota Tomioka, and Milan Vojnovic.
 546 Qsgd: Communication-efficient sgd via gradient quantization and encod-
 547 ing. *Advances in neural information processing systems*, 30, 2017. URL
 548 https://proceedings.neurips.cc/paper_files/paper/2017/file/6c340f25839e6acdc73414517203f5f0-Paper.pdf.
 549

550 Matias D Cattaneo, Jason Matthew Klusowski, and Boris Shigida. On the implicit bias of adam. In
 551 *International Conference on Machine Learning*, pp. 5862–5906. PMLR, 2024.
 552

553 Congliang Chen, Li Shen, Haozhi Huang, and Wei Liu. Quantized adam with error feedback. *ACM*
 554 *Transactions on Intelligent Systems and Technology (TIST)*, 12(5):1–26, 2021.
 555 Congliang Chen, Li Shen, Fangyu Zou, and Wei Liu. Towards practical adam: Non-convexity,
 556 convergence theory, and mini-batch acceleration. *Journal of Machine Learning Research*, 23
 557 (229):1–47, 2022.
 558

559 Xiangyi Chen, Sijia Liu, Ruoyu Sun, and Mingyi Hong. On the convergence of a class of Adam-type
 560 algorithms for non-convex optimization. *arXiv preprint arXiv:1808.02941*, 2018.
 561

562 Xiangyi Chen, Sijia Liu, Ruoyu Sun, and Mingyi Hong. On the convergence of a class of adam-type
 563 algorithms for non-convex optimization. In *International Conference on Learning Representa-
 564 tions*, 2019. URL <https://openreview.net/forum?id=H1x-x309tm>.
 565

566 Soham De, Anirbit Mukherjee, and Enayat Ullah. Convergence guarantees for RMSProp and Adam
 567 in non-convex optimization and an empirical comparison to Nesterov acceleration. *arXiv preprint
 568 arXiv:1807.06766*, 2018.
 569

570 Aaron Defazio, Xingyu Alice Yang, Ahmed Khaled, Konstantin Mishchenko, Harsh Mehta, and
 571 Ashok Cutkosky. The road less scheduled. In *The Thirty-eighth Annual Conference on Neu-
 572 ral Information Processing Systems*, 2024. URL <https://openreview.net/forum?id=0XeNkkENuI>.
 573

574 Alexandre Défossez, Leon Bottou, Francis Bach, and Nicolas Usunier. A simple convergence proof
 575 of adam and adagrad. *Transactions on Machine Learning Research*, 2022. ISSN 2835-8856. URL
 576 <https://openreview.net/forum?id=ZPQhzTSWA7>.
 577

578 Tim Dettmers, Mike Lewis, Sam Shleifer, and Luke Zettlemoyer. 8-bit optimizers via block-wise
 579 quantization. *arXiv preprint arXiv:2110.02861*, 2021.
 580

581 John Duchi, Elad Hazan, and Yoram Singer. Adaptive subgradient methods for online learning and
 582 stochastic optimization. *Journal of Machine Learning Research*, 12(7), 2011.
 583

584 Matthew Faw, Isidoros Tziotis, Constantine Caramanis, Aryan Mokhtari, Sanjay Shakkottai, and
 585 Rachel Ward. The power of adaptivity in sgd: Self-tuning step sizes with unbounded gradients
 586 and affine variance. In Po-Ling Loh and Maxim Raginsky (eds.), *Proceedings of Thirty Fifth
 587 Conference on Learning Theory*, Proceedings of Machine Learning Research. PMLR, 2022.
 588

589 Maxim Fishman, Brian Chmiel, Ron Banner, and Daniel Soudry. Scaling FP8 training to trillion-
 590 token LLMs. In *The Thirteenth International Conference on Learning Representations*, 2025.
 591 URL <https://openreview.net/forum?id=E1EH00imOb>.
 592

593 Aaron Gokaslan, Vanya Cohen, Ellie Pavlick, and Stefanie Tellex. Openwebtext corpus. <http://Skylion007.github.io/OpenWebTextCorpus>, 2019.
 594

595 Zhishuai Guo, Yi Xu, Wotao Yin, Rong Jin, and Tianbao Yang. A novel convergence analysis for
 596 algorithms of the Adam family and beyond. *arXiv preprint arXiv:2104.14840*, 2021.
 597

598 G Hinton, N Srivastava, and K Swersky. Lecture 6d-a separate, adaptive learning rate for each
 599 connection. *Slides of Lecture Neural Networks for Machine Learning*, 1:1–31, 2012.
 600

594 Yusu Hong and Junhong Lin. High probability convergence of Adam under unbounded gradients
 595 and affine variance noise. *arXiv preprint arXiv:2311.02000*, 2023.

596

597 Yusu Hong and Junhong Lin. On convergence of adam for stochastic optimization under relaxed
 598 assumptions. *Advances in Neural Information Processing Systems*, 37:10827–10877, 2024.

599

600 Lu Hou, Ruiliang Zhang, and James T Kwok. Analysis of quantized models. In *International
 Conference on Learning Representations*, 2019.

601

602 IEEE. Ieee standard for floating-point arithmetic. *IEEE Std 754-2019 (Revision of IEEE 754-2008)*,
 603 pp. 1–84, 2019. doi: 10.1109/IEEEESTD.2019.8766229.

604

605 Peng Jiang and Gagan Agrawal. A linear speedup analysis of distributed deep learning with sparse
 606 and quantized communication. In S. Bengio, H. Wallach, H. Larochelle, K. Grauman, N. Cesa-
 607 Bianchi, and R. Garnett (eds.), *Advances in Neural Information Processing Systems*, volume 31.
 608 Curran Associates, Inc., 2018. URL https://proceedings.neurips.cc/paper_files/paper/2018/file/17326d10d511828f6b34fa6d751739e2-Paper.pdf.

609

610 Keller Jordan, Yuchen Jin, Vlado Boza, Jiacheng You, Franz Cesista, Laker Newhouse, and Jeremy
 611 Bernstein. Muon: An optimizer for hidden layers in neural networks, 2024. URL <https://kellerjordan.github.io/posts/muon/>.

612

613 Dhiraj Kalamkar, Dheevatsa Mudigere, Naveen Mellemudi, Dipankar Das, Kunal Banerjee,
 614 Sasikanth Avancha, Dharma Teja Vooturi, Nataraj Jammalamadaka, Jianyu Huang, Hector Yuen,
 615 et al. A study of bfloat16 for deep learning training. *arXiv preprint arXiv:1905.12322*, 2019.

616

617 Sai Praneeth Karimireddy, Quentin Rebjock, Sebastian Stich, and Martin Jaggi. Error feedback
 618 fixes signsgd and other gradient compression schemes. In *International conference on machine
 learning*, pp. 3252–3261. PMLR, 2019.

619

620 Diederik P Kingma. Adam: A method for stochastic optimization. *arXiv preprint arXiv:1412.6980*,
 621 2014.

622

623 Anastasia Koloskova, Tao Lin, Sebastian U Stich, and Martin Jaggi. Decentralized deep learning
 624 with arbitrary communication compression. In *International Conference on Learning Representations*,
 625 2020. URL <https://openreview.net/forum?id=SkgGCKrKvH>.

626

627 Dmitry Kovalev. Understanding gradient orthogonalization for deep learning via non-euclidean
 628 trust-region optimization. *arXiv preprint arXiv:2503.12645*, 2025.

629

630 Alex Krizhevsky, Geoffrey Hinton, et al. Learning multiple layers of features from tiny images.
 2009.

631

632 Andrey Kuzmin, Mart Van Baalen, Yuwei Ren, Markus Nagel, Jorn Peters, and Tijmen Blankevoort.
 633 Fp8 quantization: The power of the exponent. *Advances in Neural Information Processing Systems*,
 35:14651–14662, 2022.

634

635 Bingrui Li, Jianfei Chen, and Jun Zhu. Memory efficient optimizers with 4-bit states. *Advances in
 636 Neural Information Processing Systems*, 36, 2024.

637

638 Haochuan Li, Alexander Rakhlin, and Ali Jadbabaie. Convergence of adam under relaxed assump-
 639 tions. *Advances in Neural Information Processing Systems*, 36:52166–52196, 2023.

640

641 Huan Li, Yiming Dong, and Zhouchen Lin. On the $O(\sqrt{d}/T^{1/4})$ convergence rate of RMSProp and
 642 its momentum extension measured by l_1 norm. *Journal of Machine Learning Research*, 26(131):
 1–25, 2025. URL <http://jmlr.org/papers/v26/24-0523.html>.

643

644 Xiaoyu Li and Francesco Orabona. On the convergence of stochastic gradient descent with adaptive
 645 stepsizes. In *AI Stats*, 2019.

646

647 Aixin Liu, Bei Feng, Bing Xue, Bingxuan Wang, Bochao Wu, Chengda Lu, Chenggang Zhao,
 648 Chengqi Deng, Chenyu Zhang, Chong Ruan, et al. Deepseek-v3 technical report. *arXiv preprint
 arXiv:2412.19437*, 2024.

648 Jingyuan Liu, Jianlin Su, Xingcheng Yao, Zhejun Jiang, Guokun Lai, Yulun Du, Yidao Qin,
 649 Weixin Xu, Enzhe Lu, Junjie Yan, et al. Muon is scalable for lilm training. *arXiv preprint*
 650 *arXiv:2502.16982*, 2025.

651 Shih-yang Liu, Zechun Liu, Xijie Huang, Pingcheng Dong, and Kwang-Ting Cheng. Lilm-fp4: 4-bit
 652 floating-point quantized transformers. *arXiv preprint arXiv:2310.16836*, 2023.

654 Ilya Loshchilov and Frank Hutter. Decoupled weight decay regularization. In *International Confer-
 655 ence on Learning Representations*, 2019. URL <https://openreview.net/forum?id=Bkg6RiCqY7>.

657 Ilia Markov, Adrian Vladu, Qi Guo, and Dan Alistarh. Quantized distributed training of large models
 658 with convergence guarantees. In *International Conference on Machine Learning*, pp. 24020–
 659 24044. PMLR, 2023.

661 Paulius Micikevicius, Sharan Narang, Jonah Alben, Gregory Diamos, Erich Elsen, David Garcia,
 662 Boris Ginsburg, Michael Houston, Oleksii Kuchaiev, Ganesh Venkatesh, et al. Mixed precision
 663 training. *arXiv preprint arXiv:1710.03740*, 2017.

664 Paulius Micikevicius, Dusan Stosic, Neil Burgess, Marius Cornea, Pradeep Dubey, Richard Grisen-
 665 thwaite, Sangwon Ha, Alexander Heinecke, Patrick Judd, John Kamalu, et al. Fp8 formats for
 666 deep learning. *arXiv preprint arXiv:2209.05433*, 2022.

668 Konstantin Mishchenko and Aaron Defazio. Prodigy: An expeditiously adaptive parameter-free
 669 learner. *arXiv preprint arXiv:2306.06101*, 2023.

670 Ionut-Vlad Modoranu, Mher Safaryan, Grigory Malinovsky, Eldar Kurtić, Thomas Robert, Peter
 671 Richtárik, and Dan Alistarh. Microadam: Accurate adaptive optimization with low space over-
 672 head and provable convergence. *Advances in Neural Information Processing Systems*, 37:1–43,
 673 2024.

675 NVIDIA. Nvidia h100 tensor core gpu architecture, 2022. URL <https://resources.nvidia.com/en-us-tensor-core>.

677 Kaan Ozkara, Tao Yu, and Youngsuk Park. Stochastic rounding for LLM training: Theory and
 678 practice. In *The 28th International Conference on Artificial Intelligence and Statistics*, 2025.
 679 URL <https://openreview.net/forum?id=3j3NtXcc95>.

680 Houwen Peng, Kan Wu, Yixuan Wei, Guoshuai Zhao, Yuxiang Yang, Ze Liu, Yifan Xiong, Ziyue
 681 Yang, Bolin Ni, Jingcheng Hu, et al. Fp8-lm: Training fp8 large language models. *arXiv preprint*
 682 *arXiv:2310.18313*, 2023.

684 Thomas Pethick, Wanyun Xie, Kimon Antonakopoulos, Zhenyu Zhu, Antonio Silveti-Falls, and
 685 Volkan Cevher. Training deep learning models with norm-constrained LMOs. In *Forty-second
 686 International Conference on Machine Learning*, 2025. URL <https://openreview.net/forum?id=20qm2IzTy9>.

688 Sashank J Reddi, Satyen Kale, and Sanjiv Kumar. On the convergence of Adam and beyond. In
 689 *Proc. of the International Conference on Learning Representations (ICLR)*, 2018.

691 Thomas Robert, Mher Safaryan, Ionut-Vlad Modoranu, and Dan Alistarh. Ldadam: Adaptive opti-
 692 mization from low-dimensional gradient statistics. *arXiv preprint arXiv:2410.16103*, 2025.

693 HoHo Rosenbrock. An automatic method for finding the greatest or least value of a function. *The
 694 computer journal*, 3(3):175–184, 1960.

696 Naoki Sato, Hiroki Naganuma, and Hideaki Iiduka. Convergence bound and critical batch size of
 697 muon optimizer, 2025. URL <https://arxiv.org/abs/2507.01598>.

698 Andrei Semenov, Matteo Pagliardini, and Martin Jaggi. Benchmarking optimizers for large language
 699 model pretraining. *arXiv preprint arXiv:2509.01440*, 2025.

701 Wei Shen, Ruichuan Huang, Minhui Huang, Cong Shen, and Jiawei Zhang. On the convergence
 702 analysis of muon. *arXiv preprint arXiv:2505.23737*, 2025.

702 Naichen Shi, Dawei Li, Mingyi Hong, and Ruoyu Sun. RMSProp converges with proper hyper-
 703 parameter. In *International Conference on Learning Representations*, 2020.

704

705 Hanlin Tang, Xiangru Lian, Shuang Qiu, Lei Yuan, Ce Zhang, Tong Zhang, and Ji Liu. Deepsqueeze:
 706 Decentralization meets error-compensated compression. *arXiv preprint arXiv:1907.07346*, 2019.

707

708 Georgios Vlassis, Saleh Ashkboos, Alexandra Volkova, Torsten Hoefer, and Dan Alistarh. Beyond
 709 outliers: A study of optimizers under quantization. *arXiv preprint arXiv:2509.23500*, 2025.

710

711 Bohan Wang, Yushun Zhang, Huishuai Zhang, Qi Meng, Zhi-Ming Ma, Tie-Yan Liu, and Wei Chen.
 712 Provable adaptivity in Adam. *arXiv preprint arXiv:2208.09900*, 2022.

713

714 Bohan Wang, Jingwen Fu, Huishuai Zhang, Nanning Zheng, and Wei Chen. Closing the gap between
 715 the upper bound and lower bound of adam's iteration complexity. In *Thirty-seventh Conference on
 716 Neural Information Processing Systems*, 2023. URL <https://openreview.net/forum?id=yDvb3mlogA>.

717

718 Bohan Wang, Yushun Zhang, Huishuai Zhang, Qi Meng, Ruoyu Sun, Zhi-Ming Ma, Tie-Yan Liu,
 719 Zhi-Quan Luo, and Wei Chen. Provable adaptivity of adam under non-uniform smoothness. In
 720 *Proceedings of the 30th ACM SIGKDD Conference on Knowledge Discovery and Data Mining*,
 721 pp. 2960–2969, 2024.

722

723 Naigang Wang, Jungwook Choi, Daniel Brand, Chia-Yu Chen, and Kailash Gopalakrishnan. Training
 724 deep neural networks with 8-bit floating point numbers. *Advances in neural information
 725 processing systems*, 31, 2018.

726

727 Ruizhe Wang, Yeyun Gong, Xiao Liu, Guoshuai Zhao, Ziyue Yang, Baining Guo, Zhengjun Zha,
 728 and Peng Cheng. Optimizing large language model training using fp4 quantization. In *Forty-
 729 second International Conference on Machine Learning*, 2025.

730

731 Shibo Wang and Pankaj Kanwar. Bfloat16: The secret to high performance on cloud tpus.
 732 *Google Cloud Blog*, 2019. URL <https://cloud.google.com/blog/products/ai-machine-learning/bfloat16-the-secret-to-high-performance-on-cloud-tpus>. Accessed:
 2025-09-21.

733

734 Kaiyue Wen, David Hall, Tengyu Ma, and Percy Liang. Fantastic pretraining optimizers and where
 735 to find them. *arXiv preprint arXiv:2509.02046*, 2025.

736

737 Wei Wen, Cong Xu, Feng Yan, Chunpeng Wu, Yandan Wang, Yiran Chen, and Hai Li. Terngrad:
 738 Ternary gradients to reduce communication in distributed deep learning. *Advances in neural
 739 information processing systems*, 30, 2017.

740

741 Mitchell Wortsman, Tim Dettmers, Luke Zettlemoyer, Ari Morcos, Ali Farhadi, and Ludwig
 742 Schmidt. Stable and low-precision training for large-scale vision-language models. *Advances
 743 in Neural Information Processing Systems*, 36:10271–10298, 2023.

744

745 Haocheng Xi, Yuxiang Chen, Kang Zhao, Kaijun Zheng, Jianfei Chen, and Jun Zhu. Jetfire: Efficient
 746 and accurate transformer pretraining with int8 data flow and per-block quantization. *arXiv
 747 preprint arXiv:2403.12422*, 2024.

748

749 Haocheng Xi, Han Cai, Ligeng Zhu, Yao Lu, Kurt Keutzer, Jianfei Chen, and Song Han. COAT:
 750 Compressing optimizer states and activations for memory-efficient FP8 training. In *The Thirteenth
 751 International Conference on Learning Representations*, 2025. URL <https://openreview.net/forum?id=XfKSDgqIRj>.

752

753 Tao Yu, Gaurav Gupta, Karthick Gopalswamy, Amith R Mamidala, Hao Zhou, Jeffrey Huynh,
 754 Youngsuk Park, Ron Diamant, Anoop Deoras, and Luke Huan. Collage: Light-weight low-
 755 precision strategy for LLM training. In Ruslan Salakhutdinov, Zico Kolter, Katherine Heller,
 756 Adrian Weller, Nuria Oliver, Jonathan Scarlett, and Felix Berkenkamp (eds.), *Proceedings
 757 of the 41st International Conference on Machine Learning*, volume 235 of *Proceedings of
 758 Machine Learning Research*, pp. 57459–57479. PMLR, 21–27 Jul 2024. URL <https://proceedings.mlr.press/v235/yu24d.html>.

756 Manzil Zaheer, Sashank Reddi, Devendra Sachan, Satyen Kale, and Sanjiv Kumar. Adaptive meth-
757 ods for nonconvex optimization. *Advances in Neural Information Processing Systems*, 31, 2018.
758

759 Chenyang Zhang, Difan Zou, and Yuan Cao. The implicit bias of adam on separable data. *Advances*
760 *in Neural Information Processing Systems*, 37:23988–24021, 2024.

761 Jingzhao Zhang, Tianxing He, Suvrit Sra, and Ali Jadbabaie. Why gradient clipping accelerates
762 training: A theoretical justification for adaptivity. In *International Conference on Learning Rep-
763 resentations*, 2020. URL <https://openreview.net/forum?id=BJgnXpVYwS>.
764

765 Qi Zhang, Yi Zhou, and Shaofeng Zou. Convergence guarantees for rmsprop and adam in
766 generalized-smooth non-convex optimization with affine noise variance, 2025. URL <https://arxiv.org/abs/2404.01436>.
767

768 Yushun Zhang, Congliang Chen, Naichen Shi, Ruoyu Sun, and Zhi-Quan Luo. Adam can converge
769 without any modification on update rules. *Advances in Neural Information Processing Systems*,
770 35:28386–28399, 2022.

771 Shuai Zheng, Ziyue Huang, and James Kwok. Communication-efficient distributed blockwise mo-
772 mentum sgd with error-feedback. *Advances in Neural Information Processing Systems*, 32, 2019.
773

774 Jiecheng Zhou, Ding Tang, Rong Fu, Boni Hu, Haoran Xu, Yi Wang, Zhilin Pei, Zhongling Su,
775 Liang Liu, Xingcheng Zhang, and Weiming Zhang. Towards efficient pre-training: Exploring fp4
776 precision in large language models. *arXiv preprint arXiv:2502.11458*, 2025.

777 Difan Zou, Yuan Cao, Yuanzhi Li, and Quanquan Gu. Understanding the generalization of adam
778 in learning neural networks with proper regularization. In *The Eleventh International Confer-
779 ence on Learning Representations*, 2023. URL <https://openreview.net/forum?id=iUYpN14qjTF>.
781

782 Fangyu Zou, Li Shen, Zequn Jie, Weizhong Zhang, and Wei Liu. A sufficient condition for conver-
783 gences of Adam and RMSProp. In *Proceedings of the IEEE/CVF Conference on computer vision*
784 *and pattern recognition*, pp. 11127–11135, 2019.

785
786
787
788
789
790
791
792
793
794
795
796
797
798
799
800
801
802
803
804
805
806
807
808
809

810 USE OF LARGE LANGUAGE MODELS
811

812 **Polishing writing.** We used multiple large language models (LLMs) to polish the presentation of
813 the paper, focusing on grammar, fluency, and readability while preserving the technical meaning of
814 the content. For each passage, we generated outputs from several LLMs and selected the best version
815 based on clarity and accuracy. The LLMs served only as editorial assistants, and all suggested
816 outputs were carefully checked and revised by the authors. The prompt used for polishing is as
817 follows:

818 I am preparing a paper for ICLR in Optimization.
819 Please help me polish the following
820 [sentence/paragraph/section] to make it more logical,
821 precise, clear, and accurate, while preserving the
822 technical meaning and mathematical correctness. Focus
823 on improving sentence structure, clarity, flow, and
824 readability, and enhance logical coherence between
825 statements. Highlight any ambiguities or imprecise
826 statements and suggest more rigorous alternatives.
827 [sentence/paragraph/section]

828 **Assisting L^AT_EX code.** We also used github copilot/cursor as a typing assistant to conveniently type
829 L^AT_EX code for mathematical formulas and derivations. All generated code was manually checked,
830 corrected, and integrated by the authors.

833 A PROOF OF THEOREM 4.5
834835 A.1 PRELIMINARIES
836

837 We consider an optimization problem in a d -dimensional space (let $d = mn$ be the number of train-
838 able parameters), where coordinates are indexed by $i \in [d] = \{1, 2, \dots, d\}$. Our algorithm generates
839 a sequence of vectors $(\mathbf{u}_t)_{t \in \mathbb{N}}$, with the i -th component of \mathbf{u}_t denoted by $u_{t,i}$. The objective is to
840 find a critical point of a global function $F: \mathbb{R}^d \rightarrow \mathbb{R}$ within a stochastic framework, where we have
841 access to a sequence of i.i.d. sample functions $(f_t)_{t \in \mathbb{N}^*}$ (e.g., the loss on a data minibatch). For any
842 differentiable function $h: \mathbb{R}^d \rightarrow \mathbb{R}$, we denote its gradient by ∇h and its i -th component by $\nabla_i h$.
843 Finally, we use a small constant $\epsilon > 0$ for numerical stability and let $\mathbb{E}_t[\cdot]$ denote the conditional ex-
844 pectation given the history of samples f_1, \dots, f_{t-1} . We use $\text{vec}(\cdot)$ to vectorize a matrix and $\text{mat}(\cdot)$
845 for the inverse operation.

846 Recall the dynamic system of our theoretical Quantized Adam. In the proof, we denote $\mathbf{w}_t =$
847 $\text{vec}(\mathbf{W}_t)$, $\widehat{\mathbf{g}}_t = \text{vec}(\mathbf{G}_t)$ and the dimension $d = m \cdot n$. For an iteration $t \in \mathbb{N}^*$, we define:

$$\begin{cases} m_{t,i} &= \beta_1 m_{t-1,i}^Q + \widehat{g}_{t,i} = \beta_1(m_{t-1,i} + \xi_{t-1,i}) + (\nabla_i f_t(\mathbf{w}_{t-1}) + \delta_{t,i}), \\ v_{t,i} &= \beta_2 v_{t-1,i}^Q + \widehat{g}_{t,i}^2 = \beta_2(v_{t-1,i} + \theta_{t-1,i}) + (\nabla_i f_t(\mathbf{w}_{t-1}) + \delta_{t,i})^2, \\ w_{t,i} &= w_{t-1,i} - \eta_t \frac{m_{t,i}}{\sqrt{\epsilon + v_{t,i}}}. \end{cases} \quad (\text{A.1})$$

853 with the step size given by

$$\eta_t = \eta(1 - \beta_1) \sqrt{\frac{1 - \beta_2^t}{1 - \beta_2}}. \quad (\text{A.2})$$

854 Here, $\delta_{t,i}$, $\xi_{t-1,i}$, and $\theta_{t-1,i}$ represent the quantization errors for the gradient, first mo-
855 ment, and second moment, respectively. Especially, $\nabla_i f_t(\mathbf{w}_{t-1}) = \frac{1}{B} \sum_{j=1}^B \nabla_i f(\mathbf{w}_{t-1}; \gamma_{t,j})$,
856 $\delta_{t,i} = \frac{1}{B} \sum_{j=1}^B \nabla_i^Q f(\mathbf{w}_{t-1}^Q; \gamma_{t,j}) - \frac{1}{B} \sum_{j=1}^B \nabla_i f_t(\mathbf{w}_{t-1}; \gamma_{t,j})$. And we have $\mathbb{E}[\nabla_i f_t(\mathbf{w}_{t-1})] =$
857 $\nabla_i F(\mathbf{w}_{t-1})$

863 Our convergence analysis for Quantized Adam is predicated on a specific, analytically convenient
864 formulation of the algorithm. This section serves to rigorously justify our theoretical framework

864 by establishing two foundational equivalences. First, we demonstrate that our representation of the
 865 Adam update is equivalent to the standard formulation. Following the methodology of Défossez
 866 et al. (2022), we absorb the scaling factor into the learning rate, which simplifies the recursive
 867 structure of the momentum term. Second, and more critically for our work, we prove that the
 868 theoretical analysis of quantizing these weighted-sum states is directly applicable to the practical
 869 scenario of quantizing the standard weighted-average states.

870
 871 **Equivalence with Standard Adam** Our formulation in (A.1) utilizes a weighted sum for the
 872 moments, which differs slightly from the standard weighted-average approach in the original
 873 Adam algorithm (Kingma, 2014). The standard first moment, often expressed as $\tilde{m}_{t,i} = (1 -$
 874 $\beta_1) \sum_{k=1}^t \beta_1^{t-k} \hat{g}_{k,i}$, is simply a scaled version of our definition, i.e., $\tilde{m}_{t,i} = (1 - \beta_1)m_{t,i}$. This
 875 constant scaling factor can be directly absorbed into the learning rate.

876 Furthermore, the standard Adam algorithm includes bias correction terms to counteract the zero-
 877 initialization of moments. These corrections are equivalent to using a time-dependent step size of
 878 the form:

$$\eta_{t,\text{Adam}} = \eta \cdot \frac{1 - \beta_1}{\sqrt{1 - \beta_2}} \cdot \frac{\sqrt{1 - \beta_1^t}}{1 - \beta_1^t}. \quad (\text{A.3})$$

879 For analytical tractability, our analysis adopts the simplified step size η_t from (A.2), which omits
 880 the bias correction for the first moment ($m_{t,i}$). This simplification is motivated by several practical
 881 and theoretical considerations. First, it ensures that our step size η_t is monotonic with respect to t ,
 882 which is advantageous for the convergence proof. Second, for typical hyperparameter values (e.g.,
 883 $\beta_1 = 0.9, \beta_2 = 0.999$), the omitted term $1/(1 - \beta_1^t)$ converges to its limit of 1 much more rapidly
 884 than the retained term $\sqrt{1 - \beta_2^t}$. Finally, removing this term effectively implements a learning
 885 rate warm-up, a common and beneficial practice, while retaining the correction for $v_{t,i}$ prevents an
 886 undesirably large initial step size that could lead to training instability.

887
 888 **Equivalence of Quantization Schemes.** A subtle but crucial aspect of our setup is the object
 889 of quantization. Our theoretical framework analyzes the quantization of weighted-sum moments
 890 ($\mathbf{m}_t, \mathbf{v}_t$), while a practical implementation would quantize the standard weighted-average moments
 891 ($\tilde{\mathbf{m}}_t, \tilde{\mathbf{v}}_t$). We now prove that these two approaches are, in fact, analytically equivalent.

892 To establish this rigorously, we first abstract the core dynamic behavior into a general mathematical
 893 lemma. We will show that two discrete-time systems, representing the weighted-sum and weighted-
 894 average accumulation methods under relative error perturbations, are analytically indistinguishable.
 895 We will then apply this result to the specific case of Quantized Adam.

896 **Lemma A.1** (Equivalence of Perturbed Dynamical Systems). Consider two scalar sequences
 897 $\{a_k\}_{k \geq 0}$ and $\{c_k\}_{k \geq 0}$ evolving according to the following dynamics for $k \geq 1$, with initial con-
 898 ditions $a_0 = c_0 = 0$:

$$a_k = \beta(a_{k-1} + d_{k-1}) + b_k \quad (\text{A.4})$$

$$c_k = \beta(c_{k-1} + e_{k-1}) + (1 - \beta)b_k \quad (\text{A.5})$$

900 where $\beta \in (0, 1)$ is a decay factor, $\{b_k\}$ is an external input sequence, and $\{d_k\}, \{e_k\}$ are perturba-
 901 tion sequences. These perturbations are bounded by a relative error model with factor $q \in [0, 1)$:

$$|d_{k-1}| \leq q|a_{k-1}| \quad \text{and} \quad |e_{k-1}| \leq q|c_{k-1}|. \quad (\text{A.6})$$

902 Then, the sequence $\{c_k\}$ and the scaled sequence $\{a'_k\} \triangleq (1 - \beta)a_k$ are analytically equivalent.
 903 Specifically, they follow identical recurrence relations where their respective perturbation terms
 904 satisfy identical relative error bounds with respect to their own states.

905
 906 *Proof.* To prove the equivalence, we derive the recurrence relation for the scaled sequence $\{a'_k\}$ and
 907 compare its structure and error properties to that of $\{c_k\}$.

908 **Step 1: Derive the recurrence for $\{a'_k\}$.** Starting from the definition $a'_k = (1 - \beta)a_k$ and substi-
 909 tuting the dynamics from (A.4):

$$\begin{aligned} a'_k &= (1 - \beta)[\beta(a_{k-1} + d_{k-1}) + b_k] \\ &= \beta(1 - \beta)a_{k-1} + \beta(1 - \beta)d_{k-1} + (1 - \beta)b_k. \end{aligned}$$

918 Now, we replace a_{k-1} with $a'_{k-1}/(1-\beta)$:

$$\begin{aligned} 919 \quad a'_k &= \beta(1-\beta) \left(\frac{a'_{k-1}}{1-\beta} \right) + \beta(1-\beta)d_{k-1} + (1-\beta)b_k \\ 920 \quad &= \beta a'_{k-1} + \beta(1-\beta)d_{k-1} + (1-\beta)b_k. \\ 921 \end{aligned}$$

924 **Step 2: Compare recurrence structures.** Let us place the recurrence relations for $\{c_k\}$ and $\{a'_k\}$ 925 side-by-side:

$$\begin{aligned} 926 \quad c_k &= \beta c_{k-1} + \beta e_{k-1} + (1-\beta)b_k \\ 927 \quad a'_k &= \beta a'_{k-1} + \beta(1-\beta)d_{k-1} + (1-\beta)b_k. \\ 928 \end{aligned}$$

929 Both sequences share the identical structure: $X_k = \beta X_{k-1} + \text{Perturbation}_k + (1-\beta)b_k$. The only 930 difference lies in the form of their respective perturbation terms.

931 **Step 3: Compare relative bounds of the perturbation terms.** The equivalence hinges on whether 932 these different perturbation terms satisfy the same relative error property with respect to their own 933 system's state.

934 For system $\{c_k\}$, the perturbation term is βe_{k-1} . Using the bound from (A.6):

$$935 \quad |\text{Perturbation}_c| = |\beta e_{k-1}| = \beta |e_{k-1}| \leq \beta q |c_{k-1}|.$$

937 For system $\{a'_k\}$, the effective perturbation term is $\beta(1-\beta)d_{k-1}$. Using the bound from (A.6) and 938 the scaling relationship $a_{k-1} = a'_{k-1}/(1-\beta)$:

$$939 \quad |\text{Perturbation}_a| = |\beta(1-\beta)d_{k-1}| = \beta(1-\beta)|d_{k-1}| \leq \beta(1-\beta)q|a_{k-1}| = \beta(1-\beta)q \frac{|a'_{k-1}|}{1-\beta} = \beta q |a'_{k-1}|.$$

942 **Conclusion of Proof.** Both systems, $\{c_k\}$ and the scaled $\{a'_k\}$, adhere to the same mathematical 943 dynamics. Their evolution is governed by an identical recurrence structure, and their respective 944 perturbation terms are bounded by the exact same relative factor βq with respect to their own 945 previous state. Therefore, from an analytical standpoint, the two systems are indistinguishable. Any 946 conclusion regarding the long-term behavior (e.g., convergence, stability) of $\{c_k\}$ under its perturbation 947 model will apply directly to $\{a'_k\}$ (and thus proportionally to $\{a_k\}$) under its own perturbation 948 model. \square

949 With Lemma A.1 established, we can now apply this general result to our specific case of Quantized 950 Adam. The weighted-sum moment \mathbf{m}_t from our analysis corresponds to the abstract sequence 951 $\{a_k\}$, while the standard weighted-average moment $\tilde{\mathbf{m}}_t$ corresponds to $\{c_k\}$. The gradient term 952 \mathbf{g}_t corresponds to $\{b_k\}$, and the relative quantization errors in both schemes are modeled by the 953 perturbations $\{d_k\}$ and $\{e_k\}$ with the bound factor q .

954 Lemma A.1 thus formally proves that analyzing the quantization of our weighted-sum moment \mathbf{m}_t 955 is analytically equivalent to analyzing the quantization of the standard weighted-average moment 956 $\tilde{\mathbf{m}}_t$. This rigorously justifies our proof strategy and ensures that our theoretical findings are directly 957 relevant to practical implementations of Quantized Adam. A parallel argument holds for the second 958 moments \mathbf{v}_t and $\tilde{\mathbf{v}}_t$ with decay factor β_2 .

960 A.2 DETAILED PROOF

962 To systematically analyze the effects of quantization, we begin by isolating the different sources of 963 error. We introduce auxiliary moment estimates, $m'_{t,i}$ and $v'_{t,i}$, which are defined to incorporate the 964 quantization error from the stochastic gradient, $\delta_{t,i}$, but are themselves assumed to be stored with 965 perfect precision. Their dynamics are given by:

$$\begin{aligned} 966 \quad m'_{t,i} &= \beta_1 m'_{t-1,i} + (\nabla_i f_t(\mathbf{w}_{t-1}) + \delta_{t,i}) \\ 967 \quad v'_{t,i} &= \beta_2 v'_{t-1,i} + (\nabla_i f_t(\mathbf{w}_{t-1}) + \delta_{t,i})^2 \end{aligned} \tag{A.7}$$

969 Throughout the following proof we note $\mathbb{E}_{t-1}[\cdot]$ the conditional expectation with respect to 970 f_1, \dots, f_{t-1} . In particular, $\mathbf{w}_{t-1}, \mathbf{v}_{t-1}$ is deterministic knowing f_1, \dots, f_{t-1} . With slightly abuse 971 of notation in the detailed proof, We introduce

$$972 \quad \mathcal{G}_t = \nabla F(\mathbf{w}_{t-1}) \quad \text{and} \quad \mathbf{g}_t = \nabla f_t(\mathbf{w}_{t-1}). \tag{A.8}$$

972 We introduce the update $\mathbf{u}_t \in \mathbb{R}^d$, as well as the update without momentum $\mathbf{U}_t \in \mathbb{R}^d$:
 973

$$974 \quad u_{t,i} = \frac{m_{t,i}}{\sqrt{\epsilon + v_{t,i}}} \quad \text{and} \quad U_{t,i} = \frac{g_{t,i} + \delta_{t,i}}{\sqrt{\epsilon + v'_{t,i}}}. \quad (\text{A.9})$$

$$975$$

$$976$$

977 For any $k \in \mathbb{N}$ with $k < t$, we define $\tilde{v}_{t,k} \in \mathbb{R}^d$ by
 978

$$979 \quad \tilde{v}_{t,k,i} = \beta_2^k v'_{t-k,i} + \mathbb{E}_{t-k} \left[\sum_{j=t-k+1}^t \beta_2^{t-j} (g_{j,i} + \delta_{j,i})^2 \right], \quad (\text{A.10})$$

$$980$$

$$981$$

982 i.e. the contribution from the k last gradients are replaced by their expected value for known values
 983 of f_1, \dots, f_{t-k-1} .
 984

985 Using the smoothness of F , we have

$$986 \quad F(\mathbf{w}_t) \leq F(\mathbf{w}_{t-1}) - \eta_t \mathcal{G}_t^T \mathbf{u}_t + \frac{\eta_t^2 L}{2} \|\mathbf{u}_t\|_2^2.$$

$$987$$

$$988$$

989 The overall motivation of our proof is to find a lower bound for $\eta_t \mathcal{G}_t^T \mathbf{u}_t$.
 990

$$991 \quad \mathcal{G}_t^T \mathbf{u}_t = \sum_{i \in [d]} \mathcal{G}_{t,i} \frac{m_{t,i}}{\sqrt{\epsilon + v_{t,i}}} \quad (\text{A.11})$$

$$992$$

$$993$$

994 We can rewrite $\mathcal{G}_t^T \mathbf{u}_t$ as:
 995

$$996 \quad \sum_{i \in [d]} \mathcal{G}_{t,i} \frac{m_{t,i}}{\sqrt{\epsilon + v_{t,i}}} = \underbrace{\left(\sum_{i \in [d]} \mathcal{G}_{t,i} \frac{m_{t,i}}{\sqrt{\epsilon + v_{t,i}}} - \sum_{i \in [d]} \mathcal{G}_{t,i} \frac{m'_{t,i}}{\sqrt{\epsilon + v'_{t,i}}} \right)}_A + \underbrace{\sum_{i \in [d]} \mathcal{G}_{t,i} \frac{m'_{t,i}}{\sqrt{\epsilon + v'_{t,i}}}}_B \quad (\text{A.12})$$

$$997$$

$$998$$

$$999$$

1000 Here, Term A represents the error component arising from the quantization of the momentum accumulators ($\mathbf{m}_t, \mathbf{v}_t$), while Term B represents the behavior of the update driven by an ideal accumulator.
 1001

1002 Now we can bound term A. We split A into two parts as before:
 1003

$$1004 \quad |A| \leq \underbrace{\left| \sum_{i \in [d]} \mathcal{G}_{t,i} \frac{m_{t,i} - m'_{t,i}}{\sqrt{\epsilon + v_{t,i}}} \right|}_{A_1} + \underbrace{\left| \sum_{i \in [d]} \mathcal{G}_{t,i} \left(\frac{m'_{t,i}}{\sqrt{\epsilon + v_{t,i}}} - \frac{m'_{t,i}}{\sqrt{\epsilon + v'_{t,i}}} \right) \right|}_{A_2} \quad (\text{A.13})$$

$$1005$$

$$1006$$

$$1007$$

$$1008$$

$$1009$$

1010 The first term, A_1 , which arises from the quantization noise on the first moment \mathbf{m} , is bounded using
 1011 Lemma A.3 (with $q = q_M$) and Lemma A.5:
 1012

$$1013 \quad |A_1| \leq \sum_{i \in [d]} R \frac{|m_{t,i} - m'_{t,i}|}{\sqrt{v_{t,i}}}$$

$$1014 \leq R \sum_{i \in [d]} \frac{\sum_{k=0}^t (\beta_1^{t-k} ((1+q_M)^{t-k} - 1)) |\nabla_i f_k(\mathbf{w}_{k-1}) + \delta_{k,i}|}{\sqrt{\sum_{k=0}^t \beta_2^{t-k} (1-q_V)^{t-k} (\nabla_i f_k(\mathbf{w}_{k-1}) + \delta_{k,i})^2}} \leq q_M \cdot dR \cdot C_q \quad (\text{A.14})$$

$$1015$$

$$1016$$

$$1017$$

$$1018$$

1019 where $C_q = \frac{\sqrt{r'(1+r')}}{(1+q_M)(1-r')^{3/2}}$ and $r' = \frac{\beta_1^2(1+q_M)^2}{\beta_2(1-q_V)}$.
 1020

1021 For the second term, A_2 , we use the bound on the gradient $\|\mathcal{G}_t\|_\infty \leq R$ and apply Lemma A.2,
 1022 which requires a case analysis.
 1023

$$1024 \quad |A_2| \leq \sum_{i \in [d]} R |m'_{t,i}| \left| \frac{1}{\sqrt{\epsilon + v_{t,i}}} - \frac{1}{\sqrt{\epsilon + v'_{t,i}}} \right|$$

$$1025$$

$$1026 \leq \sum_{i \in [d]} R |m'_{t,i}| \max \left\{ \frac{1}{\sqrt{\epsilon + LB_{t,i}}} - \frac{1}{\sqrt{\epsilon + v'_{t,i}}}, \frac{1}{\sqrt{\epsilon + v'_{t,i}}} - \frac{1}{\sqrt{\epsilon + UB_{t,i}}} \right\} \quad (\text{A.15})$$

1029 Let $g_{k,i} = \nabla_i f_k(\mathbf{w}_{k-1}) + \delta_{k,i}$. We analyze the two terms inside the max for a single coordinate i .

1030 **Case I (Deviation from Lower Bound):** Following the approximation in the provided sketch, we
1031 have

$$1033 |m'_{t,i}| \left(\frac{1}{\sqrt{\epsilon + LB_{t,i}}} - \frac{1}{\sqrt{\epsilon + v'_{t,i}}} \right) = |m'_{t,i}| \left(\frac{v'_{t,i} - LB_{t,i}}{\sqrt{\epsilon + LB_{t,i}} \sqrt{\epsilon + v'_{t,i}} (\sqrt{\epsilon + LB_{t,i}} + \sqrt{\epsilon + v'_{t,i}})} \right) \\ 1034 = \frac{|m'_{t,i}|}{\sqrt{\epsilon + LB_{t,i}}} \frac{v'_{t,i} - LB_{t,i}}{\sqrt{\epsilon + v'_{t,i}} (\sqrt{\epsilon + LB_{t,i}} + \sqrt{\epsilon + v'_{t,i}})} \\ 1035 \leq \frac{|m'_{t,i}|}{\sqrt{\epsilon + LB_{t,i}}} \frac{v'_{t,i} - LB_{t,i}}{\epsilon + v'_{t,i}} \\ 1036 = \frac{\sum_{k=0}^t \beta_1^{t-k} |g_{k,i} + \delta_{k,i}|}{\sqrt{\epsilon + \sum_{k=0}^t (\beta_2(1 - q_V))^{t-k} (g_{k,i} + \delta_{k,i})^2}} \cdot \frac{\sum_{k=0}^t (\beta_2^{t-k} - (\beta_2(1 - q_V))^{t-k}) (g_{k,i} + \delta_{k,i})^2}{\epsilon + \sum_{k=0}^t \beta_2^{t-k} (g_{k,i} + \delta_{k,i})^2} \quad (\text{A.16})$$

1037 The first fraction is bounded by Lemma A.4: $\frac{\sum_{k=0}^t \beta_1^k |a_{t-k,i}|}{\sqrt{\epsilon + \sum_{k=0}^t (\beta_2(1 - q_V))^k a_{t-k,i}}} \leq \frac{1}{\sqrt{1 - \beta_1^2 / (\beta_2(1 - q_V))}}$. The
1038 second fraction is a ratio of weighted sums $\frac{\sum_{k=0}^t (\beta_2^k - (\beta_2(1 - q_V))^k) a_{t-k,i}}{\epsilon + \sum_{k=0}^t \beta_2^k a_{t-k,i}}$. This ratio is bounded by
1039 the maximum ratio of its coefficients:

$$1040 \max_{k \in \{0, \dots, t\}} \frac{\beta_2^k - (\beta_2(1 - q_V))^k}{\beta_2^k} = \max_{k \in \{0, \dots, t\}} (1 - (1 - q_V)^k) = 1 - (1 - q_V)^t.$$

1041 Combining these bounds, the term for Case I is bounded by $\frac{1}{\sqrt{1 - \beta_1^2 / (\beta_2(1 - q_V))}} (1 - (1 - q_V)^t)$.

1042 **Case II (Deviation from Upper Bound):** Similarly, we bound the second term:

$$1043 |m'_{t,i}| \left(\frac{1}{\sqrt{\epsilon + v'_{t,i}}} - \frac{1}{\sqrt{\epsilon + UB_{t,i}}} \right) \leq \frac{|m'_{t,i}|}{\sqrt{\epsilon + v'_{t,i}}} \frac{UB_{t,i} - v'_{t,i}}{\epsilon + UB_{t,i}}$$

1044 Applying Lemma A.4 and the maximum ratio:

$$1045 \leq \frac{1}{\sqrt{1 - \beta_1^2 / \beta_2}} \cdot (1 - (1 + q_V)^{-t})$$

1046 Comparing the bounds from the two cases, the bound from Case I is larger since $1 - (1 - q_V)^t >$
1047 $1 - (1 + q_V)^{-t}$ and the denominator term $\sqrt{1 - \beta_1^2 / (\beta_2(1 - q_V))}$ is smaller than $\sqrt{1 - \beta_1^2 / \beta_2}$.
1048 Therefore, taking the maximum and summing over d dimensions:

$$1049 |A_2| \leq \sum_{i \in [d]} R \frac{1 - (1 - q_V)^t}{\sqrt{1 - \frac{\beta_1^2}{\beta_2(1 - q_V)}}} = \frac{dR(1 - (1 - q_V)^t)}{\sqrt{1 - \frac{\beta_1^2}{\beta_2(1 - q_V)}}} \quad (\text{A.17})$$

1050 Combining the bounds for $|A_1|$ and $|A_2|$, we can get the bound for term A:

$$1051 |A| \leq |A_1| + |A_2| \leq q_M \cdot dR \cdot C_q + \frac{dR(1 - (1 - q_V)^t)}{\sqrt{1 - \frac{\beta_1^2}{\beta_2(1 - q_V)}}} \triangleq Q(t) \quad (\text{A.18})$$

1052 Now we move on to bound Term B. Let us now focus on bounding Term B from (A.12). By
1053 expanding the definition of the first moment estimate $m'_{t,i}$, we can decompose Term B into two
1054 parts, which we will call Term C and Term D:

$$1055 \sum_{i \in [d]} \mathcal{G}_{t,i} \frac{m'_{t,i}}{\sqrt{\epsilon + v'_{t,i}}} = \sum_{i \in [d]} \mathcal{G}_{t,i} \sum_{k=0}^{t-1} \beta_1^k \frac{g_{t-k,i} + \delta_{t-k,i}}{\sqrt{\epsilon + v'_{t,i}}} \quad (\text{A.19})$$

$$\begin{aligned}
 &= \underbrace{\sum_{i \in [d]} \sum_{k=0}^{t-1} \beta_1^k \mathcal{G}_{t-k,i} \frac{g_{t-k,i} + \delta_{t-k,i}}{\sqrt{\epsilon + v'_{t,i}}} + \sum_{i \in [d]} \sum_{k=0}^{t-1} \beta_1^k (\mathcal{G}_{t,i} - \mathcal{G}_{t-k,i}) \frac{g_{t-k,i} + \delta_{t-k,i}}{\sqrt{\epsilon + v'_{t,i}}}}_C + \underbrace{\sum_{i \in [d]} \sum_{k=0}^{t-1} \beta_1^k (\mathcal{G}_{t,i} - \mathcal{G}_{t-k,i}) \frac{g_{t-k,i} + \delta_{t-k,i}}{\sqrt{\epsilon + v'_{t,i}}}}_D.
 \end{aligned} \tag{A.20}$$

The magnitude of Term D, which captures the error from gradient drift, is bounded by Lemma A.8:

$$|D| \leq \frac{\eta_t^2 L^2 \sqrt{1 - \beta_1}}{4(1 + q_G)R} \left(\sum_{l=1}^{t-1} \|\mathbf{u}_{t-l}\|_2^2 \sum_{k=l}^{t-1} \beta_1^k \sqrt{k} \right) + \frac{(1 + q_G)R}{\sqrt{1 - \beta_1}} \sum_{k=0}^{t-1} \left(\frac{\beta_1}{\beta_2} \right)^k \sqrt{k+1} \|\mathbf{U}_{t-k}\|_2^2. \tag{A.21}$$

For Term C, we establish a lower bound on its expectation in Lemma A.9:

$$\begin{aligned}
 \mathbb{E}[C] &\geq \frac{1}{2} \left(\sum_{i \in [d]} \sum_{k=0}^{t-1} \beta_1^k \mathbb{E} \left[\frac{\mathcal{G}_{t-k,i}^2}{\sqrt{\epsilon + \tilde{v}_{t,k+1,i}}} \right] \right) - \frac{2(1 + q_G)R}{\sqrt{1 - \beta_1}} \left(\sum_{i \in [d]} \sum_{k=0}^{t-1} \left(\frac{\beta_1}{\beta_2} \right)^k \sqrt{k+1} \mathbb{E} [\|\mathbf{U}_{t-k}\|_2^2] \right) \\
 &\quad - d \sum_{k=0}^{t-1} \beta_1^k M_{t-k}.
 \end{aligned} \tag{A.22}$$

where $M_{t-k} = \frac{q_G R^2 + L q_W R \|\mathbf{w}_{t-k-1}\|_2}{\sqrt{\epsilon}}$. Injecting (A.22), (A.21) and (A.20) into (A.12). We get the final lower bound for $\mathcal{G}_t^T \mathbf{u}_t$:

$$\begin{aligned}
 \mathbb{E} \left[\sum_{i \in [d]} \mathcal{G}_{t,i} \frac{m_{t,i}}{\sqrt{\epsilon + v_{t,i}}} \right] &\geq \frac{1}{2} \left(\sum_{i \in [d]} \sum_{k=0}^{t-1} \beta_1^k \mathbb{E} \left[\frac{\mathcal{G}_{t-k,i}^2}{\sqrt{\epsilon + \tilde{v}_{t,k+1,i}}} \right] \right) - Q(t) - d \sum_{k=0}^{t-1} \beta_1^k M_{t-k} \\
 &\quad - \frac{\eta_t^2 L^2}{4(1 + q_G)R} \sqrt{1 - \beta_1} \left(\sum_{l=1}^{t-1} \|\mathbf{u}_{t-l}\|_2^2 \sum_{k=l}^{t-1} \beta_1^k \sqrt{k} \right) - \frac{3(1 + q_G)R}{\sqrt{1 - \beta_1}} \left(\sum_{k=0}^{t-1} \left(\frac{\beta_1}{\beta_2} \right)^k \sqrt{k+1} \|\mathbf{U}_{t-k}\|_2^2 \right).
 \end{aligned} \tag{A.23}$$

Now lets look back at:

$$F(\mathbf{w}_t) \leq F(\mathbf{w}_{t-1}) - \eta_t \mathcal{G}_t^T \mathbf{u}_t + \frac{\eta_t^2 L}{2} \|\mathbf{u}_t\|_2^2.$$

inject (A.23) into it:

$$\begin{aligned}
 \mathbb{E}[F(\mathbf{w}_t)] &\leq \mathbb{E}[F(\mathbf{w}_{t-1})] - \frac{\eta_t}{2} \left(\sum_{i \in [d]} \sum_{k=0}^{t-1} \beta_1^k \mathbb{E} \left[\frac{\mathcal{G}_{t-k,i}^2}{\sqrt{\epsilon + \tilde{v}_{t,k+1,i}}} \right] \right) + \frac{\eta_t^2 L}{2} \mathbb{E} [\|\mathbf{u}_t\|_2^2] + \eta_t Q(t) + \eta_t d \sum_{k=0}^{t-1} \beta_1^k M_{t-k} \\
 &\quad + \frac{\eta_t^3 L^2}{4(1 + q_G)R} \sqrt{1 - \beta_1} \left(\sum_{l=1}^{t-1} \|\mathbf{u}_{t-l}\|_2^2 \sum_{k=l}^{t-1} \beta_1^k \sqrt{k} \right) + \frac{3\eta_t(1 + q_G)R}{\sqrt{1 - \beta_1}} \left(\sum_{k=0}^{t-1} \left(\frac{\beta_1}{\beta_2} \right)^k \sqrt{k+1} \|\mathbf{U}_{t-k}\|_2^2 \right).
 \end{aligned} \tag{A.24}$$

We have for any $k \in \mathbb{N}$, $k < t$, and any coordinate $i \in [d]$, $\sqrt{\epsilon + \tilde{v}_{t,k+1,i}} \leq (1 + q_G)R \sqrt{\sum_{j=0}^{t-1} \beta_2^j}$.

Introducing $\Omega_t = \sqrt{\sum_{j=0}^{t-1} \beta_2^j}$, we have

$$\begin{aligned}
 \mathbb{E}[F(\mathbf{w}_t)] &\leq \mathbb{E}[F(\mathbf{w}_{t-1})] - \frac{\eta_t}{2(1 + q_G)R\Omega_t} \sum_{k=0}^{t-1} \beta_1^k \mathbb{E} [\|\mathcal{G}_{t-k}\|_2^2] + \frac{\eta_t^2 L}{2} \mathbb{E} [\|\mathbf{u}_t\|_2^2] + \eta_t Q(t) + \eta_t d \mathbb{E} \left[\sum_{k=0}^{t-1} \beta_1^k M_{t-k} \right] \\
 &\quad + \frac{\eta_t^3 L^2}{4(1 + q_G)R} \sqrt{1 - \beta_1} \left(\sum_{l=1}^{t-1} \|\mathbf{u}_{t-l}\|_2^2 \sum_{k=l}^{t-1} \beta_1^k \sqrt{k} \right) + \frac{3\eta_t(1 + q_G)R}{\sqrt{1 - \beta_1}} \left(\sum_{k=0}^{t-1} \left(\frac{\beta_1}{\beta_2} \right)^k \sqrt{k+1} \|\mathbf{U}_{t-k}\|_2^2 \right).
 \end{aligned} \tag{A.25}$$

Now summing over all iterations $t \in [T]$ for $T \in \mathbb{N}^*$, and η_t is non-decreasing, as well the fact that F is bounded below by F_* , we get

$$\begin{aligned}
 & \underbrace{\frac{1}{2(1+q_G)R} \sum_{t=1}^T \frac{\eta_t}{\Omega_t} \sum_{k=0}^{t-1} \beta_1^k \mathbb{E} [\|\mathcal{G}_{t-k}\|_2^2]}_{\tilde{A}} \leq F(\mathbf{w}_0) - F_* + \underbrace{\frac{\eta_T^2 L}{2} \sum_{t=1}^T \mathbb{E} [\|\mathbf{u}_t\|_2^2]}_{\tilde{B}} + \underbrace{\eta_T \sum_{t=1}^T Q(t)}_{E_Q} + \underbrace{\eta_T d \sum_{t=1}^T \mathbb{E} \left[\sum_{k=0}^{t-1} \beta_1^k M_{t-k} \right]}_M \\
 & + \underbrace{\frac{\eta_T^3 L^2}{4(1+q_G)R} \sqrt{1-\beta_1} \sum_{t=1}^T \sum_{l=1}^{t-1} \mathbb{E} [\|\mathbf{u}_{t-l}\|_2^2] \sum_{k=l}^{t-1} \beta_1^k \sqrt{k}}_{\tilde{C}} + \underbrace{\frac{3\eta_T(1+q_G)R}{\sqrt{1-\beta_1}} \sum_{t=1}^T \sum_{k=0}^{t-1} \left(\frac{\beta_1}{\beta_2} \right)^k \sqrt{k+1} \mathbb{E} [\|\mathbf{U}_{t-k}\|_2^2]}_{\tilde{D}}. \tag{A.26}
 \end{aligned}$$

First lets bound Term \tilde{A} . We have $\eta_t = (1-\beta_1)\Omega_t\eta$. Thus, we can simplify the \tilde{A} term from (A.26), also using the usual change of index $j = t - k$, to get

$$\begin{aligned}
 \tilde{A} &= \frac{1}{2(1+q_G)R} \sum_{t=1}^T \frac{\eta_t}{\Omega_t} \sum_{j=1}^t \beta_1^{t-j} \mathbb{E} [\|\mathcal{G}_j\|_2^2] \\
 &= \frac{\eta(1-\beta_1)}{2(1+q_G)R} \sum_{j=1}^T \mathbb{E} [\|\mathcal{G}_j\|_2^2] \sum_{t=j}^T \beta_1^{t-j} \\
 &= \frac{\eta}{2(1+q_G)R} \sum_{j=1}^T (1 - \beta_1^{T-j+1}) \mathbb{E} [\|\mathcal{G}_j\|_2^2] \\
 &= \frac{\eta}{2(1+q_G)R} \sum_{j=1}^T (1 - \beta_1^{T-j+1}) \mathbb{E} [\|\nabla F(\mathbf{w}_{j-1})\|_2^2] \\
 &= \frac{\eta}{2(1+q_G)R} \sum_{j=0}^{T-1} (1 - \beta_1^{T-j}) \mathbb{E} [\|\nabla F(\mathbf{w}_j)\|_2^2]. \tag{A.27}
 \end{aligned}$$

To establish our convergence guarantee, we analyze the expected gradient norm at a randomly selected iteration τ , drawn from the set $\{0, \dots, T-1\}$. The selection is not uniform but is instead weighted to properly account for the influence of the momentum term over the iterations. The probability of selecting a specific iteration t is defined as:

$$\forall t \in \{0, \dots, T-1\}, \quad \mathbb{P}(\tau = t) \propto 1 - \beta_1^{T-t}. \tag{A.28}$$

We can notice that

$$\sum_{j=0}^{T-1} (1 - \beta_1^{T-j}) = T - \beta_1 \frac{1 - \beta_1^T}{1 - \beta_1} \geq T - \frac{\beta_1}{1 - \beta_1}. \tag{A.29}$$

Introducing

$$\tilde{T} = T - \frac{\beta_1}{1 - \beta_1}, \tag{A.30}$$

we then have

$$\tilde{A} \geq \frac{\eta \tilde{T}}{2(1+q_G)R} \mathbb{E} [\|\nabla F(\mathbf{w}_\tau)\|_2^2]. \tag{A.31}$$

Next looking at \tilde{B} , we apply Lemma A.13,

$$\tilde{B} \leq B' \left(\ln \left(1 + \frac{((1+q_G)R)^2}{\epsilon(1-\beta_2(1-q_V))} \right) - T \ln(\beta_2(1-q_V)) \right) \tag{A.32}$$

1188 with

$$1190 \quad B' = \frac{d\eta_T^2 L}{2(1 - \beta_1(1 + q_M))(1 - \frac{\beta_1(1+q_M)}{\beta_2(1-q_V)})}. \quad (A.33)$$

1193 Then looking at \tilde{C} and introducing the change of index $j = t - l$,

$$1195 \quad \begin{aligned} \tilde{C} &= \frac{\eta_T^3 L^2}{4(1 + q_G)R} \sqrt{1 - \beta_1} \sum_{t=1}^T \sum_{j=1}^t \mathbb{E} [||\mathbf{u}_j||_2^2] \sum_{k=t-j}^{t-1} \beta_1^k \sqrt{k} \\ 1196 &= \frac{\eta_T^3 L^2}{4(1 + q_G)R} \sqrt{1 - \beta_1} \sum_{j=1}^T \mathbb{E} [||\mathbf{u}_j||_2^2] \sum_{t=j}^T \sum_{k=t-j}^{t-1} \beta_1^k \sqrt{k} \\ 1197 &= \frac{\eta_T^3 L^2}{4(1 + q_G)R} \sqrt{1 - \beta_1} \sum_{j=1}^T \mathbb{E} [||\mathbf{u}_j||_2^2] \sum_{k=0}^{T-1} \beta_1^k \sqrt{k} \sum_{t=j}^{j+k} 1 \\ 1201 &= \frac{\eta_T^3 L^2}{4(1 + q_G)R} \sqrt{1 - \beta_1} \sum_{j=1}^T \mathbb{E} [||\mathbf{u}_j||_2^2] \sum_{k=0}^{T-1} \beta_1^k \sqrt{k} (k+1) \\ 1205 &\leq \frac{\eta_T^3 L^2}{(1 + q_G)R} \sum_{j=1}^T \mathbb{E} [||\mathbf{u}_j||_2^2] \frac{\beta_1}{(1 - \beta_1)^2}. \end{aligned} \quad (A.34)$$

1210 using Lemma A.12. Finally, using Lemma A.13, we get

$$1212 \quad \tilde{C} \leq C' \left(\ln \left(1 + \frac{((1 + q_G)R)^2}{\epsilon(1 - \beta_2(1 - q_V))} \right) - T \ln(\beta_2(1 - q_V)) \right). \quad (A.35)$$

1215 with

$$1216 \quad C' = \frac{d\eta_T^3 L^2 \beta_1}{(1 + q_G)R(1 - \beta_1)^2(1 - \beta_1(1 + q_M))(1 - \frac{\beta_1(1+q_M)}{\beta_2(1-q_V)})}. \quad (A.36)$$

1219 introducing the same change of index $j = t - k$ for \tilde{D} , we get

$$1221 \quad \begin{aligned} \tilde{D} &= \frac{3\eta_T(1 + q_G)R}{\sqrt{1 - \beta_1}} \sum_{t=1}^T \sum_{j=1}^t \left(\frac{\beta_1}{\beta_2} \right)^{t-j} \sqrt{1 + t - j} \mathbb{E} [||\mathbf{U}_j||_2^2] \\ 1222 &= \frac{3\eta_T(1 + q_G)R}{\sqrt{1 - \beta_1}} \sum_{j=1}^T \mathbb{E} [||\mathbf{U}_j||_2^2] \sum_{t=j}^T \left(\frac{\beta_1}{\beta_2} \right)^{t-j} \sqrt{1 + t - j} \\ 1224 &\leq \frac{6\eta_T(1 + q_G)R}{\sqrt{1 - \beta_1}} \sum_{j=1}^T \mathbb{E} [||\mathbf{U}_j||_2^2] \frac{1}{(1 - \beta_1/\beta_2)^{3/2}}, \end{aligned} \quad (A.37)$$

1230 using Lemma A.11. Finally, using Lemma A.10, we get

$$1232 \quad \begin{aligned} \tilde{D} &\leq \frac{6\eta_T(1 + q_G)R}{\sqrt{1 - \beta_1}(1 - \beta_1/\beta_2)^{3/2}} \sum_{i \in [d]} \left(\ln \left(1 + \frac{v'_{T,i}}{\epsilon} \right) - T \ln(\beta_2) \right) \\ 1233 &\leq \frac{6d\eta_T(1 + q_G)R}{\sqrt{1 - \beta_1}(1 - \beta_1/\beta_2)^{3/2}} \left(\ln \left(1 + \frac{((1 + q_G)R)^2}{\epsilon(1 - \beta_2)} \right) - T \ln(\beta_2) \right) \end{aligned} \quad (A.38)$$

1238 Then we rewrite the quantization error term E_Q :

$$1240 \quad E_Q = \eta_T \sum_{t=1}^T \left(q_M \cdot dR \cdot C_q + \frac{dR(1 - (1 - q_V)^t)}{\sqrt{1 - \frac{\beta_1^2}{\beta_2(1-q_V)}}} \right)$$

$$\begin{aligned}
&= \eta_T \left(\sum_{t=1}^T \left(q_M \cdot dR \cdot C_q + \frac{dR}{\sqrt{1 - \frac{\beta_1^2}{\beta_2(1-q_V)}}} \right) - \sum_{t=1}^T \frac{dR(1-q_V)^t}{\sqrt{1 - \frac{\beta_1^2}{\beta_2(1-q_V)}}} \right) \\
&= \eta_T \left(T \left(q_M \cdot dR \cdot C_q + \frac{dR}{\sqrt{1 - \frac{\beta_1^2}{\beta_2(1-q_V)}}} \right) - \frac{dR}{\sqrt{1 - \frac{\beta_1^2}{\beta_2(1-q_V)}}} \sum_{t=1}^T (1-q_V)^t \right) \\
&= \eta_T \left(T \cdot q_M \cdot dR \cdot C_q + \frac{T dR}{\sqrt{1 - \frac{\beta_1^2}{\beta_2(1-q_V)}}} - \frac{dR}{\sqrt{1 - \frac{\beta_1^2}{\beta_2(1-q_V)}}} \left(\frac{1-q_V}{q_V} (1 - (1-q_V)^T) \right) \right)
\end{aligned} \tag{A.39}$$

Finally, we bound Term M using Lemma A.14:

$$M \leq \frac{\eta_T dT}{\sqrt{\epsilon(1-\beta_1)}} (q_G R^2 + L q_W R \|\mathbf{w}_0\|_2) + \frac{\eta_T^2 d^{\frac{3}{2}} L q_W R T^2}{2\sqrt{\epsilon(1-\beta_1)} \sqrt{1 - \frac{\beta_1^2(1+q_M)^2}{\beta_2(1-q_V)}}}, \tag{A.40}$$

Now putting (A.31), (A.32), (A.35), (A.38), (A.39) and (A.40) together into (A.26) and noting that $\eta_T \leq \eta \frac{1-\beta_1}{\sqrt{1-\beta_2}}$, we get:

$$\begin{aligned}
\mathbb{E} [\|\nabla F(\mathbf{w}_\tau)\|_2^2] &\leq 2(1+q_G)R \frac{F_0 - F_*}{\eta \tilde{T}} + \frac{E}{\tilde{T}} \left(\ln \left(1 + \frac{((1+q_G)R)^2}{\epsilon(1-\beta_2)} \right) - T \ln(\beta_2) \right) \\
&\quad + \frac{H}{\tilde{T}} \left(\ln \left(1 + \frac{((1+q_G)R)^2}{\epsilon(1-\beta_2(1-q_V))} \right) - T \ln(\beta_2(1-q_V)) \right) + \frac{Q(T)}{\tilde{T}} \\
&\quad + \frac{2(1+q_G)dT}{\tilde{T}\sqrt{\epsilon(1-\beta_2)}} (q_G R^3 + L q_W R^2 \|\mathbf{w}_0\|_2) + \frac{(1-\beta_1)d^{\frac{3}{2}}\eta L q_W (1+q_G)R^2 T^2}{\tilde{T}\sqrt{\epsilon(1-\beta_2)} \sqrt{1 - \frac{\beta_1^2(1+q_M)^2}{\beta_2(1-q_V)}}}.
\end{aligned} \tag{A.41}$$

with

$$\begin{aligned}
E &= \frac{12d((1+q_G)R)^2 \sqrt{1-\beta_1}}{(1-\beta_1/\beta_2)^{3/2} \sqrt{1-\beta_2}} \\
H &= \frac{d\eta L(1+q_G)R(1-\beta_1)^2}{(1-\beta_1(1+q_M))(1-\frac{\beta_1(1+q_M)}{\beta_2(1-q_V)})(1-\beta_2)} + \frac{2d\eta^2 L^2 \beta_1(1-\beta_1)}{(1-\beta_1(1+q_M))(1-\frac{\beta_1(1+q_M)}{\beta_2(1-q_V)})(1-\beta_2)^{\frac{3}{2}}} \\
Q(T) &= \frac{2(1+q_G)q_M dR^2(1-\beta_1)T}{\sqrt{1-\beta_2}} \cdot \frac{\sqrt{r'(1+r')}}{(1+q_M)(1-r')^{3/2}} + \frac{2(1+q_G)dR^2(1-\beta_1)T}{\sqrt{(1-\frac{\beta_1^2}{\beta_2(1-q_V)})(1-\beta_2)}} \\
&\quad - \frac{2(1+q_G)dR^2(1-\beta_1)}{\sqrt{(1-\frac{\beta_1^2}{\beta_2(1-q_V)})(1-\beta_2)}} \left(\frac{1-q_V}{q_V} (1 - (1-q_V)^T) \right) \\
\text{where } r' &= \frac{\beta_1^2(1+q_M)^2}{\beta_2(1-q_V)}
\end{aligned} \tag{A.42}$$

For clarity in the main theorem statement, we can present a slightly looser but more accessible version of this bound. By noting that for a sufficiently large T , we have $\tilde{T} \geq T/2$, and

$$\left(\ln \left(1 + \frac{((1+q_G)R)^2}{\epsilon(1-\beta_2)} \right) - T \ln(\beta_2) \right) < \left(\ln \left(1 + \frac{((1+q_G)R)^2}{\epsilon(1-\beta_2(1-q_V))} \right) - T \ln(\beta_2(1-q_V)) \right),$$

we can state the simplified bound presented in Theorem 4.5:

$$\mathbb{E} [\|\nabla F(\mathbf{w}_\tau)\|_2^2] \leq 4(1+q_G)R \frac{F_0 - F_*}{\eta T} + \frac{C}{T} \left(\ln \left(1 + \frac{((1+q_G)R)^2}{\epsilon(1-\beta_2(1-q_V))} \right) - T \ln(\beta_2(1-q_V)) \right)$$

$$+ \frac{\tilde{Q}(T)}{T} + \frac{4(1+q_G)d}{\sqrt{\epsilon(1-\beta_2)}} (q_G R^3 + L q_W R^2 D) + \frac{2(1-\beta_1)d^{\frac{3}{2}}\eta L q_W (1+q_G) R^2 T}{\sqrt{\epsilon(1-\beta_2)} \sqrt{1 - \frac{\beta_1^2(1+q_M)^2}{\beta_2(1-q_V)}}},$$

1299
1300 with
1301

$$C = \frac{24d((1+q_G)R)^2\sqrt{1-\beta_1}}{(1-\beta_1/\beta_2)^{3/2}\sqrt{1-\beta_2}} + \frac{2d\eta L(1+q_G)R(1-\beta_1)^2}{(1-\beta_1(1+q_M))(1-\frac{\beta_1(1+q_M)}{\beta_2(1-q_V)})(1-\beta_2)} \\ + \frac{4d\eta^2 L^2 \beta_1(1-\beta_1)}{(1-\beta_1(1+q_M))(1-\frac{\beta_1(1+q_M)}{\beta_2(1-q_V)})(1-\beta_2)^{\frac{3}{2}}},$$

$$\tilde{Q}(T) = \frac{4(1+q_G)q_M d R^2 (1-\beta_1) T}{\sqrt{1-\beta_2}} \cdot \frac{\sqrt{r'(1+r')}}{(1+q_M)(1-r')^{3/2}} + \frac{4(1+q_G)d R^2 (1-\beta_1) T}{\sqrt{(1-\frac{\beta_1^2}{\beta_2(1-q_V)})(1-\beta_2)}} \\ - \frac{4(1+q_G)d R^2 (1-\beta_1)}{\sqrt{(1-\frac{\beta_1^2}{\beta_2(1-q_V)})(1-\beta_2)}} \left(\frac{1-q_V}{q_V} (1 - (1-q_V)^T) \right)$$

1313 where $r' = \frac{\beta_1^2(1+q_M)^2}{\beta_2(1-q_V)}$
1314
1315

1316 Theory 4.5 states that under a specific schedule for the hyperparameters and a gradual reduction in
1317 quantization error, Quantized Adam achieves the same convergence rate as its full-precision counter-
1318 part. We prove this by performing a detailed asymptotic analysis of each term in the main bound
1319 from Theorem 4.5 as the total number of iterations $T \rightarrow \infty$.

1320 However, to perform a precise asymptotic analysis and derive the tightest possible convergence rate
1321 from our framework, we will now analyze the order of each component from the more detailed
1322 bound in A.41:

$$\mathbb{E} [\|\nabla F(\text{vec}(\mathbf{W})_\tau)\|_2^2] \leq \underbrace{2(1+q_G)R \frac{F_0 - F_*}{\eta \tilde{T}}}_{\text{Term 1}} \\ + \underbrace{\frac{12d((1+q_G)R)^2\sqrt{1-\beta_1}}{\tilde{T}(1-\beta_1/\beta_2)^{3/2}\sqrt{1-\beta_2}} \left(\ln \left(1 + \frac{((1+q_G)R)^2}{\epsilon(1-\beta_2)} \right) - T \ln(\beta_2) \right)}_{\text{Term 2}} \\ + \underbrace{\frac{E}{\tilde{T}} \left(\ln \left(1 + \frac{((1+q_G)R)^2}{\epsilon(1-\beta_2(1-q_V))} \right) - T \ln(\beta_2(1-q_V)) \right)}_{\text{Term 3}} \\ + \underbrace{\frac{Q(T)}{\tilde{T}} + \frac{2(1+q_G)dT}{\tilde{T}\sqrt{\epsilon(1-\beta_2)}} (q_G R^3 + L q_W R^2 \|\text{vec}(\mathbf{W}_0)\|_2)}_{\text{Term 4, Term 5}} \\ + \underbrace{\frac{(1-\beta_1)d^{\frac{3}{2}}\eta L q_W (1+q_G) R^2 T^2}{\tilde{T}\sqrt{\epsilon(1-\beta_2)} \sqrt{1 - \frac{\beta_1^2(1+q_M)^2}{\beta_2(1-q_V)}}}}_{\text{Term 6}}.$$

1344 Our proof strategy is to analyze the asymptotic order of each term under the following scaling
1345 assumptions.
1346

1347 **Scaling Assumptions.** We adopt the scaling assumptions provided in the Theorem:

1348
1349 • **Quantization Error Schedules:** The quantization errors are annealed over time such that $q_G = \mathcal{O}(T^{-1})$, $q_M = \mathcal{O}(T^{-1})$, $q_W = \mathcal{O}(T^{-2})$, and $q_V = \mathcal{O}(T^{-2})$.

1350 • **Adam Hyperparameters:** The learning rate and second-moment decay are set as $\eta = \Theta(T^{-1/2})$
 1351 and $1 - \beta_2 = \Theta(1/T)$, while β_1 is treated as a constant.
 1352

1353 **Asymptotic Analysis of Bound Terms.** We now analyze the order of magnitude for each of the
 1354 six terms.
 1355

1356 **Term 1 (Initial Condition Term):** This term is given by $T_1 = 2(1 + q_G)R \frac{F_0 - F_*}{\eta \tilde{T}}$. We analyze the
 1357 components of its denominator. The effective number of iterations is $\tilde{T} = T - \frac{\beta_1}{1 - \beta_1} = \Theta(T)$. The
 1358 learning rate scales as $\eta = \Theta(T^{-1/2})$. The denominator thus scales as $\eta \tilde{T} = \Theta(T^{-1/2})\Theta(T) =$
 1359 $\Theta(T^{1/2})$. Since all other quantities are constants and $q_G \rightarrow 0$, the entire term scales as:
 1360

$$1361 T_1 = \Theta\left(\frac{1}{\eta \tilde{T}}\right) = \Theta\left(\frac{1}{T^{1/2}}\right) = \Theta(T^{-1/2}).$$

1364 **Term 2 (First Logarithmic Term):** This term is:
 1365

$$1366 T_2 = \frac{12d((1 + q_G)R)^2 \sqrt{1 - \beta_1}}{\tilde{T}(1 - \beta_1/\beta_2)^{3/2} \sqrt{1 - \beta_2}} \left(\ln\left(1 + \frac{(1 + q_G)R)^2}{\epsilon(1 - \beta_2)}\right) - T \ln(\beta_2) \right)$$

1369 The leading fraction's order is determined by its denominator, $\tilde{T}\sqrt{1 - \beta_2}$. With $\tilde{T} = \Theta(T)$ and
 1370 $1 - \beta_2 = \Theta(1/T)$, we have $\sqrt{1 - \beta_2} = \Theta(T^{-1/2})$. Thus, the fraction scales as $\Theta(\frac{1}{T \cdot T^{-1/2}}) =$
 1371 $\Theta(T^{-1/2})$. The term in the parenthesis scales as $\ln(1 + \Theta(T)) - \Theta(1) = \Theta(\ln T)$. The overall
 1372 order is:
 1373

$$1374 T_2 = \Theta\left(\frac{1}{\tilde{T}\sqrt{1 - \beta_2}}\right) \cdot \Theta(\ln T) = \Theta\left(T^{-1/2}\right) \cdot \Theta(\ln T) = \Theta\left(\frac{\ln T}{\sqrt{T}}\right).$$

1377 **Term 3 (Second Logarithmic Term):** This term is $T_3 = \frac{E}{\tilde{T}} (\ln(\dots) - T \ln(\dots))$. First, we determine
 1378 the asymptotic order of E , which is defined as:
 1379

$$1380 E = \frac{d\eta L(1 + q_G)R(1 - \beta_1)^2}{(1 - \beta_1(1 + q_M))(1 - \frac{\beta_1(1 + q_M)}{\beta_2(1 - q_V)})(1 - \beta_2)} + \frac{2d\eta^2 L^2 \beta_1(1 - \beta_1)}{(1 - \beta_1(1 + q_M))(1 - \frac{\beta_1(1 + q_M)}{\beta_2(1 - q_V)})(1 - \beta_2)^{\frac{3}{2}}}.$$

1383 For the first part of E , the numerator scales as $\eta = \Theta(T^{-1/2})$ and the denominator is dominated
 1384 by $(1 - \beta_2) = \Theta(T^{-1})$. This part is $\Theta(T^{-1/2})/\Theta(T^{-1}) = \Theta(T^{1/2})$. For the second part, the
 1385 numerator scales as $\eta^2 = \Theta(T^{-1})$ and the denominator is dominated by $(1 - \beta_2)^{3/2} = \Theta(T^{-3/2})$.
 1386 This part is $\Theta(T^{-1})/\Theta(T^{-3/2}) = \Theta(T^{1/2})$. Thus, $E = \Theta(T^{1/2})$. The logarithmic part scales as
 1387 $\Theta(\ln T)$, so the entire term scales as:
 1388

$$1389 T_3 = \Theta\left(\frac{E}{\tilde{T}}\right) \cdot \Theta(\ln T) = \Theta\left(\frac{T^{1/2}}{T}\right) \cdot \Theta(\ln T) = \Theta\left(\frac{\ln T}{\sqrt{T}}\right).$$

1391 **Term 4 (Moment Quantization Error):** We rewrite this term as:
 1392

$$1393 T_4 = \frac{2(1 + q_G)dR^2T(1 - \beta_1)}{\tilde{T}\sqrt{1 - \beta_2}} Q, \quad (\text{A.44})$$

$$1396 \text{where } Q = q_M \cdot \frac{\sqrt{r'(1+r')}}{(1+q_M)(1-r')^{3/2}} + \frac{1}{\sqrt{1 - \frac{\beta_1^2}{\beta_2(1-q_V)}}} - \frac{1}{T} \frac{1}{\sqrt{1 - \frac{\beta_1^2}{\beta_2(1-q_V)}}} \left(\frac{1}{q_V} (1 - (1 - q_V)^T) \right).$$

1399 Our goal is to show that $T_4 = \mathcal{O}(T^{-1/2})$.
 1400

1401 First, the pre-factor has an asymptotic order of:
 1402

$$1403 \frac{2(1 + q_G)dR^2T(1 - \beta_1)}{T\sqrt{1 - \beta_2}} = \Theta\left(\frac{T}{T \cdot T^{-1/2}}\right) = \Theta(T^{1/2}).$$

The core of the analysis thus lies in determining the order of Q . We can rewrite Q by combining its second and third components:

$$Q = q_M \cdot \frac{\sqrt{r'(1+r')}}{(1+q_M)(1-r')^{3/2}} + \frac{1}{\sqrt{1 - \frac{\beta_1^2}{\beta_2(1-q_V)}}} \left[1 - \frac{1}{T} \left(\frac{1-q_V}{q_V} (1 - (1-q_V)^T) \right) \right].$$

The first part of Q is clearly $\mathcal{O}(q_M) = \mathcal{O}(T^{-1})$. The common factor in the second part, $\frac{1}{\sqrt{1-\dots}}$, converges to a constant as $T \rightarrow \infty$, so it is $\mathcal{O}(1)$. The analysis therefore simplifies to finding the order of the bracketed term.

Let $x = q_V = \mathcal{O}(T^{-2})$. We perform a Taylor expansion on $(1-x)^T$:

$$(1-x)^T = 1 - Tx + \frac{T(T-1)}{2}x^2 + \mathcal{O}(T^3x^3).$$

This allows us to analyze the term inside the bracket:

$$\begin{aligned} 1 - \frac{1}{T} \left(\frac{1-x}{x} (1 - (1-x)^T) \right) &= 1 - \frac{1}{T} \frac{1-x}{x} \left(Tx - \frac{T(T-1)}{2}x^2 + \mathcal{O}(T^3x^3) \right) \\ &= 1 - \frac{1}{T} (1-x) \left(T - \frac{T(T-1)}{2}x + \mathcal{O}(T^3x^2) \right) \\ &= 1 - \frac{1}{T} \left(T - \frac{T(T-1)}{2}x - Tx + \mathcal{O}(T^3x^2) \right) \\ &= 1 - \left(1 - \frac{T(T+1)}{2T}x + \mathcal{O}(T^2x^2) \right) \\ &= \frac{T+1}{2}x - \mathcal{O}(T^2x^2). \end{aligned}$$

Substituting back $x = q_V = \mathcal{O}(T^{-2})$, the bracketed term has an order of:

$$\mathcal{O}(T \cdot q_V) = \mathcal{O}(T \cdot T^{-2}) = \mathcal{O}(T^{-1}).$$

Therefore, the entire second component of Q is $\mathcal{O}(1) \cdot \mathcal{O}(T^{-1}) = \mathcal{O}(T^{-1})$. Combining both components of Q , we find its overall order:

$$Q = \mathcal{O}(T^{-1}) + \mathcal{O}(T^{-1}) = \mathcal{O}(T^{-1}).$$

Finally, we compute the order of Term 4 by combining the pre-factor and Q :

$$T_4 = \Theta(T^{1/2}) \cdot \mathcal{O}(T^{-1}) = \mathcal{O}(T^{-1/2}).$$

Term 5 (Initial W/G Quantization Error): This term is:

$$T_5 = \frac{2(1+q_G)dT}{\tilde{T}\sqrt{\epsilon(1-\beta_2)}} (q_G R^3 + Lq_W R^2 \|\text{vec}(\mathbf{W}_0)\|_2)$$

The leading fraction scales as $\frac{T}{\tilde{T}\sqrt{1-\beta_2}} = \frac{\Theta(T)}{\Theta(T)\Theta(T^{-1/2})} = \Theta(T^{1/2})$. The parenthesis scales with its dominant term $q_G = \mathcal{O}(T^{-1})$. The total order is:

$$T_5 = \Theta(T^{1/2}) \cdot \mathcal{O}(q_G + q_W) = \Theta(T^{1/2}) \cdot (\mathcal{O}(T^{-1}) + \mathcal{O}(T^{-2})) = \mathcal{O}(T^{-1/2}).$$

Term 6 (Weight Growth Quantization Error): This term is $T_6 = \frac{(1-\beta_1)d^{\frac{3}{2}}\eta Lq_W(1+q_G)R^2T^2}{\tilde{T}\sqrt{\epsilon(1-\beta_2)}\sqrt{1-\frac{\beta_1^2(1+q_M)^2}{\beta_2(1-q_V)}}}$.

First, we analyze $\sqrt{\frac{1}{1-\frac{\beta_1^2(1+q_M)^2}{\beta_2(1-q_V)}}}$. As $T \rightarrow \infty$, the denominator converges to the constant $1 - \beta_1^2$, so its contribution is $\mathcal{O}(1)$. The term's order is determined by the scaling of its other components: $\eta = \Theta(T^{-1/2})$, $q_W = \mathcal{O}(T^{-2})$, $\tilde{T} = \Theta(T)$, and $(1 - \beta_2) = \Theta(T^{-1})$. The total order is:

$$T_6 = \Theta \left(\frac{\eta \cdot q_W \cdot T^2}{\tilde{T} \cdot (1 - \beta_2)} \right) = \Theta \left(\frac{T^{-1/2} \cdot T^{-2} \cdot T^2}{T \cdot T^{-1}} \right) = \Theta(T^{-1/2}).$$

1458 **Conclusion.** By comparing the asymptotic orders of all terms, we identify those that converge to
 1459 zero at the slowest rate, as they will dominate the overall convergence bound. The orders are:
 1460

1461 • Term 1, 4, 5, 6: $\mathcal{O}(T^{-1/2})$ or $\Theta(T^{-1/2})$.
 1462 • Term 2, 3: $\Theta(T^{-1/2} \ln T)$.
 1463

1464 The dominant terms are the second and third, which are of order $\Theta(T^{-1/2} \ln T)$. These terms form
 1465 the bottleneck that determines the overall convergence rate. Thus, under the specified parameter
 1466 schedule, the expected squared gradient norm converges to zero at the following rate:
 1467

1468
$$\mathbb{E} [\|\nabla F(\mathbf{w}_\tau)\|_2^2] = \Theta\left(\frac{\ln T}{\sqrt{T}}\right) = \tilde{\mathcal{O}}\left(\frac{1}{\sqrt{T}}\right).$$

 1469

1470 This matches the known convergence rate for full-precision Adam.
 1471

1472 Furthermore, we derive the convergence rate for the expected gradient norm, $\mathbb{E} [\|\nabla F(\mathbf{w}_\tau)\|_2]$, from
 1473 the rate of its squared value. We use Jensen's inequality, which states that for a convex function ϕ
 1474 and a random variable X , $\phi(\mathbb{E}[X]) \leq \mathbb{E}[\phi(X)]$.

1475 Let the random variable be $X = \|\nabla F(\mathbf{w}_\tau)\|_2$ and the convex function be $\phi(x) = x^2$. Applying
 1476 Jensen's inequality yields:

1477
$$(\mathbb{E} [\|\nabla F(\mathbf{w}_\tau)\|_2])^2 \leq \mathbb{E} [\|\nabla F(\mathbf{w}_\tau)\|_2^2].$$

 1478

1479 By taking the square root of both sides, we obtain a bound on the expected norm:
 1480

1481
$$\mathbb{E} [\|\nabla F(\mathbf{w}_\tau)\|_2] \leq \sqrt{\mathbb{E} [\|\nabla F(\mathbf{w}_\tau)\|_2^2]}.$$

 1482

1483 Substituting our previously derived convergence rate:

1484
$$\begin{aligned} \mathbb{E} [\|\nabla F(\mathbf{w}_\tau)\|_2] &\leq \sqrt{\tilde{\mathcal{O}}\left(\frac{1}{\sqrt{T}}\right)} \\ 1485 &= \tilde{\mathcal{O}}\left(\sqrt{T^{-1/2}}\right) \\ 1486 &= \tilde{\mathcal{O}}\left(T^{-1/4}\right). \end{aligned}$$

 1487
 1488
 1489
 1490

1491 Thus, the expected gradient norm converges to zero at a rate of $\tilde{\mathcal{O}}(T^{-1/4})$. This finalizes the proof
 1492 of the theorem.
 1493

1494 A.3 PROOF OF LEMMA A.2

1495 **Lemma A.2** (The value range of $v_{t,i}$ and the upper bound of $|\frac{1}{\sqrt{\epsilon+v_{t,i}}}-\frac{1}{\sqrt{\epsilon+v'_{t,i}}}|$). Let $LB_{t,i} =$
 1496 $\sum_{k=0}^t \beta_2^{t-k} (1-q_V)^{t-k} (\nabla_i f_k(\mathbf{w}_{k-1}) + \delta_{k,i})^2$ and $UB_{t,i} = \sum_{k=0}^t \beta_2^{t-k} (1+q_V)^{t-k} (\nabla_i f_k(\mathbf{w}_{k-1}) +$
 1497 $\delta_{k,i})^2$. We have:

1498
$$\sum_{k=0}^t \beta_2^{t-k} (1-q_V)^{t-k} (\nabla_i f_k(\mathbf{w}_{k-1}) + \delta_{k,i})^2 \leq v_{t,i} \leq \sum_{k=0}^t \beta_2^{t-k} (1+q_V)^{t-k} (\nabla_i f_k(\mathbf{w}_{k-1}) + \delta_{k,i})^2$$

 1499
 1500
 1501 (A.45)

1502
$$\left| \frac{1}{\sqrt{\epsilon+v_{t,i}}} - \frac{1}{\sqrt{\epsilon+v'_{t,i}}} \right| \leq \max \left\{ \frac{1}{\sqrt{\epsilon+LB_{t,i}}} - \frac{1}{\sqrt{\epsilon+v'_{t,i}}}, \frac{1}{\sqrt{\epsilon+v'_{t,i}}} - \frac{1}{\sqrt{\epsilon+UB_{t,i}}} \right\}$$

 1503
 1504
 1505
 1506
 1507
 1508
 1509
 1510
 1511

1512 *Proof.* The proof consists of two parts.

1513 **Part 1: Bounding $v_{t,i}$**

The update rule for the second moment estimate is $v_{t,i} = \beta_2(v_{t-1,i} + \theta_{t-1,i}) + (\nabla_i f_t(\mathbf{w}_{t-1}) + \delta_{t,i})^2$. The quantization noise is assumed to be a relative error, bounded by $|\theta_{t-1,i}| \leq q_V |v_{t-1,i}|$. This implies that $(1 - q_V)v_{t-1,i} \leq v_{t-1,i} + \theta_{t-1,i} \leq (1 + q_V)v_{t-1,i}$.

Applying this to the update rule, we can establish the lower bound by recursively unrolling the inequality:

$$\begin{aligned} v_{t,i} &\geq \beta_2(1 - q_V)v_{t-1,i} + (\nabla_i f_t(\mathbf{w}_{t-1}) + \delta_{t,i})^2 \\ &\geq \beta_2(1 - q_V)[\beta_2(1 - q_V)v_{t-2,i} + (\nabla_i f_{t-1}(\mathbf{w}_{t-2}) + \delta_{t-1,i})^2] + (\nabla_i f_t(\mathbf{w}_{t-1}) + \delta_{t,i})^2 \\ &= \dots \\ &= \sum_{k=0}^t \beta_2^{t-k}(1 - q_V)^{t-k}(\nabla_i f_k(\mathbf{w}_{k-1}) + \delta_{k,i})^2 \end{aligned} \quad (\text{A.47})$$

Similarly, we can establish the upper bound:

$$\begin{aligned} v_{t,i} &\leq \beta_2(1 + q_V)v_{t-1,i} + (\nabla_i f_t(\mathbf{w}_{t-1}) + \delta_{t,i})^2 \\ &= \sum_{k=0}^t \beta_2^{t-k}(1 + q_V)^{t-k}(\nabla_i f_k(\mathbf{w}_{k-1}) + \delta_{k,i})^2 \end{aligned} \quad (\text{A.48})$$

This completes the proof of the first statement in the lemma.

Part 2: Bounding the difference of the inverse square roots

Let $v'_{t,i}$ be the idealized second moment estimate, updated without the quantization noise θ . Its explicit form is:

$$v'_{t,i} = \sum_{k=0}^t \beta_2^{t-k}(\nabla_i f_k(\mathbf{w}_{k-1}) + \delta_{k,i})^2 \quad (\text{A.49})$$

From Part 1, we know that $v_{t,i}$ is in the interval $[LB_{t,i}, UB_{t,i}]$, where $LB_{t,i}$ and $UB_{t,i}$ are the bounds established.

Now, we compare $v'_{t,i}$ with these bounds. Since $0 < \beta_2 < 1$ and we assume $0 < q_V < 1$, we have $\beta_2(1 - q_V) < \beta_2 < \beta_2(1 + q_V)$. This implies a term-by-term inequality, leading to:

$$LB_{t,i} < v'_{t,i} < UB_{t,i} \quad (\text{A.50})$$

Consider the function $f(y) = 1/\sqrt{\epsilon + y}$ for $y \geq 0$. This function is monotonically decreasing and convex. The value $v_{t,i}$ lies in the interval $[LB_{t,i}, UB_{t,i}]$, and $v'_{t,i}$ is a point within this interval. The maximum absolute difference $|f(v_{t,i}) - f(v'_{t,i})|$ must occur when $v_{t,i}$ is at one of the endpoints of the interval. Therefore, we can bound the difference as:

$$\left| \frac{1}{\sqrt{\epsilon + v_{t,i}}} - \frac{1}{\sqrt{\epsilon + v'_{t,i}}} \right| \leq \max \left\{ \left| \frac{1}{\sqrt{\epsilon + LB_{t,i}}} - \frac{1}{\sqrt{\epsilon + v'_{t,i}}} \right|, \left| \frac{1}{\sqrt{\epsilon + UB_{t,i}}} - \frac{1}{\sqrt{\epsilon + v'_{t,i}}} \right| \right\} \quad (\text{A.51})$$

Since $LB_{t,i} < v'_{t,i} < UB_{t,i}$ and the function is decreasing, we have $1/\sqrt{\epsilon + UB_{t,i}} < 1/\sqrt{\epsilon + v'_{t,i}} < 1/\sqrt{\epsilon + LB_{t,i}}$. We can therefore remove the absolute value signs:

$$\left| \frac{1}{\sqrt{\epsilon + v_{t,i}}} - \frac{1}{\sqrt{\epsilon + v'_{t,i}}} \right| \leq \max \left\{ \frac{1}{\sqrt{\epsilon + LB_{t,i}}} - \frac{1}{\sqrt{\epsilon + v'_{t,i}}}, \frac{1}{\sqrt{\epsilon + v'_{t,i}}} - \frac{1}{\sqrt{\epsilon + UB_{t,i}}} \right\} \quad (\text{A.52})$$

This completes the proof of the second statement. \square

1566 A.4 PROOF OF LEMMA A.3
15671568 **Lemma A.3** (Bound on Discrete Error). Given two discrete-time systems defined for $t \geq 1$:1569
1570 • System A: $a_t = k(a_{t-1} + c_{t-1}) + d_t$
1571 • System B: $b_t = kb_{t-1} + d_t$
15721573 where the perturbation term c_t is bounded by $|c_t| \leq q|a_t|$ for all t , and the constants k, q satisfy
1574 $0 < k < 1$ and $q < k$.1575 Under zero initial conditions, where $a_0 = b_0 = 0$, the absolute error between the states of the two
1576 systems is bounded by:

1577
1578
$$|a_t - b_t| \leq \sum_{j=1}^{t-1} [(k(1+q))^{t-j} - k^{t-j}] |d_j| \quad (\text{A.53})$$

1579
1580

1581 *Proof.* First, define the error as $e_t = a_t - b_t$. Subtracting the two system equations yields the error
1582 recurrence relation:

1583
$$e_t = ke_{t-1} + kc_{t-1} \quad (\text{A.54})$$

1584

1585 The explicit solution to this recurrence is $e_t = k^t e_0 + \sum_{j=0}^{t-1} k^{t-j} c_j$. Under the zero initial condition
1586 $a_0 = b_0 = 0$, this simplifies to:

1587
1588
$$e_t = \sum_{j=0}^{t-1} k^{t-j} c_j \quad (\text{A.55})$$

1589

1590 Taking the absolute value and applying the given condition $|c_j| \leq q|a_j|$, we have:

1591
1592
$$|e_t| \leq \sum_{j=0}^{t-1} k^{t-j} |c_j| \leq q \sum_{j=0}^{t-1} k^{t-j} |a_j| \quad (\text{A.56})$$

1593

1594 Since $a_0 = 0$, the sum starts from $j = 1$. The state $|a_j|$ can be bounded from its own recurrence
1595 $|a_t| \leq k(1+q)|a_{t-1}| + |d_t|$, which for $a_0 = 0$ unrolls to:

1596
1597
$$|a_j| \leq \sum_{i=1}^j (k(1+q))^{j-i} |d_i| \quad (\text{A.57})$$

1598

1599 Substituting the bound for $|a_j|$ into the inequality for $|e_t|$ gives a double summation:

1600
1601
$$|e_t| \leq q \sum_{j=1}^{t-1} k^{t-j} \left(\sum_{i=1}^j (k(1+q))^{j-i} |d_i| \right) \quad (\text{A.58})$$

1602
1603

1604 By swapping the order of summation and evaluating the inner geometric series, we obtain the final
1605 result:

1606
1607
$$|a_t - b_t| \leq \sum_{j=1}^{t-1} [(k(1+q))^{t-j} - k^{t-j}] |d_j| \quad (\text{A.59})$$

1608
1609 \square

1610 A.5 PROOF OF LEMMA A.4
16111612 **Lemma A.4** (Finite Geometric Series Ratio Bounded by Infinite Sum). Let $(g_k)_{k=0}^t$ be a sequence
1613 of scalars for any finite $t \in \mathbb{N}$. Let the weights be terms of two geometric series, $A_k = a^k$ and
1614 $B_k = b^k$, where $a, b \in (0, 1)$ are the base ratios.1615 If the condition $a^2 < b$ holds, then the ratio of the weighted sum is bounded by a constant derived
1616 from the corresponding infinite series:

1617
1618
$$\frac{\sum_{k=0}^t a^k |g_k|}{\sqrt{\sum_{k=0}^t b^k g_k^2}} \leq \sqrt{\frac{1}{1 - a^2/b}} \quad (\text{A.60})$$

1619

1620 *Proof.* Let the numerator be $N_t = \sum_{k=0}^t a^k |g_k|$ and the denominator be $D_t = \sqrt{\sum_{k=0}^t b^k g_k^2}$.
 1621

1622 We rewrite the numerator as:
 1623

$$1624 N_t = \sum_{k=0}^t \left(\frac{a^k}{\sqrt{b^k}} \right) \cdot \left(\sqrt{b^k} |g_k| \right) \quad (A.61)$$

1626 Applying the Cauchy-Schwarz inequality to these finite sums, we get:
 1627

$$\begin{aligned} 1628 N_t^2 &\leq \left(\sum_{k=0}^t \left(\frac{a^k}{\sqrt{b^k}} \right)^2 \right) \cdot \left(\sum_{k=0}^t \left(\sqrt{b^k} |g_k| \right)^2 \right) \\ 1629 &= \left(\sum_{k=0}^t \frac{a^{2k}}{b^k} \right) \cdot \left(\sum_{k=0}^t b^k g_k^2 \right) \\ 1630 &= \left(\sum_{k=0}^t \left(\frac{a^2}{b} \right)^k \right) \cdot D_t^2 \end{aligned} \quad (A.62)$$

1637 The first term is a finite geometric series. Since the condition $a^2 < b$ implies that the ratio $r = a^2/b$
 1638 is positive and less than 1, all terms in the series are positive. Therefore, the finite sum is always less
 1639 than or equal to the sum of the infinite series:

$$1640 \sum_{k=0}^t \left(\frac{a^2}{b} \right)^k \leq \sum_{k=0}^{\infty} \left(\frac{a^2}{b} \right)^k = \frac{1}{1 - a^2/b} \quad (A.63)$$

1643 Substituting this upper bound back into the inequality for N_t^2 , we have:
 1644

$$1645 N_t^2 \leq \left(\frac{1}{1 - a^2/b} \right) \cdot D_t^2 \quad (A.64)$$

1647 Taking the square root of both sides gives:
 1648

$$1649 N_t \leq \sqrt{\frac{1}{1 - a^2/b}} \cdot D_t \quad (A.65)$$

1652 Finally, dividing by D_t yields the desired result for any finite t :
 1653

$$1654 \frac{N_t}{D_t} = \frac{\sum_{k=0}^t a^k |g_k|}{\sqrt{\sum_{k=0}^t b^k g_k^2}} \leq \sqrt{\frac{1}{1 - a^2/b}} \quad (A.66)$$

1657 \square

1659 A.6 PROOF OF LEMMA A.5

1660 **Lemma A.5** (Bound on the Quantized Momentum Error Ratio). Let $(g_k)_{k=0}^t$ be a sequence of
 1661 scalars. Let the weights be $A_k = \beta_1^k ((1 + q_M)^k - 1)$ and $B_k = (\beta_2 (1 - q_V))^k$. If the condition
 1662 $\beta_1^2 (1 + q_M)^2 < \beta_2 (1 - q_V)$ holds, then the ratio of the weighted sum is bounded by:
 1663

$$1664 \frac{\sum_{k=0}^t A_k |g_k|}{\sqrt{\sum_{k=0}^t B_k g_k^2}} \leq q_M \cdot \frac{\sqrt{r'(1+r')}}{(1+q_M)(1-r')^{3/2}}$$

1667 where $r' = \frac{\beta_1^2 (1+q_M)^2}{\beta_2 (1-q_V)}$.
 1668

1670 *Proof.* Following the proof of Lemma A.4, we apply the Cauchy-Schwarz inequality to get:
 1671

$$1672 \left(\sum_{k=0}^t A_k |g_k| \right)^2 \leq \left(\sum_{k=0}^t \frac{A_k^2}{B_k} \right) \cdot \left(\sum_{k=0}^t B_k g_k^2 \right). \quad (A.67)$$

1674 This implies that the ratio is bounded by the square root of the first term on the right-hand side. We
 1675 now focus on bounding the term $\sum_{k=0}^t \frac{A_k^2}{B_k}$. First, we express the ratio $\frac{A_k^2}{B_k}$ as:
 1676

$$\begin{aligned} \frac{A_k^2}{B_k} &= \frac{(\beta_1^k((1+q_M)^k - 1))^2}{(\beta_2(1-q_V))^k} \\ &= \left(\frac{\beta_1^2}{\beta_2(1-q_V)} \right)^k ((1+q_M)^k - 1)^2. \end{aligned} \quad (\text{A.68})$$

1682 To bound the term $((1+q_M)^k - 1)^2$, we first establish an inequality for $(1+q_M)^k - 1$ using the
 1683 Mean Value Theorem. Let $f(x) = x^k$. For $q_M > 0$, by the Mean Value Theorem, there exists a
 1684 $c \in (1, 1+q_M)$ such that:
 1685

$$\frac{f(1+q_M) - f(1)}{(1+q_M) - 1} = f'(c) \implies (1+q_M)^k - 1 = q_M \cdot (kc^{k-1}). \quad (\text{A.69})$$

1688 Since $c < 1+q_M$, and for $k \geq 1$, we have $c^{k-1} \leq (1+q_M)^{k-1}$. This leads to the inequality:
 1689

$$(1+q_M)^k - 1 \leq k \cdot q_M \cdot (1+q_M)^{k-1}. \quad (\text{A.70})$$

1690 Squaring both sides of (A.70) gives:
 1691

$$\begin{aligned} ((1+q_M)^k - 1)^2 &\leq k^2 q_M^2 (1+q_M)^{2(k-1)} \\ &= \frac{k^2 q_M^2}{(1+q_M)^2} (1+q_M)^{2k}. \end{aligned} \quad (\text{A.71})$$

1692 Substituting this back into (A.68), and using the definition $r' = \frac{\beta_1^2(1+q_M)^2}{\beta_2(1-q_V)}$, we get:
 1693

$$\begin{aligned} \frac{A_k^2}{B_k} &\leq \left(\frac{\beta_1^2}{\beta_2(1-q_V)} \right)^k \frac{k^2 q_M^2}{(1+q_M)^2} (1+q_M)^{2k} \\ &= \frac{q_M^2}{(1+q_M)^2} k^2 \left(\frac{\beta_1^2(1+q_M)^2}{\beta_2(1-q_V)} \right)^k \\ &= \frac{q_M^2}{(1+q_M)^2} k^2 (r')^k. \end{aligned} \quad (\text{A.72})$$

1707 Now we sum this term. The condition $r' < 1$ ensures the convergence of the infinite series. We first
 1708 derive the closed-form expression for $\sum_{k=0}^{\infty} k^2 x^k$ for $|x| < 1$. We start with the geometric series:
 1709

$$\sum_{k=0}^{\infty} x^k = \frac{1}{1-x}. \quad (\text{A.73})$$

1712 Differentiating with respect to x and multiplying by x gives:
 1713

$$\sum_{k=0}^{\infty} kx^k = x \frac{d}{dx} \left(\frac{1}{1-x} \right) = \frac{x}{(1-x)^2}. \quad (\text{A.74})$$

1717 Differentiating one more time and multiplying by x yields:
 1718

$$\sum_{k=0}^{\infty} k^2 x^k = x \frac{d}{dx} \left(\frac{x}{(1-x)^2} \right) = x \frac{1(1-x)^2 - x(2(1-x)(-1))}{(1-x)^4} = \frac{x(1+x)}{(1-x)^3}. \quad (\text{A.75})$$

1721 Using this result with $x = r'$, we can bound the sum $\sum_{k=0}^t \frac{A_k^2}{B_k}$ by extending it to an infinite series:
 1722

$$\begin{aligned} \sum_{k=0}^t \frac{A_k^2}{B_k} &\leq \sum_{k=0}^{\infty} \frac{A_k^2}{B_k} \\ &\leq \sum_{k=0}^{\infty} \frac{q_M^2}{(1+q_M)^2} k^2 (r')^k \end{aligned}$$

$$\begin{aligned}
&= \frac{q_M^2}{(1+q_M)^2} \sum_{k=0}^{\infty} k^2 (r')^k \\
&= \frac{q_M^2}{(1+q_M)^2} \frac{r'(1+r')}{(1-r')^3}.
\end{aligned} \tag{A.76}$$

Finally, taking the square root of (A.76) and substituting it back into the result from the Cauchy-Schwarz inequality (A.67) gives the desired bound:

$$\sqrt{\sum_{k=0}^t A_k |g_k|} \leq \sqrt{\sum_{k=0}^t \frac{A_k^2}{B_k}} \leq \sqrt{\frac{q_M^2}{(1+q_M)^2} \frac{r'(1+r')}{(1-r')^3}} = q_M \cdot \frac{\sqrt{r'(1+r')}}{(1+q_M)(1-r')^{3/2}}. \tag{A.77}$$

□

A.7 PROOF OF LEMMA A.6

Lemma A.6 (Bound on the Quantized Gradient Estimator). Let the stochastic gradient be bounded in infinity norm almost surely by $\|\nabla f_t(\mathbf{w}; \gamma)\|_\infty \leq R - \sqrt{\epsilon}$ for any parameters \mathbf{w} . Let the gradient quantization operator satisfy the relative error model $|Q(z) - z| \leq q_G |z|$ for any scalar z . The quantized gradient estimator $\hat{\mathbf{g}}_t$ is defined component-wise for $i \in [d]$ as:

$$\hat{g}_{t,i} = \frac{1}{B} \sum_{j=1}^B [\nabla^Q f(\mathbf{w}_{t-1}^Q; \gamma_{t,j})]_i, \tag{A.78}$$

where we use $\nabla^Q f(\cdot)$ as shorthand for $Q(\nabla f(\cdot))$ and $[\cdot]_i$ to denote the i -th component. Then, the infinity norm of the estimator is bounded almost surely:

$$\|\hat{\mathbf{g}}_t\|_\infty \leq (1+q_G)(R - \sqrt{\epsilon}). \tag{A.79}$$

For notational simplicity in subsequent proofs, we will use the slightly looser bound $\|\hat{\mathbf{g}}_t\|_\infty \leq (1+q_G)R$.

Proof. We first bound the infinity norm of a single quantized gradient vector $\nabla^Q f(\cdot)$. For any component $i \in [d]$, we have:

$$\begin{aligned}
\left| \nabla_i^Q f(\mathbf{w}_{t-1}^Q; \gamma_{t,j}) \right| &= \left| \nabla_i f(\mathbf{w}_{t-1}^Q; \gamma_{t,j}) + \left(\nabla_i^Q f(\mathbf{w}_{t-1}^Q; \gamma_{t,j}) - \nabla_i f(\mathbf{w}_{t-1}^Q; \gamma_{t,j}) \right) \right| \\
&\leq \left| \nabla_i f(\mathbf{w}_{t-1}^Q; \gamma_{t,j}) \right| + \left| \nabla_i^Q f(\mathbf{w}_{t-1}^Q; \gamma_{t,j}) - \nabla_i f(\mathbf{w}_{t-1}^Q; \gamma_{t,j}) \right| \\
&\leq \left| \nabla_i f(\mathbf{w}_{t-1}^Q; \gamma_{t,j}) \right| + q_G \left| \nabla_i f(\mathbf{w}_{t-1}^Q; \gamma_{t,j}) \right| \\
&= (1+q_G) \left| \nabla_i f(\mathbf{w}_{t-1}^Q; \gamma_{t,j}) \right|.
\end{aligned} \tag{A.80}$$

Since this holds for any component, it also holds for the component with the maximum absolute value. Therefore, by taking the maximum over $i \in [d]$, we can bound the infinity norm:

$$\begin{aligned}
\|\nabla^Q f(\mathbf{w}_{t-1}^Q; \gamma_{t,j})\|_\infty &\leq (1+q_G) \|\nabla f(\mathbf{w}_{t-1}^Q; \gamma_{t,j})\|_\infty \\
&\leq (1+q_G)(R - \sqrt{\epsilon}).
\end{aligned} \tag{A.81}$$

Finally, we apply the triangle inequality to the full estimator $\hat{\mathbf{g}}_t$, which is the average over B such vectors:

$$\begin{aligned}
\|\hat{\mathbf{g}}_t\|_\infty &= \left\| \frac{1}{B} \sum_{j=1}^B \nabla^Q f(\mathbf{w}_{t-1}^Q; \gamma_{t,j}) \right\|_\infty \\
&\leq \frac{1}{B} \sum_{j=1}^B \|\nabla^Q f(\mathbf{w}_{t-1}^Q; \gamma_{t,j})\|_\infty \\
&\leq \frac{1}{B} \sum_{j=1}^B (1+q_G)(R - \sqrt{\epsilon}) \\
&= (1+q_G)(R - \sqrt{\epsilon}).
\end{aligned} \tag{A.82}$$

This concludes the proof. □

1782 A.8 PROOF OF LEMMA A.7
1783

1784 **Lemma A.7** (Bound on the Expected Gradient Error with Biased Quantization). Under the assumptions
1785 that the infinity norm of stochastic gradient is up bounded (Assumption 4.2), the objective F is
1786 L-smooth (Assumption 4.3), and the quantization relative error model holds (Assumption 3.1), the
1787 magnitude of the conditional expectation of the total error term $\delta_{t,i}$ is bounded by:

$$1788 |\mathbb{E}_{t-1} [\delta_{t,i}]| \leq q_G R + Lq_W \|\mathbf{w}_{t-1}\|_2. \\ 1789$$

1790 *Proof.* We start from the decomposition of the conditional expectation of $\delta_{t,i}$, which we derived
1791 previously:

$$1793 \mathbb{E}_{t-1} [\delta_{t,i}] = \mathbb{E}_\gamma \left[\nabla_i^Q f(\mathbf{w}_{t-1}^Q; \gamma) - \nabla_i f(\mathbf{w}_{t-1}^Q; \gamma) \right] + \mathbb{E}_\gamma \left[\nabla_i f(\mathbf{w}_{t-1}^Q; \gamma) - \nabla_i f(\mathbf{w}_{t-1}; \gamma) \right] \\ 1794 = \underbrace{\mathbb{E}_\gamma \left[\nabla_i^Q f(\mathbf{w}_{t-1}^Q; \gamma) - \nabla_i f(\mathbf{w}_{t-1}^Q; \gamma) \right]}_{\text{Term I: Gradient Quantization Bias}} + \underbrace{\left(\nabla_i F(\mathbf{w}_{t-1}^Q) - \nabla_i F(\mathbf{w}_{t-1}) \right)}_{\text{Term II: Weight Quantization Bias}} \quad (\text{A.83}) \\ 1795 \\ 1796 \\ 1797$$

1798 Using the triangle inequality, we can bound the magnitude as:

$$1799 |\mathbb{E}_{t-1} [\delta_{t,i}]| \leq |\text{Term I}| + |\text{Term II}|. \quad (\text{A.84}) \\ 1800$$

1801 We bound each term separately.

1802 **Bounding Term I:** This term is the expected bias from the (potentially biased) gradient quantization.
1803 We first apply Jensen's inequality for absolute values, i.e., $|\mathbb{E}[X]| \leq \mathbb{E}[|X|]$:

$$1805 |\text{Term I}| = \left| \mathbb{E}_\gamma \left[\nabla_i^Q f(\mathbf{w}_{t-1}^Q; \gamma) - \nabla_i f(\mathbf{w}_{t-1}^Q; \gamma) \right] \right| \\ 1806 \leq \mathbb{E}_\gamma \left[\left| \nabla_i^Q f(\mathbf{w}_{t-1}^Q; \gamma) - \nabla_i f(\mathbf{w}_{t-1}^Q; \gamma) \right| \right]. \quad (\text{A.85}) \\ 1807 \\ 1808$$

1809 By the relative error model for gradient quantization (Assumption 3.1 with factor q_G):

$$1810 |\text{Term I}| \leq \mathbb{E}_\gamma \left[q_G \left| \nabla_i f(\mathbf{w}_{t-1}^Q; \gamma) \right| \right] \leq q_G R. \quad (\text{A.86}) \\ 1811 \\ 1812$$

1813 **Bounding Term II:** This term represents the bias from weight quantization. Using the L-smoothness
1814 of F (Assumption 4.3) and the relative error for weights (Assumption 3.1):

$$1815 |\text{Term II}| = |\nabla_i F(\mathbf{w}_{t-1}^Q) - \nabla_i F(\mathbf{w}_{t-1})| \leq \|\nabla F(\mathbf{w}_{t-1}^Q) - \nabla F(\mathbf{w}_{t-1})\|_2 \leq Lq_W \|\mathbf{w}_{t-1}\|_2. \\ 1816 \quad (\text{A.87}) \\ 1817$$

1818 **Combining the Bounds:** Summing the bounds for Term I and Term II, we arrive at the final result:
1819

$$1820 |\mathbb{E}_{t-1} [\delta_{t,i}]| \leq |\text{Term I}| + |\text{Term II}| \leq q_G R + Lq_W \|\mathbf{w}_{t-1}\|_2. \quad (\text{A.88}) \\ 1821 \\ 1822 \quad \square$$

1823 A.9 PROOF OF LEMMA A.8 (BOUND ON TERM D)
1824

1825 **Lemma A.8** (Bound on Term D). The term D, which captures the error from gradient drift as defined
1826 in (A.20), is bounded by:

$$1827 |D| \leq \frac{\eta_t^2 L^2 \sqrt{1-\beta_1}}{4(1+q_G)R} \left(\sum_{l=1}^{t-1} \|\mathbf{u}_{t-l}\|_2^2 \sum_{k=l}^{t-1} \beta_1^k \sqrt{k} \right) + \frac{(1+q_G)R}{\sqrt{1-\beta_1}} \sum_{k=0}^{t-1} \left(\frac{\beta_1}{\beta_2} \right)^k \sqrt{k+1} \|\mathbf{U}_{t-k}\|_2^2. \\ 1828 \quad (\text{A.89}) \\ 1829 \\ 1830 \\ 1831$$

1832 *Proof.* We start with the definition of Term D:
1833

$$1834 D = \sum_{i \in [d]} \sum_{k=0}^{t-1} \beta_1^k (\mathcal{G}_{t,i} - \mathcal{G}_{t-k,i}) \frac{g_{t-k,i} + \delta_{t-k,i}}{\sqrt{\epsilon + v'_{t,i}}} \\ 1835$$

To tackle this, we employ the weighted Young's inequality, which states that for any $\lambda > 0$,

$$xy \leq \frac{\lambda}{2}x^2 + \frac{1}{2\lambda}y^2 \quad (\text{A.90})$$

We apply this inequality to each product within the summation for Term D, setting

$$x = |\mathcal{G}_{t,i} - \mathcal{G}_{t-k,i}|, \quad y = \frac{|g_{t-k,i} + \delta_{t-k,i}|}{\sqrt{\epsilon + v'_{t,i}}}, \quad \text{and} \quad \lambda = \frac{\sqrt{1-\beta_1}}{2(1+q_G)R\sqrt{k+1}}.$$

This application gives us an initial bound on the magnitude of D:

$$|D| \leq \sum_{i \in [d]} \sum_{k=0}^{t-1} \beta_1^k \left(\frac{\sqrt{1-\beta_1}}{4(1+q_G)R\sqrt{k+1}} (\mathcal{G}_{t,i} - \mathcal{G}_{t-k,i})^2 + \frac{(1+q_G)R\sqrt{k+1}}{\sqrt{1-\beta_1}} \frac{(g_{t-k,i} + \delta_{t-k,i})^2}{\epsilon + v'_{t,i}} \right). \quad (\text{A.91})$$

To simplify this expression further, we must establish bounds for two of its key components.

First, we can find a lower bound for the denominator term. For any coordinate $i \in [d]$, the recursive definition of $v'_{t,i}$ implies that $\epsilon + v'_{t,i} \geq \epsilon + \beta_2^k v'_{t-k,i} \geq \beta_2^k (\epsilon + v'_{t-k,i})$. This allows us to bound the fraction as:

$$\frac{(g_{t-k,i} + \delta_{t-k,i})^2}{\epsilon + v'_{t,i}} \leq \frac{1}{\beta_2^k} U_{t-k,i}^2. \quad (\text{A.92})$$

Second, we bound the squared gradient difference using the L-smoothness of the objective function F .

$$\begin{aligned} \|\mathcal{G}_t - \mathcal{G}_{t-k}\|_2^2 &\leq L^2 \|\mathbf{w}_{t-1} - \mathbf{w}_{t-k-1}\|_2^2 = L^2 \left\| \sum_{l=1}^k \eta_{t-l} \mathbf{u}_{t-l} \right\|_2^2 \\ &\leq \eta_t^2 L^2 k \sum_{l=1}^k \|\mathbf{u}_{t-l}\|_2^2. \end{aligned} \quad (\text{A.93})$$

The final step above follows from Jensen's inequality and the fact that the step size schedule η_t is non-decreasing.

With these two intermediate results, (A.92) and (A.93), we can return to our main inequality (A.91). Substituting these bounds yields:

$$\begin{aligned} |D| &\leq \left(\sum_{k=0}^{t-1} \frac{\eta_t^2 L^2 \sqrt{1-\beta_1} \beta_1^k}{4(1+q_G)R\sqrt{k+1}} \left(k \sum_{l=1}^k \|\mathbf{u}_{t-l}\|_2^2 \right) \right) + \left(\sum_{k=0}^{t-1} \frac{(1+q_G)R\beta_1^k \sqrt{k+1}}{\sqrt{1-\beta_1} \beta_2^k} \|\mathbf{U}_{t-k}\|_2^2 \right) \\ &\leq \frac{\eta_t^2 L^2 \sqrt{1-\beta_1}}{4(1+q_G)R} \left(\sum_{k=0}^{t-1} \beta_1^k \sqrt{k} \sum_{l=1}^k \|\mathbf{u}_{t-l}\|_2^2 \right) + \frac{(1+q_G)R}{\sqrt{1-\beta_1}} \sum_{k=0}^{t-1} \left(\frac{\beta_1}{\beta_2} \right)^k \sqrt{k+1} \|\mathbf{U}_{t-k}\|_2^2. \end{aligned}$$

Finally, by rearranging the order of summation in the first term, we arrive at our desired bound:

$$|D| \leq \frac{\eta_t^2 L^2 \sqrt{1-\beta_1}}{4(1+q_G)R} \left(\sum_{l=1}^{t-1} \|\mathbf{u}_{t-l}\|_2^2 \sum_{k=l}^{t-1} \beta_1^k \sqrt{k} \right) + \frac{(1+q_G)R}{\sqrt{1-\beta_1}} \sum_{k=0}^{t-1} \left(\frac{\beta_1}{\beta_2} \right)^k \sqrt{k+1} \|\mathbf{U}_{t-k}\|_2^2. \quad (\text{A.94})$$

□

A.10 PROOF OF LEMMA A.9 (LOWER BOUND ON TERM C)

Lemma A.9 (Lower Bound on the Expectation of Term C). The expectation of term C, defined in (A.20), is lower-bounded by:

$$\mathbb{E}[C] \geq \frac{1}{2} \left(\sum_{i \in [d]} \sum_{k=0}^{t-1} \beta_1^k \mathbb{E} \left[\frac{\mathcal{G}_{t-k,i}^2}{\sqrt{\epsilon + \tilde{v}_{t,k+1,i}}} \right] \right) - \frac{2(1+q_G)R}{\sqrt{1-\beta_1}} \left(\sum_{i \in [d]} \sum_{k=0}^{t-1} \left(\frac{\beta_1}{\beta_2} \right)^k \sqrt{k+1} \mathbb{E} [\|\mathbf{U}_{t-k}\|_2^2] \right)$$

$$1890 \quad - d \sum_{k=0}^{t-1} \beta_1^k M_{t-k}. \quad (A.95)$$

$$1893 \quad \text{where } M_{t-k} = \frac{q_G R^2 + L q_W R \|\mathbf{w}_{t-k-1}\|_2}{\sqrt{\epsilon}}.$$

1895 *Proof.* We study the main term of the summation in C, i.e. for $i \in [d]$ and $k < t$:

$$1897 \quad \mathbb{E} \left[\mathcal{G}_{t-k,i} \frac{g_{t-k,i} + \delta_{t-k,i}}{\sqrt{\epsilon + v_{t,i}}} \right] = \mathbb{E} \left[\nabla_i F(\mathbf{w}_{t-k-1}) \frac{\nabla_i f_{t-k}(\mathbf{w}_{t-k-1}) + \delta_{t-k,i}}{\sqrt{\epsilon + v_{t,i}}} \right]. \quad (A.96)$$

1900 We will further drop indices in the rest of the proof, noting $\mathcal{G} = \mathcal{G}_{t-k,i}$, $g = g_{t-k,i}$, $\delta = \delta_{t-k,i}$, $\tilde{v} =$
1901 $\tilde{v}_{t,k+1,i}$ and $v = v'_{t,i}$. Finally, let us note

$$1902 \quad s^2 = \sum_{j=t-k}^t \beta_2^{t-j} (g_{j,i} + \delta_{j,i})^2 \quad \text{and} \quad r^2 = \mathbb{E}_{t-k-1} [s^2]. \quad (A.97)$$

1905 In particular we have $\tilde{v} - v = r^2 - s^2$. With our new notations, we can rewrite (A.96) as

$$1907 \quad \mathbb{E} \left[\mathcal{G} \frac{g + \delta}{\sqrt{\epsilon + v}} \right] = \mathbb{E} \left[\mathcal{G} \frac{g + \delta}{\sqrt{\epsilon + \tilde{v}}} + \mathcal{G}(g + \delta) \left(\frac{1}{\sqrt{\epsilon + v}} - \frac{1}{\sqrt{\epsilon + \tilde{v}}} \right) \right] \\ 1908 \quad = \mathbb{E} \left[\mathbb{E}_{t-k-1} \left[\mathcal{G} \frac{g + \delta}{\sqrt{\epsilon + \tilde{v}}} \right] + \mathcal{G}(g + \delta) \frac{r^2 - s^2}{\sqrt{\epsilon + v} \sqrt{\epsilon + \tilde{v}} (\sqrt{\epsilon + v} + \sqrt{\epsilon + \tilde{v}})} \right] \\ 1909 \quad = \mathbb{E} \left[\frac{\mathcal{G}^2}{\sqrt{\epsilon + \tilde{v}}} \right] + \mathbb{E} \left[\frac{\mathcal{G} \mathbb{E}_{t-k-1} [\delta]}{\sqrt{\epsilon + \tilde{v}}} \right] + \mathbb{E} \left[\underbrace{\mathcal{G}(g + \delta) \frac{r^2 - s^2}{\sqrt{\epsilon + v} \sqrt{\epsilon + \tilde{v}} (\sqrt{\epsilon + v} + \sqrt{\epsilon + \tilde{v}})}}_E \right] \\ 1910 \quad \geq \mathbb{E} \left[\frac{\mathcal{G}^2}{\sqrt{\epsilon + \tilde{v}}} \right] - \frac{q_G R^2 + L q_W R \|\mathbf{w}_{t-k-1}\|_2}{\sqrt{\epsilon}} + \mathbb{E} [E]. \quad (A.98)$$

1919 The inequality uses Lemma A.7 and the bound for $\|\nabla F(\cdot)\|_\infty$. We denote $\frac{q_G R^2 + L q_W R \|\mathbf{w}_{t-k-1}\|_2}{\sqrt{\epsilon}} \triangleq$
1920 M_{t-k} .

1921 Then we focus on E :

$$1923 \quad |E| \leq \underbrace{|\mathcal{G}(g + \delta)| \frac{r^2}{\sqrt{\epsilon + v} (\epsilon + \tilde{v})}}_{\kappa} + \underbrace{|\mathcal{G}(g + \delta)| \frac{s^2}{(\epsilon + v) \sqrt{\epsilon + \tilde{v}}}}_{\rho},$$

1927 due to the fact that $\sqrt{\epsilon + v} + \sqrt{\epsilon + \tilde{v}} \geq \max(\sqrt{\epsilon + v}, \sqrt{\epsilon + \tilde{v}})$ and $|r^2 - s^2| \leq r^2 + s^2$.

1929 Applying Young's inequality to κ with

$$1930 \quad \lambda = \frac{\sqrt{1 - \beta_1} \sqrt{\epsilon + \tilde{v}}}{2}, \quad x = \frac{|\mathcal{G}|}{\sqrt{\epsilon + \tilde{v}}}, \quad y = \frac{|g + \delta| r^2}{\sqrt{\epsilon + \tilde{v}} \sqrt{\epsilon + v}},$$

1933 we obtain

$$1934 \quad \kappa \leq \frac{\mathcal{G}^2}{4 \sqrt{\epsilon + \tilde{v}}} + \frac{1}{\sqrt{1 - \beta_1}} \frac{(g + \delta)^2 r^4}{(\epsilon + \tilde{v})^{3/2} (\epsilon + v)}.$$

1937 Given that $\epsilon + \tilde{v} \geq r^2$ and taking the conditional expectation, we can simplify as

$$1938 \quad \mathbb{E}_{t-k-1} [\kappa] \leq \frac{\mathcal{G}^2}{4 \sqrt{\epsilon + \tilde{v}}} + \frac{1}{\sqrt{1 - \beta_1}} \frac{r^2}{\sqrt{\epsilon + \tilde{v}}} \mathbb{E}_{t-k-1} \left[\frac{(g + \delta)^2}{\epsilon + v} \right]. \quad (A.99)$$

1941 Now turning to ρ , we use Young's inequality with

$$1943 \quad \lambda = \frac{\sqrt{1 - \beta_1} \sqrt{\epsilon + \tilde{v}}}{2 r^2}, \quad x = \frac{|\mathcal{G} s|}{\sqrt{\epsilon + \tilde{v}}}, \quad y = \frac{|s(g + \delta)|}{\epsilon + v},$$

1944 we obtain

$$1946 \quad \rho \leq \frac{\mathcal{G}^2}{4\sqrt{\epsilon + \tilde{v}}} \frac{s^2}{r^2} + \frac{1}{\sqrt{1 - \beta_1}} \frac{r^2}{\sqrt{\epsilon + \tilde{v}}} \frac{(g + \delta)^2 s^2}{(\epsilon + v)^2}. \quad (\text{A.100})$$

1948 Given that $\epsilon + v \geq s^2$, and $\mathbb{E}_{t-k-1} \left[\frac{s^2}{r^2} \right] = 1$, we obtain after taking the conditional expectation,

$$1951 \quad \mathbb{E}_{t-k-1} [\rho] \leq \frac{\mathcal{G}^2}{4\sqrt{\epsilon + \tilde{v}}} + \frac{1}{\sqrt{1 - \beta_1}} \frac{r^2}{\sqrt{\epsilon + \tilde{v}}} \mathbb{E}_{t-k-1} \left[\frac{(g + \delta)^2}{\epsilon + v} \right]. \quad (\text{A.101})$$

1953 Notice that in (A.100), we possibly divide by zero. It suffice to notice that if $r^2 = 0$ then $s^2 = 0$ a.s.
1954 so that $\rho = 0$ and (A.101) is still verified. Summing (A.99) and (A.101), we get

$$1956 \quad \mathbb{E}_{t-k-1} [|E|] \leq \frac{\mathcal{G}^2}{2\sqrt{\epsilon + \tilde{v}}} + \frac{2}{\sqrt{1 - \beta_1}} \frac{r^2}{\sqrt{\epsilon + \tilde{v}}} \mathbb{E}_{t-k-1} \left[\frac{(g + \delta)^2}{\epsilon + v} \right]. \quad (\text{A.102})$$

1958 Given that $r \leq \sqrt{\epsilon + \tilde{v}}$ by definition of \tilde{v} , and that $r \leq \sqrt{k+1}(1+q_G)R$, reintroducing the indices
1959 we had dropped

$$1961 \quad \mathbb{E}_{t-k-1} [|E|] \leq \frac{\mathcal{G}_{t-k,i}^2}{2\sqrt{\epsilon + \tilde{v}_{t,k+1,i}}} + \frac{2(1+q_G)R}{\sqrt{1 - \beta_1}} \sqrt{k+1} \mathbb{E}_{t-k-1} \left[\frac{(g_{t-k,i} + \delta_{t-k,i})^2}{\epsilon + v'_{t,i}} \right]. \quad (\text{A.103})$$

1964 Taking the complete expectation and using that by definition $\epsilon + v'_{t,i} \geq \epsilon + \beta_2^k v'_{t-k,i} \geq \beta_2^k (\epsilon + v'_{t-k,i})$
1965 we get

$$1967 \quad \mathbb{E} [|E|] \leq \frac{1}{2} \mathbb{E} \left[\frac{\mathcal{G}_{t-k,i}^2}{\sqrt{\epsilon + \tilde{v}_{t,k+1,i}}} \right] + \frac{2(1+q_G)R}{\sqrt{1 - \beta_1 \beta_2^k}} \sqrt{k+1} \mathbb{E} \left[\frac{(g_{t-k,i} + \delta_{t-k,i})^2}{\epsilon + v'_{t-k,i}} \right]. \quad (\text{A.104})$$

1970 Injecting (A.104) into (A.98) gives us

$$1971 \quad \sum_{i \in [d]} \sum_{k=0}^{t-1} \beta_1^k \mathbb{E} \left[\frac{\mathcal{G}_{t-k,i} g_{t-k,i} + \delta_{t-k,i}}{\sqrt{\epsilon + v_{t,i}}} \right] \\ 1972 \quad \geq \sum_{i \in [d]} \sum_{k=0}^{t-1} \beta_1^k \left(\mathbb{E} \left[\frac{\mathcal{G}_{t-k,i}^2}{\sqrt{\epsilon + \tilde{v}_{t,k+1,i}}} \right] - \mathbb{E} [|E|] - M_{t-k} \right) \quad (\text{A.105}) \\ 1973 \quad \geq \sum_{i \in [d]} \sum_{k=0}^{t-1} \beta_1^k \left(\mathbb{E} \left[\frac{\mathcal{G}_{t-k,i}^2}{\sqrt{\epsilon + \tilde{v}_{t,k+1,i}}} \right] - \left(\frac{1}{2} \mathbb{E} \left[\frac{\mathcal{G}_{t-k,i}^2}{\sqrt{\epsilon + \tilde{v}_{t,k,i}}} \right] + \frac{2(1+q_G)R\sqrt{k+1}}{\sqrt{1 - \beta_1 \beta_2^k}} \mathbb{E} \left[\frac{(g_{t-k,i} + \delta_{t-k,i})^2}{\epsilon + v'_{t-k,i}} \right] + M_{t-k} \right) \right) \\ 1974 \quad \geq \frac{1}{2} \left(\sum_{i \in [d]} \sum_{k=0}^{t-1} \beta_1^k \mathbb{E} \left[\frac{\mathcal{G}_{t-k,i}^2}{\sqrt{\epsilon + \tilde{v}_{t,k+1,i}}} \right] \right) - \frac{2(1+q_G)R}{\sqrt{1 - \beta_1}} \left(\sum_{i \in [d]} \sum_{k=0}^{t-1} \left(\frac{\beta_1}{\beta_2} \right)^k \sqrt{k+1} \mathbb{E} [|E|] \right) - d \sum_{k=0}^{t-1} \beta_1^k M_{t-k}. \quad (\text{A.106})$$

1985 This is the desired lower bound for $\mathbb{E} [C]$. □

A.11 PROOF OF LEMMA A.10

1989 **Lemma A.10** (Lemma A.2 in Défossez et al. (2022)). Assume we have $0 < \beta_1 < \beta_2 \leq 1$ and a
1990 sequence of real numbers $(a_n)_{n \in \mathbb{N}^*}$. We define for all $n \in \mathbb{N}^*$:

$$1992 \quad b_n = \sum_{j=1}^n \beta_2^{n-j} a_j^2 \quad \text{and} \quad c_n = \sum_{j=1}^n \beta_1^{n-j} a_j.$$

1994 Then for any $\epsilon > 0$, we have the following inequality:

$$1996 \quad \sum_{j=1}^n \frac{c_j^2}{\epsilon + b_j} \leq \frac{1}{(1 - \beta_1)(1 - \beta_1/\beta_2)} \left(\ln \left(1 + \frac{b_n}{\epsilon} \right) - n \ln(\beta_2) \right). \quad (\text{A.107})$$

1998
1999

Proof. First, we use Jensen's inequality on c_j^2 , noting that $\sum_{l=1}^j \beta_1^{j-l} = \frac{1-\beta_1^j}{1-\beta_1} \leq \frac{1}{1-\beta_1}$, to get:

2000
2001
2002
2003

$$c_j^2 = \left(\sum_{l=1}^j \beta_1^{j-l} a_l \right)^2 \leq \left(\sum_{l=1}^j \beta_1^{j-l} \right) \left(\sum_{l=1}^j \beta_1^{j-l} a_l^2 \right) \leq \frac{1}{1-\beta_1} \sum_{l=1}^j \beta_1^{j-l} a_l^2.$$

2004
2005

Dividing by $\epsilon + b_j$ and using the fact that for $l \leq j$, $b_j \geq \beta_2^{j-l} b_l$, which implies $\epsilon + b_j \geq \beta_2^{j-l} (\epsilon + b_l)$, we obtain:

2006
2007
2008

$$\frac{c_j^2}{\epsilon + b_j} \leq \frac{1}{1-\beta_1} \sum_{l=1}^j \beta_1^{j-l} \frac{a_l^2}{\epsilon + b_j} \leq \frac{1}{1-\beta_1} \sum_{l=1}^j \left(\frac{\beta_1}{\beta_2} \right)^{j-l} \frac{a_l^2}{\epsilon + b_l}. \quad (\text{A.108})$$

2009
2010

Now, we sum over $j \in [n]$ and swap the order of summation:

2011
2012
2013
2014
2015
2016

$$\begin{aligned} \sum_{j=1}^n \frac{c_j^2}{\epsilon + b_j} &\leq \frac{1}{1-\beta_1} \sum_{j=1}^n \sum_{l=1}^j \left(\frac{\beta_1}{\beta_2} \right)^{j-l} \frac{a_l^2}{\epsilon + b_l} = \frac{1}{1-\beta_1} \sum_{l=1}^n \frac{a_l^2}{\epsilon + b_l} \sum_{j=l}^n \left(\frac{\beta_1}{\beta_2} \right)^{j-l} \\ &\leq \frac{1}{(1-\beta_1)(1-\beta_1/\beta_2)} \sum_{l=1}^n \frac{a_l^2}{\epsilon + b_l}, \end{aligned} \quad (\text{A.109})$$

2017

where the last step uses the sum of a geometric series, since $\beta_1/\beta_2 < 1$.

2018
2019
2020
2021

The next step is to bound the final sum. Let's denote $x_l = a_l^2$. The sum is $\sum_{l=1}^n \frac{x_l}{\epsilon + b_l}$, where $b_l = \sum_{k=1}^l \beta_2^{l-k} x_k$. Note that $b_l - x_l = \beta_2 b_{l-1}$ (with $b_0 = 0$). Using the inequality $\frac{x}{y} \leq \ln(y) - \ln(y-x)$ for $0 < x < y$, we have:

2022
2023
2024
2025
2026
2027

$$\begin{aligned} \frac{x_l}{\epsilon + b_l} &\leq \ln(\epsilon + b_l) - \ln(\epsilon + b_l - x_l) \\ &= \ln(\epsilon + b_l) - \ln(\epsilon + \beta_2 b_{l-1}) \\ &= \ln\left(\frac{\epsilon + b_l}{\epsilon + b_{l-1}}\right) + \ln\left(\frac{\epsilon + b_{l-1}}{\epsilon + \beta_2 b_{l-1}}\right). \end{aligned}$$

2028
2029
2030
2031
2032

Summing from $l = 1$ to n , the first term forms a telescoping series equal to $\ln(\epsilon + b_n) - \ln(\epsilon) = \ln(1 + b_n/\epsilon)$. For the second term, since $\beta_2 \leq 1$ and $b_{l-1} \geq 0$, we have $\frac{\epsilon + \beta_2 b_{l-1}}{\epsilon + b_{l-1}} \geq \beta_2$, which implies $\ln\left(\frac{\epsilon + b_{l-1}}{\epsilon + \beta_2 b_{l-1}}\right) \leq -\ln(\beta_2)$. Thus, summing over l gives:

2033
2034
2035

$$\sum_{l=1}^n \frac{a_l^2}{\epsilon + b_l} \leq \ln\left(1 + \frac{b_n}{\epsilon}\right) - n \ln(\beta_2). \quad (\text{A.110})$$

2036
2037

This inequality is a useful result in itself, corresponding to the special case where c_j^2 is replaced by a_j^2 (or equivalently $\beta_1 \rightarrow 0$ and a_j is replaced by a_j^2).

2038
2039

Finally, substituting the bound from (A.110) into (A.109) yields the desired result. \square

2040
2041

A.12 PROOF OF LEMMA A.11

2042
2043

Lemma A.11 (Lemma A.3 in Défossez et al. (2022)). For any scalar $\rho \in (0, 1)$ and any integer $K \in \mathbb{N}$, the following bound holds for the finite geometric sum:

2044
2045
2046
2047

$$\sum_{k=0}^{K-1} \rho^k \sqrt{k+1} \leq \frac{2}{(1-\rho)^{3/2}}. \quad (\text{A.111})$$

2048
2049

Proof. Let the sum be denoted by $S_K = \sum_{k=0}^{K-1} \rho^k \sqrt{k+1}$. We analyze the term $(1-\rho)S_K$:

2050
2051

$$(1-\rho)S_K = \sum_{k=0}^{K-1} \rho^k \sqrt{k+1} - \sum_{j=1}^K \rho^j \sqrt{j}$$

$$= 1 + \sum_{k=1}^{K-1} \rho^k (\sqrt{k+1} - \sqrt{k}) - \rho^K \sqrt{K}.$$

By the concavity of the square root function, $\sqrt{k+1} - \sqrt{k} \leq \frac{1}{2\sqrt{k}}$. This implies:

$$(1 - \rho)S_K \leq 1 + \sum_{k=1}^{K-1} \frac{\rho^k}{2\sqrt{k}} \leq 1 + \int_0^\infty \frac{\rho^t}{2\sqrt{t}} dt.$$

The integral is a standard Gaussian integral form which evaluates to $\frac{\sqrt{\pi}}{2\sqrt{-\ln(\rho)}}$. Using the inequality $-\ln(\rho) \geq 1 - \rho$, we have:

$$(1 - \rho)S_K \leq 1 + \frac{\sqrt{\pi}}{2\sqrt{1 - \rho}} \leq \frac{2}{\sqrt{1 - \rho}}.$$

Dividing by $(1 - \rho)$ yields the desired result. \square

A.13 PROOF OF LEMMA A.12

Lemma A.12 (Lemma A.4 in Défossez et al. (2022)). For any scalar $\rho \in (0, 1)$ and any integer $K \in \mathbb{N}$, the following bound holds:

$$\sum_{k=0}^{K-1} \rho^k \sqrt{k}(k+1) \leq \frac{4\rho}{(1 - \rho)^{5/2}}. \quad (\text{A.112})$$

Proof. Let the sum be denoted by $S_K = \sum_{k=0}^{K-1} \rho^k \sqrt{k}(k+1)$. We proceed by analyzing $(1 - \rho)S_K$:

$$\begin{aligned} (1 - \rho)S_K &= \sum_{k=1}^{K-1} \rho^k \left[\sqrt{k}(k+1) - k\sqrt{k-1} \right] - \rho^K k\sqrt{K-1} \\ &\leq \sum_{k=1}^{K-1} \rho^k (2\sqrt{k}), \end{aligned}$$

where the inequality holds because $\sqrt{k}(k+1) - k\sqrt{k-1} \leq 2\sqrt{k}$. Re-indexing the sum gives:

$$(1 - \rho)S_K \leq 2\rho \sum_{k=1}^{K-1} \rho^{k-1} \sqrt{k} = 2\rho \sum_{j=0}^{K-2} \rho^j \sqrt{j+1}.$$

Applying the result from Lemma A.11 to the final sum, we get:

$$(1 - \rho)S_K \leq 2\rho \left(\frac{2}{(1 - \rho)^{3/2}} \right) = \frac{4\rho}{(1 - \rho)^{3/2}}.$$

Dividing both sides by $(1 - \rho)$ completes the proof. \square

A.14 PROOF OF LEMMA A.13

Lemma A.13 (Upper bound of $\sum_{t=1}^T \mathbb{E} [||\mathbf{u}_t||_2^2]$). Under the condition that $\beta_1(1 + q_M) < \beta_2(1 - q_V)$, the expected sum of squared updates over T iterations is bounded by:

$$\begin{aligned} \sum_{t=1}^T \mathbb{E} [||\mathbf{u}_t||_2^2] &\leq \frac{d}{(1 - \beta_1(1 + q_M))(1 - \frac{\beta_1(1 + q_M)}{\beta_2(1 - q_V)})} \\ &\times \left(\ln \left(1 + \frac{((1 + q_G)R)^2}{\epsilon(1 - \beta_2(1 - q_V))} \right) - T \ln(\beta_2(1 - q_V)) \right). \end{aligned} \quad (\text{A.113})$$

2106 *Proof.* The proof proceeds by first expanding the term of interest, applying bounds on the moment
 2107 estimates derived from their recurrence relations, and then leveraging Lemma A.10 to bound the
 2108 resulting sum.

2109 We begin by expanding the definition of $\|\mathbf{u}_t\|_2^2$, separating the sum over the dimension d , and taking
 2110 the expectation:
 2111

$$2112 \sum_{t=1}^T \mathbb{E} [\|\mathbf{u}_t\|_2^2] = \sum_{t=1}^T \mathbb{E} \left[\sum_{i \in [d]} \frac{m_{t,i}^2}{\epsilon + v_{t,i}} \right] = \sum_{i \in [d]} \sum_{t=1}^T \mathbb{E} \left[\frac{m_{t,i}^2}{\epsilon + v_{t,i}} \right]. \quad (\text{A.114})$$

2115 For each coordinate i , we bound the numerator $m_{t,i}^2$ from above and the denominator $\epsilon + v_{t,i}$ from
 2116 below. By unrolling the recurrence for $m_{t,i}$ and applying the triangle inequality along with the
 2117 relative error model, we get an upper bound on its magnitude:
 2118

$$2119 |m_{t,i}| \leq \sum_{k=1}^t \beta_1^{t-k} (1 + q_M)^{t-k} |\nabla_i f_k(\mathbf{w}_{k-1}) + \delta_{k,i}|. \quad (\text{A.115})$$

2120 For the denominator, Lemma A.2 provides a lower bound for $v_{t,i}$:
 2121

$$2122 v_{t,i} \geq \sum_{k=1}^t \beta_2^{t-k} (1 - q_V)^{t-k} (\nabla_i f_k(\mathbf{w}_{k-1}) + \delta_{k,i})^2. \quad (\text{A.116})$$

2123 Substituting these into the sum gives the inequality:
 2124

$$2125 \sum_{t=1}^T \mathbb{E} [\|\mathbf{u}_t\|_2^2] \leq \sum_{i \in [d]} \sum_{t=1}^T \mathbb{E} \left[\frac{\left(\sum_{k=1}^t \beta_1^{t-k} (1 + q_M)^{t-k} |\hat{g}_{k,i}| \right)^2}{\epsilon + \sum_{k=1}^t \beta_2^{t-k} (1 - q_V)^{t-k} \hat{g}_{k,i}^2} \right], \quad (\text{A.117})$$

2126 where for brevity we denote $\hat{g}_{k,i} = \nabla_i f_k(\mathbf{w}_{k-1}) + \delta_{k,i}$.
 2127

2128 The inner sum over t for each coordinate i in (A.117) perfectly matches the form required by
 2129 Lemma A.10. To apply it, we make the following substitutions into the lemma's notation:
 2130

- 2131 • Let the sequence $(a_j)_{j \in \mathbb{N}^*}$ be $a_k = |\hat{g}_{k,i}|$.
- 2132 • Let the effective decay factors be $\beta'_1 = \beta_1(1 + q_M)$ and $\beta'_2 = \beta_2(1 - q_V)$. The lemma's condition
 2133 $\beta'_1 < \beta'_2$ is satisfied by our assumption.

2134 With these substitutions, the numerator term becomes $\left(\sum_{k=1}^t (\beta'_1)^{t-k} a_k \right)^2 = c_t^2$ and the sum in the
 2135 denominator becomes $\sum_{k=1}^t (\beta'_2)^{t-k} a_k^2 = b_t$. Applying Lemma A.10 to the sum over t for a fixed i
 2136 yields:
 2137

$$2138 \sum_{t=1}^T \mathbb{E} \left[\frac{c_t^2}{\epsilon + b_t} \right] \leq \frac{1}{(1 - \beta'_1)(1 - \beta'_1/\beta'_2)} \left(\ln \left(1 + \frac{b_T}{\epsilon} \right) - T \ln(\beta'_2) \right). \quad (\text{A.118})$$

2139 The final step is to find an upper bound for b_T . By definition:
 2140

$$2141 b_T = \sum_{k=1}^T (\beta'_2)^{T-k} a_k^2 = \sum_{k=1}^T (\beta_2(1 - q_V))^{T-k} \hat{g}_{k,i}^2. \quad (\text{A.119})$$

2142 From Lemma A.6, we have a uniform bound on the quantized gradient estimator, $|\hat{g}_{k,i}| \leq (1 + q_G)R$.
 2143 Therefore:
 2144

$$2145 b_T \leq \sum_{k=1}^T (\beta_2(1 - q_V))^{T-k} ((1 + q_G)R)^2$$

$$2146 = ((1 + q_G)R)^2 \sum_{j=0}^{T-1} (\beta_2(1 - q_V))^j$$

$$2160 \quad \leq ((1 + q_G)R)^2 \frac{1}{1 - \beta_2(1 - q_V)}. \quad (A.120)$$

2163 Substituting the bound for b_T back into (A.118), and re-inserting the definitions of β'_1 and β'_2 , we
2164 obtain the bound for a single coordinate i . As this bound is identical for all d coordinates, we
2165 multiply by d to get the final result stated in (A.113). This completes the proof. \square

2166 A.15 PROOF OF LEMMA A.14 (BOUND ON TERM M)

2169 **Lemma A.14** (Bound on Term M). The term M, representing the accumulated quantization bias
2170 from (A.26), is bounded by:

$$2171 \quad M \leq \frac{\eta_T d T}{\sqrt{\epsilon}(1 - \beta_1)} (q_G R^2 + L q_W R \|\mathbf{w}_0\|_2) + \frac{\eta_T^2 d L q_W U R T^2}{2\sqrt{\epsilon}(1 - \beta_1)}, \quad (A.121)$$

2173 where $U = \sqrt{\frac{d}{1 - \frac{\beta_1^2(1+q_M)^2}{\beta_2(1-q_V)}}}$.

2176 *Proof.* First, we establish a uniform bound on the update norm $\|\mathbf{u}_t\|_2$ using Lemma A.4:

$$2179 \quad \|\mathbf{u}_t\|_2 = \sqrt{\sum_{i \in [d]} \frac{m_{t,i}^2}{\epsilon + v_{t,i}}}$$

$$2182 \quad \leq \sqrt{\sum_{i \in [d]} \frac{(\sum_{k=0}^t \beta_1^{t-k} (1 + q_M)^{t-k} |\nabla_i f_k(\mathbf{w}_{k-1}) + \delta_{k,i}|)^2}{(\sum_{k=0}^t \beta_2^{t-k} (1 - q_V)^{t-k} (\nabla_i f_k(\mathbf{w}_{k-1}) + \delta_{k,i})^2)}}$$

$$2185 \quad \leq \sqrt{\frac{d}{1 - \frac{\beta_1^2(1+q_M)^2}{\beta_2(1-q_V)}}} \triangleq U \quad (A.122)$$

2188 Now, let's recall the definition of M :

$$2190 \quad M = \eta_T d \sum_{t=1}^T \mathbb{E} \left[\sum_{k=0}^{t-1} \beta_1^k M_{t-k} \right], \quad \text{where} \quad M_{t-k} = \frac{q_G R^2 + L q_W R \|\mathbf{w}_{t-k-1}\|_2}{\sqrt{\epsilon}}.$$

2193 We can split M into two components: a constant part M_{const} and a weight-dependent part M_{weights} .

$$2194 \quad M_{\text{const}} = \frac{\eta_T d q_G R^2}{\sqrt{\epsilon}} \sum_{t=1}^T \sum_{k=0}^{t-1} \beta_1^k$$

$$2198 \quad M_{\text{weights}} = \frac{\eta_T d L q_W R}{\sqrt{\epsilon}} \sum_{t=1}^T \sum_{k=0}^{t-1} \beta_1^k \mathbb{E} [\|\mathbf{w}_{t-k-1}\|_2]$$

2200 Bounding M_{const} is straightforward. The inner sum is a geometric series bounded by $\frac{1}{1 - \beta_1}$, so the
2201 double summation is bounded by $\frac{T}{1 - \beta_1}$.

$$2203 \quad M_{\text{const}} \leq \frac{\eta_T d q_G R^2 T}{\sqrt{\epsilon}(1 - \beta_1)}. \quad (A.123)$$

2205 The main challenge is to bound M_{weights} . To do this, we first need a bound on the expected weight
2206 norm $\mathbb{E} [\|\mathbf{w}_j\|_2]$. From the update rule $\mathbf{w}_j = \mathbf{w}_{j-1} - \eta_j \mathbf{u}_j$, we can unroll the recursion:

$$2208 \quad \mathbf{w}_j = \mathbf{w}_0 - \sum_{l=1}^j \eta_l \mathbf{u}_l.$$

2211 Applying the triangle inequality and taking the expectation, we get:

$$2212 \quad \mathbb{E} [\|\mathbf{w}_j\|_2] \leq \|\mathbf{w}_0\|_2 + \mathbb{E} \left[\sum_{l=1}^j \eta_l \|\mathbf{u}_l\|_2 \right].$$

2214 Using the uniform bound $\|\mathbf{u}_l\|_2 \leq U$, we have:

$$2216 \quad \mathbb{E}[\|\mathbf{w}_j\|_2] \leq \|\mathbf{w}_0\|_2 + U \sum_{l=1}^j \eta_l \leq \|\mathbf{w}_0\|_2 + U j \eta_T.$$

2219 Now we substitute this bound back into the expression for M_{weights} . We first swap the order of
2220 summation. Let $j = t - k - 1$. For a fixed $j \in \{0, \dots, T - 1\}$, the term $\mathbb{E}[\|\mathbf{w}_j\|_2]$ appears when
2221 $k = t - j - 1$. This is valid for t from $j + 1$ to T .

$$\begin{aligned} 2223 \quad \sum_{t=1}^T \sum_{k=0}^{t-1} \beta_1^k \mathbb{E}[\|\mathbf{w}_{t-k-1}\|_2] &= \sum_{j=0}^{T-1} \mathbb{E}[\|\mathbf{w}_j\|_2] \sum_{t=j+1}^T \beta_1^{t-j-1} \\ 2224 \quad &= \sum_{j=0}^{T-1} \mathbb{E}[\|\mathbf{w}_j\|_2] \sum_{m=0}^{T-j-1} \beta_1^m \\ 2225 \quad &\leq \frac{1}{1 - \beta_1} \sum_{j=0}^{T-1} \mathbb{E}[\|\mathbf{w}_j\|_2]. \end{aligned}$$

2232 Next, we substitute the linear bound:

$$\begin{aligned} 2233 \quad \frac{1}{1 - \beta_1} \sum_{j=0}^{T-1} \mathbb{E}[\|\mathbf{w}_j\|_2] &\leq \frac{1}{1 - \beta_1} \sum_{j=0}^{T-1} (\|\mathbf{w}_0\|_2 + j \cdot U \cdot \eta_T) \\ 2234 \quad &= \frac{1}{1 - \beta_1} \left(T \|\mathbf{w}_0\|_2 + U \eta_T \sum_{j=0}^{T-1} j \right). \end{aligned}$$

2239 The sum of the first $T - 1$ integers is $\frac{(T-1)T}{2} < \frac{T^2}{2}$. This gives:

$$2242 \quad \leq \frac{1}{1 - \beta_1} \left(T \|\mathbf{w}_0\|_2 + \frac{T^2}{2} U \eta_T \right).$$

2244 Finally, we assemble the complete bound for M_{weights} :

$$2245 \quad M_{\text{weights}} \leq \frac{\eta_T d L q_W R}{\sqrt{\epsilon} (1 - \beta_1)} \left(T \|\mathbf{w}_0\|_2 + \frac{T^2}{2} U \eta_T \right).$$

2248 Combining M_{const} with M_{weights} , we get the final bound for M .

$$2249 \quad M \leq \frac{\eta_T d T}{\sqrt{\epsilon} (1 - \beta_1)} (q_G R^2 + L q_W R \|\mathbf{w}_0\|_2) + \frac{\eta_T^2 d L q_W U R T^2}{2 \sqrt{\epsilon} (1 - \beta_1)} \quad (A.124)$$

2252 \square

2255 B PROOF OF THEOREM 4.6

2257 B.1 PRELIMINARIES

2259 The momentum of the quantized Muon (Algorithm 1, 3) is defined as

$$2261 \quad \mathbf{M}_t = \beta \mathbf{M}_{t-1}^Q + (1 - \beta) \frac{1}{B} \sum_{i=1}^B \nabla^Q f(\mathbf{W}_t^Q; \boldsymbol{\xi}_{t,i}), \quad \mathbf{M}_0 = \frac{1}{B} \sum_{i=1}^B \nabla^Q f(\mathbf{W}_0^Q; \boldsymbol{\xi}_{0,i}). \quad (B.1)$$

2263 We define the following auxiliary variables for analysis:

$$2265 \quad \mathbf{C}_t = \beta \mathbf{C}_{t-1} + (1 - \beta) \nabla F(\mathbf{W}_t), \quad \mathbf{C}_0 = \nabla F(\mathbf{W}_0) \quad (B.2)$$

$$2266 \quad \mathbf{X}_t = \beta \mathbf{X}_{t-1} + (1 - \beta) \frac{1}{B} \sum_{i=1}^B \nabla f(\mathbf{W}_t; \boldsymbol{\xi}_{t,i}), \quad \mathbf{X}_0 = \frac{1}{B} \sum_{i=1}^B \nabla f(\mathbf{W}_0; \boldsymbol{\xi}_{0,i}) \quad (B.3)$$

$$2268 \quad \mathbf{Y}_t = \beta \mathbf{Y}_{t-1} + (1 - \beta) \frac{1}{B} \sum_{i=1}^B \nabla^Q f(\mathbf{W}_t; \boldsymbol{\xi}_{t,i}), \quad \mathbf{Y}_0 = \frac{1}{B} \sum_{i=1}^B \nabla^Q f(\mathbf{W}_0; \boldsymbol{\xi}_{0,i}) \quad (B.4)$$

$$2271 \quad \mathbf{Z}_t = \beta \mathbf{Z}_{t-1} + (1 - \beta) \frac{1}{B} \sum_{i=1}^B \nabla^Q f(\mathbf{W}_t^Q; \boldsymbol{\xi}_{t,i}), \quad \mathbf{Z}_0 = \frac{1}{B} \sum_{i=1}^B \nabla^Q f(\mathbf{W}_0^Q; \boldsymbol{\xi}_{0,i}). \quad (B.5)$$

2274 We also define the following relative quantization errors q_G, q_W, q_M according to Assumption 3.1
2275 and Lemma B.2, i.e., for any $t \in \{0, 1, \dots, T-1\}$ and $i \in \{1, 2, \dots, B\}$,

$$\begin{aligned} 2277 \quad & \|\nabla^Q f(\mathbf{W}_t; \boldsymbol{\xi}_{t,i}) - \nabla f(\mathbf{W}_t; \boldsymbol{\xi}_{t,i})\|_F \leq q_G \|\nabla f(\mathbf{W}_t; \boldsymbol{\xi}_{t,i})\|_F, \\ 2278 \quad & \|\nabla^Q F(\mathbf{W}_t) - \nabla F(\mathbf{W}_t)\|_F \leq q_G \|\nabla F(\mathbf{W}_t)\|_F, \\ 2279 \quad & \|\nabla^Q f(\mathbf{W}_t^Q; \boldsymbol{\xi}_{t,i}) - \nabla f(\mathbf{W}_t^Q; \boldsymbol{\xi}_{t,i})\|_F \leq q_G \|\nabla f(\mathbf{W}_t^Q; \boldsymbol{\xi}_{t,i})\|_F, \\ 2280 \quad & \|\nabla^Q F(\mathbf{W}_t^Q) - \nabla F(\mathbf{W}_t^Q)\|_F \leq q_G \|\nabla F(\mathbf{W}_t^Q)\|_F, \\ 2281 \quad & \|\mathbf{W}_t^Q - \mathbf{W}_t\|_F \leq q_W \|\mathbf{W}_t\|_F, \\ 2282 \quad & \|\mathbf{M}_t^Q - \mathbf{M}_t\|_F \leq q_M \|\mathbf{M}_t\|_F. \end{aligned} \quad (B.6)$$

B.2 PROOF OF THEOREM 4.6

2288 *Proof.* Set $\eta_t = \eta$, denote $r = \min\{m, n\}$, and according to the L -smoothness of $F(\cdot)$, we have

$$\begin{aligned} 2289 \quad & \mathbb{E}[F(\mathbf{W}_t) - F(\mathbf{W}_{t+1})] \\ 2290 \quad & \geq \mathbb{E}[\langle \nabla F(\mathbf{W}_t), \mathbf{W}_t - \mathbf{W}_{t+1} \rangle] - \frac{L}{2} \|\mathbf{W}_t - \mathbf{W}_{t+1}\|_F^2 \\ 2291 \quad & = \mathbb{E}[\eta \langle \nabla F(\mathbf{W}_t), \mathbf{U}_t \mathbf{V}_t^\top \rangle] - \frac{L}{2} \eta^2 \|\mathbf{U}_t \mathbf{V}_t^\top\|_F^2 \\ 2292 \quad & \geq \mathbb{E}[\eta \langle \nabla F(\mathbf{W}_t), \mathbf{U}_t \mathbf{V}_t^\top \rangle] - \frac{L}{2} \eta^2 r \\ 2293 \quad & = \mathbb{E}[\eta \langle \mathbf{M}_t, \mathbf{U}_t \mathbf{V}_t^\top \rangle + \eta \langle \nabla F(\mathbf{W}_t) - \mathbf{M}_t, \mathbf{U}_t \mathbf{V}_t^\top \rangle] - \frac{L}{2} \eta^2 r \\ 2294 \quad & \geq \mathbb{E}[\eta \|\mathbf{M}_t\|_* - \eta \|\nabla F(\mathbf{W}_t) - \mathbf{M}_t\|_F \cdot \|\mathbf{U}_t \mathbf{V}_t^\top\|_F] - \frac{L}{2} \eta^2 r \\ 2295 \quad & \geq \mathbb{E}[\eta \|\nabla F(\mathbf{W}_t)\|_* - \eta \|\nabla F(\mathbf{W}_t) - \mathbf{M}_t\|_* - \eta \sqrt{r} \|\nabla F(\mathbf{W}_t) - \mathbf{M}_t\|_F] - \frac{L}{2} \eta^2 r \\ 2296 \quad & \geq \mathbb{E}[\eta \|\nabla F(\mathbf{W}_t)\|_* - 2\eta \sqrt{r} \|\nabla F(\mathbf{W}_t) - \mathbf{M}_t\|_F] - \frac{L}{2} \eta^2 r. \end{aligned} \quad (B.7)$$

2306 The second inequality is due to $\|\mathbf{U}_t \mathbf{V}_t^\top\|_F^2 = \text{tr}(\mathbf{V}_t \mathbf{U}_t^\top \mathbf{U}_t \mathbf{V}_t^\top) \leq r = \min\{m, n\}$. The third
2307 inequality is due to $\mathbf{M}_t = \mathbf{U}_t \mathbf{S}_t \mathbf{V}_t^\top$ and Cauchy-Schwarz inequality. The last inequality we used
2308 the fact that $\|\mathbf{A}\|_* \leq \sqrt{r} \|\mathbf{A}\|_F$ for any $\mathbf{A} \in \mathbb{R}^{m \times n}$.

2309 Summing Eq. (B.7) over $t = 0, 1, \dots, T-1$, we get

$$\begin{aligned} 2311 \quad & \frac{1}{T} \sum_{t=0}^{T-1} \mathbb{E}[\|\nabla F(\mathbf{W}_t)\|_*] \\ 2312 \quad & \leq \frac{\mathbb{E}[F(\mathbf{W}_0) - F(\mathbf{W}_T)]}{T\eta} + \frac{2\sqrt{r}}{T} \sum_{t=0}^{T-1} \mathbb{E}[\|\nabla F(\mathbf{W}_t) - \mathbf{M}_t\|_F] + \frac{\eta L r}{2}. \end{aligned} \quad (B.8)$$

2318 Next, we focus on term $\mathbb{E}[\|\nabla F(\mathbf{W}_t) - \mathbf{M}_t\|_F]$. With auxiliary variables defined in Eq. (B.2)-(B.5),
2319 we have

$$\begin{aligned} 2320 \quad & \mathbb{E}[\|\nabla F(\mathbf{W}_t) - \mathbf{M}_t\|_F] \\ 2321 \quad & \leq \mathbb{E}[\|\nabla F(\mathbf{W}_t) - \mathbf{C}_t\|_F + \|\mathbf{C}_t - \mathbf{X}_t\|_F + \|\mathbf{X}_t - \mathbf{Y}_t\|_F + \|\mathbf{Y}_t - \mathbf{Z}_t\|_F + \|\mathbf{Z}_t - \mathbf{M}_t\|_F]. \end{aligned}$$

2322 By Lemmas B.3, B.4, B.5, B.6, and B.7, we have
 2323

$$\begin{aligned}
 & \mathbb{E}[\|\nabla F(\mathbf{W}_t) - \mathbf{M}_t\|_F] \\
 & \leq \mathbb{E}[\|\nabla F(\mathbf{W}_t) - \mathbf{C}_t\|_F + \|\mathbf{C}_t - \mathbf{X}_t\|_F + \|\mathbf{X}_t - \mathbf{Y}_t\|_F + \|\mathbf{Y}_t - \mathbf{Z}_t\|_F + \|\mathbf{Z}_t - \mathbf{M}_t\|_F] \\
 & \leq \frac{\beta L \eta \sqrt{r}}{1 - \beta} + \beta^t \frac{3\sigma}{\sqrt{B}} + \sqrt{\frac{1 - \beta}{1 + \beta}} \frac{3\sigma}{\sqrt{B}} + 3q_G(\sigma + G) + 3q_G T \eta \sqrt{r} L + q_W(1 + q_G) D L + \\
 & \quad q_W(1 + q_G) T \eta \sqrt{r} L + \frac{q_M \beta}{1 - \beta(1 + q_M)} \left(\frac{\sigma}{\sqrt{B}} + \sqrt{\frac{1 - \beta}{1 + \beta}} \cdot \frac{\sigma}{\sqrt{B}} + G + q_G(\sigma + G) + \right. \\
 & \quad \left. q_W(1 + q_G) D L + (1 + q_W)(1 + q_G) T \eta \sqrt{r} L \right).
 \end{aligned}$$

2324 Summing over $t = 0, 1, \dots, T - 1$, we get
 2325

$$\begin{aligned}
 & \frac{1}{T} \sum_{t=0}^{T-1} \mathbb{E}[\|\nabla F(\mathbf{W}_t) - \mathbf{M}_t\|_F] \\
 & \leq \frac{\beta L \eta \sqrt{r}}{1 - \beta} + \frac{3\sigma}{T(1 - \beta)\sqrt{B}} + \sqrt{\frac{1 - \beta}{1 + \beta}} \frac{3\sigma}{\sqrt{B}} + 3q_G(\sigma + G) + 3q_G T \eta \sqrt{r} L + q_W(1 + q_G) D L + \\
 & \quad q_W(1 + q_G) T \eta \sqrt{r} L + \frac{q_M \beta}{1 - \beta(1 + q_M)} \left(\frac{\sigma}{\sqrt{B}} + \sqrt{\frac{1 - \beta}{1 + \beta}} \cdot \frac{\sigma}{\sqrt{B}} + G + q_G(\sigma + G) + \right. \\
 & \quad \left. q_W(1 + q_G) D L + (1 + q_W)(1 + q_G) T \eta \sqrt{r} L \right). \tag{B.9}
 \end{aligned}$$

2326 Substitute (B.9) into (B.8), with Assumption 3.1, we have
 2327

$$\begin{aligned}
 & \frac{1}{T} \sum_{t=0}^{T-1} \mathbb{E}[\|\nabla F(\mathbf{W}_t)\|_*] \\
 & \leq \frac{\mathbb{E}[F(\mathbf{W}_0) - F(\mathbf{W}_T)]}{\eta T} + \frac{L \eta r}{2} + \frac{2\sqrt{r}}{T} \sum_{t=0}^{T-1} \mathbb{E}[\|\nabla F(\mathbf{W}_t) - \mathbf{M}_t\|_F] \\
 & \leq \frac{\mathbb{E}[F(\mathbf{W}_0) - F(\mathbf{W}_T)]}{\eta T} + \frac{L \eta r}{2} + \frac{2\beta L \eta r}{1 - \beta} + \frac{6\sigma\sqrt{r}}{T(1 - \beta)\sqrt{B}} + \sqrt{\frac{1 - \beta}{1 + \beta}} \frac{6\sigma\sqrt{r}}{\sqrt{B}} + \\
 & \quad 6q_G\sqrt{r}(\sigma + G) + 6q_G T \eta r L + 2q_W(1 + q_G) D L \sqrt{r} + 2q_W(1 + q_G) T \eta r L + \\
 & \quad \frac{2q_M \beta \sqrt{r}}{1 - \beta(1 + q_M)} \left(\frac{\sigma}{\sqrt{B}} + \sqrt{\frac{1 - \beta}{1 + \beta}} \cdot \frac{\sigma}{\sqrt{B}} + G + q_G(\sigma + G) + \right. \\
 & \quad \left. q_W(1 + q_G) D L + (1 + q_W)(1 + q_G) T \eta \sqrt{r} L \right) \\
 & \leq \frac{\mathbb{E}[F(\mathbf{W}_0) - F(\mathbf{W}_T)]}{\eta T} + \frac{L \eta r}{2} + \frac{2\beta L \eta r}{1 - \beta} + \frac{6\sigma\sqrt{r}}{T(1 - \beta)\sqrt{B}} + \sqrt{\frac{1 - \beta}{1 + \beta}} \frac{6\sigma\sqrt{r}}{\sqrt{B}} + \\
 & \quad \Theta \left(q_G + q_W + q_G T \eta + q_W T \eta + \frac{q_M \beta}{1 - \beta(1 + q_M)} \left(1 + \sqrt{1 - \beta} + q_G + q_W + T \eta \right) \right).
 \end{aligned}$$

2328 Let $F(\mathbf{W}_0) - F^* \leq \Delta$, where $\Delta > 0$ is a constant. By setting $B = 1$, $1 - \beta = \Theta(T^{-1/2})$,
 2329 $\eta = \Theta((1 - \beta)^{1/2} T^{-1/2})$, we have $T \eta = \Theta(T^{1/4})$. Then we have
 2330

$$\frac{\mathbb{E}[F(\mathbf{W}_0) - F(\mathbf{W}_T)]}{\eta T} + \frac{L \eta r}{2} + \frac{2\beta L \eta r}{1 - \beta} + \frac{6\sigma\sqrt{r}}{T(1 - \beta)\sqrt{B}} + \sqrt{\frac{1 - \beta}{1 + \beta}} \frac{6\sigma\sqrt{r}}{\sqrt{B}} = \mathcal{O}\left(\frac{1}{T^{1/4}}\right).$$

2376 Moreover, with condition $\beta(1+q_M) < 1$, suppose $1-\beta = C_\beta T^{-1/2}$, $C_\beta > 0$ is a constant. Choose
 2377 $q_M = C_M T^{-1/2}$, where $C_M < C_\beta$, $C_M > 0$ is a constant, then we have
 2378

$$2379 \beta(1+q_M) = (1 - C_\beta T^{-1/2})(1 + C_M T^{-1/2}) = 1 - (C_\beta - C_M)T^{-1/2} - C_\beta C_M T^{-1} < 1. \\ 2380$$

2381 Thus, by setting $q_G = \mathcal{O}(T^{-1/2})$, $q_W = \mathcal{O}(T^{-1/2})$, $q_M = \mathcal{O}(T^{-1/2})$, we have
 2382

$$2383 \begin{aligned} q_G + q_W + q_G T \eta + q_W T \eta + \frac{q_M \beta}{1 - \beta(1 + q_M)} & \left(1 + \sqrt{1 - \beta} + q_G + q_W + T \eta \right) \\ 2384 & = \mathcal{O}(T^{-1/2} + T^{-1/2} T^{1/4} + T^{-1/2} (1 + T^{-1/4} + T^{-1/2} + T^{1/4})) \\ 2385 & = \mathcal{O}(T^{-1/4}), \\ 2386 \\ 2387 \end{aligned}$$

2388 where we used the fact $\frac{q_M \beta}{1 - \beta(1 + q_M)} = \mathcal{O}(q_M \beta(1 + \beta(1 + q_M))) = \mathcal{O}(T^{-1/2})$, and $\beta(1 + q_M) < 1$.
 2389

2390 Combining the above results, with the fact that $\|\mathbf{A}\|_* \geq \|\mathbf{A}\|_F$ for any matrix \mathbf{A} , we complete the
 2391 proof. □
 2392

2393
 2394

2395 B.3 PROOF OF LEMMA B.1 2396

2397 **Lemma B.1** (Bound of $\|\mathbf{W}\|_F$ and $\|\nabla F(\mathbf{W})\|_F$ for Muon). Suppose Assumptions 4.3 and 4.4
 2398 hold. The iterates of Muon satisfy that for any $t \geq 0$,
 2399

$$2400 \|\mathbf{W}_t\|_F \leq D + t\eta\sqrt{r}, \quad \|\nabla F(\mathbf{W}_t)\|_F \leq G + t\eta\sqrt{r}L. \\ 2401$$

2402 *Proof of Lemma B.1.* According to the update of Muon, we have
 2403

$$2404 \begin{aligned} \|\mathbf{W}_t\|_F \\ 2405 & = \|\mathbf{W}_{t-1} - \eta \mathbf{U}_t \mathbf{V}_t^\top\|_F \\ 2406 & \leq \|\mathbf{W}_{t-1}\|_F + \eta \|\mathbf{U}_t \mathbf{V}_t^\top\|_F \\ 2407 & = \|\mathbf{W}_{t-1}\|_F + \eta \sqrt{\text{tr}(\mathbf{V}_t \mathbf{U}_t^\top \mathbf{U}_t \mathbf{V}_t^\top)} \\ 2408 & \leq \|\mathbf{W}_{t-1}\|_F + \eta\sqrt{r} \\ 2409 & \leq \|\mathbf{W}_0\|_F + t\eta\sqrt{r} \\ 2410 & \leq D + t\eta\sqrt{r}. \\ 2411 \\ 2412 \end{aligned}$$

2413 The third inequality is because \mathbf{U}_t and \mathbf{V}_t are orthogonal matrices, and the last inequality is due to
 2414 Assumption 4.4.
 2415

$$2416 \begin{aligned} \|\nabla F(\mathbf{W}_t)\|_F \\ 2417 & \leq \|\nabla F(\mathbf{W}_0)\|_F + \sum_{k=0}^{t-1} \|\nabla F(\mathbf{W}_{k+1}) - \nabla F(\mathbf{W}_k)\|_F \\ 2418 & \leq G + \sum_{k=0}^{t-1} L \|\mathbf{W}_{k+1} - \mathbf{W}_k\|_F \\ 2419 & \leq G + \sum_{k=0}^{t-1} L \eta \sqrt{r} \\ 2420 & = G + t\eta\sqrt{r}L. \\ 2421 \\ 2422 \end{aligned}$$

2423 The first inequality is due to the triangle inequality, the second inequality is due to Assumption 4.3,
 2424 and the last inequality is due to the update of Muon. □
 2425

2430 B.4 PROOF OF LEMMA B.2
24312432 **Lemma B.2.** Suppose Assumption 3.1 holds. For any matrix $\mathbf{X} \in \mathbb{R}^{m \times n}$ and its quantized version
2433 \mathbf{X}^Q , we have

2434
$$\|\mathbf{X}^Q - \mathbf{X}\|_F \leq q\|\mathbf{X}\|_F.$$

2435

2436 *Proof of Lemma B.2.* According to Assumption 3.1, we have
2437

2438
$$\begin{aligned} \|\mathbf{X}^Q - \mathbf{X}\|_F^2 &= \sum_{i=1}^m \sum_{j=1}^n |X_{ij}^Q - X_{ij}|^2 \\ 2439 &\leq \sum_{i=1}^m \sum_{j=1}^n q^2 |X_{ij}|^2 \\ 2440 &= q^2 \|\mathbf{X}\|_F^2. \end{aligned}$$

2441
2442
2443
2444

2445 Taking the square root on both sides, we complete the proof. \square
24462447 B.5 PROOF OF LEMMA B.3
24482449 **Lemma B.3.** Suppose Assumptions 4.3 and 4.4 hold. For any $t \geq 0$, we have

2450
$$\mathbb{E}[\|\nabla F(\mathbf{W}_t) - \mathbf{C}_t\|_F] \leq \frac{\beta L \eta \sqrt{r}}{1 - \beta}.$$

2451
2452

2453 *Proof of Lemma B.3.* This proof is a standard technique for bounding the bias term of momentum.
2454 We have

2455
$$\begin{aligned} \mathbb{E}[\|\nabla F(\mathbf{W}_t) - \mathbf{C}_t\|_F] &= \mathbb{E}[\|\nabla F(\mathbf{W}_t) - (\beta \mathbf{C}_{t-1} + (1 - \beta) \nabla F(\mathbf{W}_t))\|_F] \\ 2456 &= \mathbb{E}[\beta \|\nabla F(\mathbf{W}_t) - \mathbf{C}_{t-1}\|_F] \\ 2457 &\leq \mathbb{E}[\beta \|\nabla F(\mathbf{W}_{t-1}) - \mathbf{C}_{t-1}\|_F + \beta \|\nabla F(\mathbf{W}_{t-1}) - \nabla F(\mathbf{W}_t)\|_F] \\ 2458 &\leq \mathbb{E}[\beta \|\nabla F(\mathbf{W}_{t-1}) - \mathbf{C}_{t-1}\|_F + \beta L \|\mathbf{W}_{t-1} - \mathbf{W}_t\|_F] \\ 2459 &= \mathbb{E}[\beta \|\nabla F(\mathbf{W}_{t-1}) - \mathbf{C}_{t-1}\|_F + \beta L \eta \|\mathbf{U}_{t-1} \mathbf{V}_{t-1}^\top\|_F] \\ 2460 &\leq \mathbb{E}[\beta \|\nabla F(\mathbf{W}_{t-1}) - \mathbf{C}_{t-1}\|_F + \beta L \eta \sqrt{r}] \\ 2461 &\leq \beta^t \|\nabla F(\mathbf{W}_0) - \mathbf{C}_0\|_F + \sum_{i=1}^t \beta^i L \eta \sqrt{r} \\ 2462 &\leq \frac{\beta L \eta \sqrt{r}}{1 - \beta}. \end{aligned}$$

2463
2464
2465
2466
2467
2468

 \square 2469 B.6 PROOF OF LEMMA B.4
24702471 **Lemma B.4.** Suppose Assumptions 4.1 and 4.2 hold. For any $t \geq 0$, we have
2472

2473
$$\mathbb{E}[\|\mathbf{C}_t - \mathbf{X}_t\|_F] \leq \beta^t \frac{\sigma}{\sqrt{B}} + \sqrt{\frac{1 - \beta}{1 + \beta} \frac{\sigma}{\sqrt{B}}}.$$

2474
2475
2476

2477 *Proof of Lemma B.4.* Expanding \mathbf{C}_t and \mathbf{X}_t by their definitions in (B.2) and (B.3), we have
2478

2479
$$\begin{aligned} \mathbf{C}_t &= \beta^t \mathbf{C}_0 + (1 - \beta) \sum_{k=1}^t \beta^{t-k} \nabla F(\mathbf{W}_k), \\ 2480 \mathbf{X}_t &= \beta^t \mathbf{X}_0 + (1 - \beta) \sum_{k=1}^t \beta^{t-k} \frac{1}{B} \sum_{i=1}^B \nabla f(\mathbf{W}_k; \boldsymbol{\xi}_{k,i}). \end{aligned}$$

2481
2482
2483

2484

Thus, we have

2485

$$2486 \quad \mathbb{E}[\|\mathbf{C}_t - \mathbf{X}_t\|_F]$$

2487

$$2488 \quad \leq \mathbb{E}[\|\beta^t(\mathbf{C}_0 - \mathbf{X}_0)\|_F] + \mathbb{E}[(1 - \beta)\|\sum_{k=1}^t \beta^{t-k}(\nabla F(\mathbf{W}_k) - \frac{1}{B} \sum_{i=1}^B \nabla f(\mathbf{W}_k; \boldsymbol{\xi}_{k,i}))\|_F]$$

2489

$$2490 \quad \leq \beta^t \mathbb{E}[\|\mathbf{C}_0 - \mathbf{X}_0\|_F] + \sqrt{\mathbb{E}[(1 - \beta)^2 \|\sum_{k=1}^t \beta^{t-k}(\nabla F(\mathbf{W}_k) - \frac{1}{B} \sum_{i=1}^B \nabla f(\mathbf{W}_k; \boldsymbol{\xi}_{k,i}))\|_F^2]}$$

2491

$$2492 \quad = \beta^t \mathbb{E}[\|\mathbf{C}_0 - \mathbf{X}_0\|_F] + \sqrt{\mathbb{E}[(1 - \beta)^2 \sum_{k=1}^t \beta^{2(t-k)} \frac{1}{B^2} \sum_{i=1}^B \|\nabla F(\mathbf{W}_k; \boldsymbol{\xi}_{k,i}) - \nabla F(\mathbf{W}_k)\|_F^2]}$$

2493

$$2494 \quad \leq \beta^t \mathbb{E}[\|\mathbf{C}_0 - \mathbf{X}_0\|_F] + \sqrt{(1 - \beta)^2 \sum_{k=1}^t \beta^{2(t-k)} \frac{\sigma^2}{B}}$$

2495

$$2496 \quad \leq \beta^t \frac{\sigma}{\sqrt{B}} + \sqrt{\frac{1 - \beta}{1 + \beta} \frac{\sigma}{\sqrt{B}}}.$$

2497

The second inequality is due to Jensen's inequality, the first equality is due to the independence of $\boldsymbol{\xi}_{k,i}$ for different k or i , and the third inequality is due to Assumptions 4.1 and 4.2. \square

2498

2499

2500 B.7 PROOF OF LEMMA B.5

2501

Lemma B.5. Suppose Assumptions 4.1, 4.2 and 3.1 hold. For any $t \geq 0$, we have

2502

$$2503 \quad \mathbb{E}[\|\mathbf{X}_t - \mathbf{Y}_t\|_F] \leq q_G(\sigma + G + t\eta\sqrt{r}L).$$

2504

2505

Proof of Lemma B.5. By the definition of \mathbf{X}_t and \mathbf{Y}_t in (B.3) and (B.4), we have

2506

2507

2508

2509

2510

2511

2512

2513

2514

$$2515 \quad \mathbb{E}[\|\mathbf{X}_t - \mathbf{Y}_t\|_F] \leq \mathbb{E}[\beta\|\mathbf{X}_{t-1} - \mathbf{Y}_{t-1}\|_F] + (1 - \beta)\frac{1}{B} \sum_{i=1}^B \mathbb{E}[\|\nabla f(\mathbf{W}_t; \boldsymbol{\xi}_{t,i}) - \nabla^Q f(\mathbf{W}_t; \boldsymbol{\xi}_{t,i})\|_F]$$

2516

$$2517 \quad \leq \mathbb{E}[\beta\|\mathbf{X}_{t-1} - \mathbf{Y}_{t-1}\|_F] + (1 - \beta)\frac{1}{B} \sum_{i=1}^B \mathbb{E}[q_G \|\nabla f(\mathbf{W}_t; \boldsymbol{\xi}_{t,i})\|_F]$$

2518

2519

$$2520 \quad \leq \mathbb{E}[\beta\|\mathbf{X}_{t-1} - \mathbf{Y}_{t-1}\|_F] + (1 - \beta)\mathbb{E}[q_G(\sigma + \|\nabla F(\mathbf{W}_t)\|_F)]$$

2521

2522

$$2523 \quad \leq \mathbb{E}[\beta\|\mathbf{X}_{t-1} - \mathbf{Y}_{t-1}\|_F] + (1 - \beta)q_G(\sigma + G + t\eta\sqrt{r}L)$$

2524

2525

$$2526 \quad \leq \beta^t \|\mathbf{X}_0 - \mathbf{Y}_0\|_F + (1 - \beta)q_G(\sigma + G + t\eta\sqrt{r}L) \sum_{k=0}^{t-1} \beta^k$$

2527

2528

2529

2530

2531

2532

2533

2534

2535

2536

2537

The second inequality is due to Assumption 3.1, Lemma B.2 and Definition B.6. The third inequality is due to Assumption 4.2. The fourth inequality is due to Lemma B.1. \square

B.8 PROOF OF LEMMA B.6

Lemma B.6. Suppose Assumptions 4.1, 4.2, 4.3 and 3.1 hold. For any $t \geq 0$, we have

2538

2539

2540

2541

2542

2543

2544

2545

2546

2547

$$2548 \quad \mathbb{E}[\|\mathbf{Y}_t - \mathbf{Z}_t\|_F] \leq \beta^t \cdot \frac{2\sigma}{\sqrt{B}} + \sqrt{\frac{1 - \beta}{1 + \beta} \cdot \frac{2\sigma}{\sqrt{B}}} + 2q_G(\sigma + G) + 2q_G t\eta\sqrt{r}L +$$

$$\begin{aligned}
& q_W(1 + q_G)DL + q_W(1 + q_G)t\eta\sqrt{r}L, \\
& \mathbb{E}[\|\mathbf{Z}_t\|_F] \leq \frac{\sigma}{\sqrt{B}} + \sqrt{\frac{1-\beta}{1+\beta}} \cdot \frac{\sigma}{\sqrt{B}} + G + q_G(\sigma + G) + q_W(1 + q_G)DL + \\
& (1 + q_W)(1 + q_G)t\eta\sqrt{r}L.
\end{aligned}$$

Proof of Lemma B.6. By the definition of \mathbf{Y}_t and \mathbf{Z}_t in (B.4) and (B.5), we have

$$\begin{aligned}
\mathbf{Y}_t &= \beta^t \mathbf{Y}_0 + (1 - \beta) \sum_{k=1}^t \beta^{t-k} \frac{1}{B} \sum_{i=1}^B \nabla^Q f(\mathbf{W}_k; \boldsymbol{\xi}_{k,i}), \\
\mathbf{Z}_t &= \beta^t \mathbf{Z}_0 + (1 - \beta) \sum_{k=1}^t \beta^{t-k} \frac{1}{B} \sum_{i=1}^B \nabla^Q f(\mathbf{W}_k^Q; \boldsymbol{\xi}_{k,i}).
\end{aligned}$$

Thus, by the triangle inequality, we have

$$\begin{aligned}
& \mathbb{E}[\|\mathbf{Y}_t - \mathbf{Z}_t\|_F] \\
& \leq \mathbb{E}[\beta^t \|\mathbf{Y}_0 - \mathbf{Z}_0\|_F] + (1 - \beta) \mathbb{E}[\|\sum_{k=1}^t \beta^{t-k} \cdot (\frac{1}{B} \sum_{i=1}^B \nabla^Q f(\mathbf{W}_k; \boldsymbol{\xi}_{k,i}) - \nabla^Q f(\mathbf{W}_k^Q; \boldsymbol{\xi}_{k,i}))\|_F] \\
& \leq \mathbb{E}[\beta^t \|\mathbf{Y}_0 - \mathbf{Z}_0\|_F] + (1 - \beta) \underbrace{\mathbb{E}[\|\sum_{k=1}^t \beta^{t-k} \cdot (\frac{1}{B} \sum_{i=1}^B \nabla^Q f(\mathbf{W}_k; \boldsymbol{\xi}_{k,i}) - \nabla f(\mathbf{W}_k; \boldsymbol{\xi}_{k,i}))\|_F]}_A + \\
& \quad \underbrace{(1 - \beta) \mathbb{E}[\|\sum_{k=1}^t \beta^{t-k} \cdot (\frac{1}{B} \sum_{i=1}^B \nabla f(\mathbf{W}_k; \boldsymbol{\xi}_{k,i}) - \nabla F(\mathbf{W}_k))\|_F]}_C + \\
& \quad \underbrace{(1 - \beta) \mathbb{E}[\|\sum_{k=1}^t \beta^{t-k} \cdot (\nabla F(\mathbf{W}_k) - \nabla F(\mathbf{W}_k^Q))\|_F]}_H + \\
& \quad \underbrace{(1 - \beta) \mathbb{E}[\|\sum_{k=1}^t \beta^{t-k} \cdot (\nabla F(\mathbf{W}_k^Q) - \frac{1}{B} \sum_{i=1}^B \nabla f(\mathbf{W}_k^Q; \boldsymbol{\xi}_{k,i}))\|_F]}_I + \\
& \quad \underbrace{(1 - \beta) \mathbb{E}[\|\sum_{k=1}^t \beta^{t-k} \cdot (\frac{1}{B} \sum_{i=1}^B \nabla f(\mathbf{W}_k^Q; \boldsymbol{\xi}_{k,i}) - \nabla^Q f(\mathbf{W}_k^Q; \boldsymbol{\xi}_{k,i}))\|_F]}_J. \tag{B.10}
\end{aligned}$$

Next, we bound each term in (B.10) one by one.

Bound on $\beta^t \mathbb{E}[\|\mathbf{Y}_0 - \mathbf{Z}_0\|_F]$. By the definitions of \mathbf{Y}_0 and \mathbf{Z}_0 in (B.4) and (B.5), we have

$$\begin{aligned}
\mathbf{Y}_0 &= \frac{1}{B} \sum_{i=1}^B \nabla^Q f(\mathbf{W}_0; \boldsymbol{\xi}_{0,i}), \\
\mathbf{Z}_0 &= \frac{1}{B} \sum_{i=1}^B \nabla^Q f(\mathbf{W}_0^Q; \boldsymbol{\xi}_{0,i}).
\end{aligned}$$

Thus, we have

$$\beta^t \mathbb{E}[\|\mathbf{Y}_0 - \mathbf{Z}_0\|_F]$$

$$\begin{aligned}
&= \beta^t \mathbb{E} \left[\left\| \frac{1}{B} \sum_{i=1}^B \nabla^Q f(\mathbf{W}_0; \boldsymbol{\xi}_{0,i}) - \frac{1}{B} \sum_{i=1}^B \nabla^Q f(\mathbf{W}_0^Q; \boldsymbol{\xi}_{0,i}) \right\|_F \right] \\
&\leq \beta^t \frac{1}{B} \sum_{i=1}^B \mathbb{E} \left[\left\| \nabla^Q f(\mathbf{W}_0; \boldsymbol{\xi}_{0,i}) - \nabla f(\mathbf{W}_0; \boldsymbol{\xi}_{0,i}) \right\|_F \right] + \\
&\quad \beta^t \mathbb{E} \left[\left\| \frac{1}{B} \sum_{i=1}^B \nabla f(\mathbf{W}_0; \boldsymbol{\xi}_{0,i}) - \nabla F(\mathbf{W}_0) \right\|_F \right] + \\
&\quad \beta^t \mathbb{E} \left[\left\| \nabla F(\mathbf{W}_0) - \nabla F(\mathbf{W}_0^Q) \right\|_F \right] + \\
&\quad \beta^t \mathbb{E} \left[\left\| \frac{1}{B} \sum_{i=1}^B \nabla F(\mathbf{W}_0^Q) - \nabla f(\mathbf{W}_0^Q; \boldsymbol{\xi}_{0,i}) \right\|_F \right] + \\
&\quad \beta^t \frac{1}{B} \sum_{i=1}^B \mathbb{E} \left[\left\| \nabla f(\mathbf{W}_0^Q; \boldsymbol{\xi}_{0,i}) - \nabla^Q f(\mathbf{W}_0^Q; \boldsymbol{\xi}_{0,i}) \right\|_F \right] \\
&\leq \beta^t \frac{1}{B} \sum_{i=1}^B q_G \mathbb{E} \left[\left\| \nabla f(\mathbf{W}_0; \boldsymbol{\xi}_{0,i}) \right\|_F \right] + \beta^t \frac{\sigma}{\sqrt{B}} + \beta^t L q_W \mathbb{E} \left[\left\| \mathbf{W}_0 \right\|_F \right] + \beta^t \frac{\sigma}{\sqrt{B}} + \\
&\quad \beta^t \frac{1}{B} \sum_{i=1}^B q_G \mathbb{E} \left[\left\| \nabla f(\mathbf{W}_0^Q; \boldsymbol{\xi}_{0,i}) \right\|_F \right] \\
&\leq \beta^t \frac{1}{B} \sum_{i=1}^B q_G (\sigma + G) + \beta^t \frac{2\sigma}{\sqrt{B}} + \beta^t q_W D L + \beta^t \frac{1}{B} \sum_{i=1}^B q_G (\sigma + q_W D L + G) \\
&= \beta^t (2q_G(\sigma + G) + q_W D L (1 + q_G) + \frac{2\sigma}{\sqrt{B}}). \tag{B.11}
\end{aligned}$$

The first inequality is due to the triangle inequality. The second inequality we used Definition B.6 for the first and last terms, Assumption 4.1, 4.2 and Jensen's inequality for the second and fourth terms, and Assumption 4.3 and Definition B.6 for the third term. The third inequality is due to Assumption 4.2, 4.4 and Definition B.6.

Bound on A.

$$\begin{aligned}
A &= (1 - \beta) \mathbb{E} \left[\left\| \sum_{k=1}^t \beta^{t-k} \cdot \left(\frac{1}{B} \sum_{i=1}^B \nabla^Q f(\mathbf{W}_k; \boldsymbol{\xi}_{k,i}) - \nabla f(\mathbf{W}_k; \boldsymbol{\xi}_{k,i}) \right) \right\|_F \right] \\
&\leq (1 - \beta) \sum_{k=1}^t \beta^{t-k} \frac{1}{B} \sum_{i=1}^B q_G \mathbb{E} \left[\left\| \nabla f(\mathbf{W}_k; \boldsymbol{\xi}_{k,i}) \right\|_F \right] \\
&\leq (1 - \beta) \sum_{k=1}^t \beta^{t-k} \frac{1}{B} \sum_{i=1}^B q_G (\sigma + \mathbb{E} \left[\left\| \nabla F(\mathbf{W}_k) \right\|_F \right]) \\
&\leq (1 - \beta) \sum_{k=1}^t \beta^{t-k} \frac{1}{B} \sum_{i=1}^B q_G (\sigma + G + t\eta\sqrt{r}L) \\
&= (1 - \beta^t) q_G (\sigma + G + t\eta\sqrt{r}L). \tag{B.12}
\end{aligned}$$

The first inequality is due to Definition B.6 and the triangle inequality. The second inequality is due to Assumption 4.2. The third inequality is due to Lemma B.1.

Bound on C. Similar to Lemma B.4, we have

$$C = (1 - \beta) \mathbb{E} \left[\left\| \sum_{k=1}^t \beta^{t-k} \cdot \left(\frac{1}{B} \sum_{i=1}^B \nabla f(\mathbf{W}_k; \boldsymbol{\xi}_{k,i}) - \nabla F(\mathbf{W}_k) \right) \right\|_F \right]$$

$$\begin{aligned}
&\leq (1-\beta) \sqrt{\mathbb{E}\left[\left\|\sum_{k=1}^t \beta^{t-k} \cdot \left(\frac{1}{B} \sum_{i=1}^B \nabla f(\mathbf{W}_k; \boldsymbol{\xi}_{k,i}) - \nabla F(\mathbf{W}_k)\right)\right\|_F^2\right]} \\
&= (1-\beta) \sqrt{\sum_{k=1}^t \beta^{2(t-k)} \frac{1}{B^2} \sum_{i=1}^B \mathbb{E}\left[\|\nabla f(\mathbf{W}_k; \boldsymbol{\xi}_{k,i}) - \nabla F(\mathbf{W}_k)\|_F^2\right]} \\
&\leq (1-\beta) \sqrt{\sum_{k=1}^t \beta^{2(t-k)} \frac{1}{B^2} \sum_{i=1}^B \sigma^2} \\
&= (1-\beta) \sqrt{\frac{1-\beta^{2t}}{1-\beta^2} \cdot \frac{\sigma^2}{B}} \\
&\leq \sqrt{\frac{1-\beta}{1+\beta}} \cdot \frac{\sigma}{\sqrt{B}}.
\end{aligned} \tag{B.13}$$

Bound on \mathbf{H} .

$$\begin{aligned}
H &= (1-\beta) \mathbb{E}\left[\left\|\sum_{k=1}^t \beta^{t-k} \cdot (\nabla F(\mathbf{W}_k) - \nabla F(\mathbf{W}_k^Q))\right\|_F\right] \\
&\leq (1-\beta) \sum_{k=1}^t \beta^{t-k} \mathbb{E}\left[\|\nabla F(\mathbf{W}_k) - \nabla F(\mathbf{W}_k^Q)\|_F\right] \\
&\leq (1-\beta) \sum_{k=1}^t \beta^{t-k} L \mathbb{E}\left[\|\mathbf{W}_k - \mathbf{W}_k^Q\|_F\right] \\
&\leq (1-\beta) \sum_{k=1}^t \beta^{t-k} L q_W \mathbb{E}\left[\|\mathbf{W}_k\|_F\right] \\
&\leq (1-\beta) \sum_{k=1}^t \beta^{t-k} L q_W (D + t\eta\sqrt{r}) \\
&\leq (1-\beta^t) q_W L (D + t\eta\sqrt{r}).
\end{aligned} \tag{B.14}$$

The first inequality is due to the triangle inequality. The second inequality is due to Assumption 4.3. The third inequality is due to Definition B.6. The fourth inequality is due to Lemma B.1.

Bound on \mathbf{I} .

Similar to Lemma B.4, we have

$$\begin{aligned}
I &= (1-\beta) \mathbb{E}\left[\left\|\sum_{k=1}^t \beta^{t-k} \cdot \left(\nabla F(\mathbf{W}_k^Q) - \frac{1}{B} \sum_{i=1}^B \nabla f(\mathbf{W}_k^Q; \boldsymbol{\xi}_{k,i})\right)\right\|_F\right] \\
&\leq (1-\beta) \sqrt{\mathbb{E}\left[\left\|\sum_{k=1}^t \beta^{t-k} \cdot \left(\nabla F(\mathbf{W}_k^Q) - \frac{1}{B} \sum_{i=1}^B \nabla f(\mathbf{W}_k^Q; \boldsymbol{\xi}_{k,i})\right)\right\|_F^2\right]} \\
&= (1-\beta) \sqrt{\sum_{k=1}^t \beta^{2(t-k)} \frac{1}{B^2} \sum_{i=1}^B \mathbb{E}\left[\|\nabla f(\mathbf{W}_k^Q; \boldsymbol{\xi}_{k,i}) - \nabla F(\mathbf{W}_k^Q)\|_F^2\right]} \\
&\leq (1-\beta) \sqrt{\sum_{k=1}^t \beta^{2(t-k)} \frac{1}{B^2} \sum_{i=1}^B \sigma^2} \\
&= (1-\beta) \sqrt{\frac{1-\beta^{2t}}{1-\beta^2} \cdot \frac{\sigma^2}{B}}
\end{aligned}$$

$$2700 \leq \sqrt{\frac{1-\beta}{1+\beta}} \cdot \frac{\sigma}{\sqrt{B}}. \quad (B.15)$$

$$2701$$

$$2702$$

$$2703$$

2704 Bound on \mathbf{J} .

$$2705 \quad J = (1-\beta) \mathbb{E} \left[\left\| \sum_{k=1}^t \beta^{t-k} \cdot \left(\frac{1}{B} \sum_{i=1}^B \nabla f(\mathbf{W}_k^Q; \boldsymbol{\xi}_{k,i}) - \nabla^Q f(\mathbf{W}_k^Q; \boldsymbol{\xi}_{k,i}) \right) \right\|_F \right]$$

$$2706 \leq (1-\beta) \sum_{k=1}^t \beta^{t-k} \frac{1}{B} \sum_{i=1}^B q_G \mathbb{E} [\|\nabla f(\mathbf{W}_k^Q; \boldsymbol{\xi}_{k,i})\|_F]$$

$$2707 \leq (1-\beta) \sum_{k=1}^t \beta^{t-k} \frac{1}{B} \sum_{i=1}^B q_G (\sigma + \mathbb{E} [\|\nabla F(\mathbf{W}_k^Q)\|_F])$$

$$2708 \leq (1-\beta) \sum_{k=1}^t \beta^{t-k} \frac{1}{B} \sum_{i=1}^B q_G (\sigma + L \mathbb{E} [\|\mathbf{W}_k^Q - \mathbf{W}_k\|_F] + \mathbb{E} [\|\nabla F(\mathbf{W}_k)\|_F])$$

$$2709 \leq (1-\beta) \sum_{k=1}^t \beta^{t-k} \frac{1}{B} \sum_{i=1}^B q_G (\sigma + L q_W \mathbb{E} [\|\mathbf{W}_k\|_F] + \mathbb{E} [\|\nabla F(\mathbf{W}_k)\|_F])$$

$$2710 \leq (1-\beta) \sum_{k=1}^t \beta^{t-k} \frac{1}{B} \sum_{i=1}^B q_G (\sigma + L q_W (D + t \eta \sqrt{r}) + G + t \eta \sqrt{r} L)$$

$$2711 \leq (1-\beta) \sum_{k=1}^t \beta^{t-k} q_G (\sigma + G + q_W D L + (1+q_W) t \eta \sqrt{r} L). \quad (B.16)$$

$$2712$$

$$2713$$

$$2714$$

$$2715$$

$$2716$$

$$2717$$

$$2718$$

$$2719$$

$$2720$$

$$2721$$

$$2722$$

$$2723$$

$$2724$$

$$2725$$

$$2726$$

$$2727$$

$$2728$$

$$2729$$

$$2730$$

$$2731$$

$$2732$$

$$2733$$

$$2734$$

$$2735$$

$$2736$$

$$2737$$

$$2738$$

$$2739$$

$$2740$$

$$2741$$

$$2742$$

$$2743$$

$$2744$$

$$2745$$

$$2746$$

$$2747$$

$$2748$$

$$2749$$

$$2750$$

$$2751$$

$$2752$$

$$2753$$

The first inequality is due to Definition B.6 and the triangle inequality. The second inequality is due to Assumption 4.2. The third inequality is due to Assumption 4.3 and the triangle inequality. The fourth inequality is due to Definition B.6. The fifth inequality is due to Lemma B.1.

2728 Bound on $\mathbb{E}[\|\mathbf{Y}_t - \mathbf{Z}_t\|_F]$. Substituting (B.11), (B.12), (B.13), (B.14), (B.15) and (B.16) into (B.10), we have

$$2731 \quad \mathbb{E}[\|\mathbf{Y}_t - \mathbf{Z}_t\|_F] \leq \beta^t \cdot \frac{2\sigma}{\sqrt{B}} + \sqrt{\frac{1-\beta}{1+\beta}} \cdot \frac{2\sigma}{\sqrt{B}} + 2q_G(\sigma + G) + (1-\beta^t)2q_G t \eta \sqrt{r} L +$$

$$2732 \quad q_W(1+q_G) D L + (1-\beta^t)q_W(1+q_G) t \eta \sqrt{r} L.$$

$$2733$$

$$2734$$

$$2735$$

$$2736$$

$$2737$$

$$2738$$

$$2739$$

$$2740$$

$$2741$$

$$2742$$

$$2743$$

$$2744$$

$$2745$$

$$2746$$

$$2747$$

$$2748$$

$$2749$$

$$2750$$

$$2751$$

$$2752$$

$$2753$$

2740 Bound on $\mathbb{E}[\|\mathbf{Z}_t\|_F]$. By the definition of \mathbf{Z}_t in (B.5), we have

$$2742 \quad \mathbb{E}[\|\mathbf{Z}_t\|_F]$$

$$2743$$

$$2744 \leq \mathbb{E}[\beta^t \|\mathbf{Z}_0\|_F] + \mathbb{E}[(1-\beta) \left\| \sum_{k=1}^t \beta^{t-k} \cdot \frac{1}{B} \sum_{i=1}^B \nabla^Q f(\mathbf{W}_k^Q; \boldsymbol{\xi}_{k,i}) \right\|_F]$$

$$2745$$

$$2746$$

$$2747 \leq \beta^t \mathbb{E}[\|\mathbf{Z}_0\|_F] + \mathbb{E}[(1-\beta) \sum_{k=1}^t \beta^{t-k} \cdot \frac{1}{B} \sum_{i=1}^B \|\nabla^Q f(\mathbf{W}_k^Q; \boldsymbol{\xi}_{k,i}) - \nabla f(\mathbf{W}_k^Q; \boldsymbol{\xi}_{k,i})\|_F] +$$

$$2748$$

$$2749$$

$$2750 \quad \mathbb{E}[(1-\beta) \sum_{k=1}^t \beta^{t-k} \cdot \left(\frac{1}{B} \sum_{i=1}^B \nabla f(\mathbf{W}_k^Q; \boldsymbol{\xi}_{k,i}) - \nabla F(\mathbf{W}_k^Q) \right) \|_F] +$$

$$2751$$

$$2752$$

$$2753 \quad \mathbb{E}[(1-\beta) \sum_{k=1}^t \beta^{t-k} \cdot (\|\nabla F(\mathbf{W}_k^Q) - \nabla F(\mathbf{W}_k)\|_F + \|\nabla F(\mathbf{W}_k)\|_F)]$$

$$\begin{aligned}
&\leq \beta^t \mathbb{E}[\|\mathbf{Z}_0\|_F] + (1 - \beta) \sum_{k=1}^t \beta^{t-k} \frac{1}{B} \sum_{i=1}^B q_G \mathbb{E}[\|\nabla f(\mathbf{W}_k^Q; \boldsymbol{\xi}_{k,i})\|_F] + \\
&\quad \sqrt{\frac{1 - \beta}{1 + \beta}} \cdot \frac{\sigma}{\sqrt{B}} + (1 - \beta) q_W L \sum_{k=1}^t \beta^{t-k} \mathbb{E}[\|\mathbf{W}_k\|_F] + (1 - \beta) \sum_{k=1}^t \beta^{t-k} \mathbb{E}[\|\nabla F(\mathbf{W}_k)\|_F] \\
&\leq \beta^t \mathbb{E}[\|\mathbf{Z}_0\|_F] + (1 - \beta) \sum_{k=1}^t \beta^{t-k} \frac{1}{B} \sum_{i=1}^B q_G (\sigma + q_W L \mathbb{E}[\|\mathbf{W}_k\|_F] + \mathbb{E}[\|\nabla F(\mathbf{W}_k)\|_F]) + \\
&\quad \sqrt{\frac{1 - \beta}{1 + \beta}} \cdot \frac{\sigma}{\sqrt{B}} + (1 - \beta) q_W L \sum_{k=1}^t \beta^{t-k} \mathbb{E}[\|\mathbf{W}_k\|_F] + (1 - \beta) \sum_{k=1}^t \beta^{t-k} \mathbb{E}[\|\nabla F(\mathbf{W}_k)\|_F] \\
&\leq \beta^t \mathbb{E}[\|\mathbf{Z}_0\|_F] + (1 - \beta^t) q_G (\sigma + q_W L (D + t\eta\sqrt{r}) + G + t\eta\sqrt{r}L) + \\
&\quad \sqrt{\frac{1 - \beta}{1 + \beta}} \cdot \frac{\sigma}{\sqrt{B}} + (1 - \beta^t) q_W L (D + t\eta\sqrt{r}) + (1 - \beta^t) (G + t\eta\sqrt{r}L) \\
&\leq \beta^t (q_G (\sigma + q_W DL + G) + \frac{\sigma}{\sqrt{B}} + q_W DL + G) + \\
&\quad (1 - \beta^t) q_G (\sigma + q_W L (D + t\eta\sqrt{r}) + G + t\eta\sqrt{r}L) + \\
&\quad \sqrt{\frac{1 - \beta}{1 + \beta}} \cdot \frac{\sigma}{\sqrt{B}} + (1 - \beta^t) q_W L (D + t\eta\sqrt{r}) + (1 - \beta^t) (G + t\eta\sqrt{r}L) \\
&\leq \beta^t \frac{\sigma}{\sqrt{B}} + \sqrt{\frac{1 - \beta}{1 + \beta}} \cdot \frac{\sigma}{\sqrt{B}} + G + q_G (\sigma + G) + q_W (1 + q_G) DL + \\
&\quad (1 - \beta^t) (1 + q_W) (1 + q_G) t\eta\sqrt{r}L \\
&\leq \frac{\sigma}{\sqrt{B}} + \sqrt{\frac{1 - \beta}{1 + \beta}} \cdot \frac{\sigma}{\sqrt{B}} + G + q_G (\sigma + G) + q_W (1 + q_G) DL + (1 + q_W) (1 + q_G) t\eta\sqrt{r}L.
\end{aligned}$$

The first and second inequalities are due to the triangle inequality. The third inequality we used Definition B.6 for the second term, Jensen's inequality, Assumptions 4.1, 4.2 for the third term, Assumption 4.3 and Definition B.6 for the fourth term. The fourth inequality we used triangle inequality, Assumptions 4.2, 4.3, Definition B.6. The fifth inequality is due to Lemma B.1.

□

B.9 PROOF OF LEMMA B.7

Lemma B.7. Suppose Assumptions 4.1, 4.2, 4.3 and 3.1 hold. For any $t \geq 0$, if $\beta(1 + q_M) < 1$, we have

$$\begin{aligned}
\mathbb{E}[\|\mathbf{Z}_t - \mathbf{M}_t\|_F] &\leq \frac{q_M \beta}{1 - \beta(1 + q_M)} \left(\frac{\sigma}{\sqrt{B}} + \sqrt{\frac{1 - \beta}{1 + \beta}} \cdot \frac{\sigma}{\sqrt{B}} + G + q_G (\sigma + G) + \right. \\
&\quad \left. q_W (1 + q_G) DL + (1 + q_W) (1 + q_G) t\eta\sqrt{r}L \right).
\end{aligned}$$

Proof of Lemma B.7. By the definitions of \mathbf{Z}_t and \mathbf{M}_t in (B.5) and (B.1), we have

$$\begin{aligned}
&\mathbb{E}[\|\mathbf{Z}_t - \mathbf{M}_t\|_F] \\
&\leq \mathbb{E}[\beta \|\mathbf{Z}_{t-1} - \mathbf{M}_{t-1}^Q\|_F] \\
&\leq \mathbb{E}[\beta \|\mathbf{Z}_{t-1} - \mathbf{M}_{t-1}\|_F + \beta \|\mathbf{M}_{t-1} - \mathbf{M}_{t-1}^Q\|_F] \\
&\leq \mathbb{E}[\beta \|\mathbf{Z}_{t-1} - \mathbf{M}_{t-1}\|_F + q_M \beta \|\mathbf{M}_{t-1}\|_F] \\
&\leq \mathbb{E}[\beta (1 + q_M) \|\mathbf{Z}_{t-1} - \mathbf{M}_{t-1}\|_F + q_M \beta \|\mathbf{Z}_{t-1}\|_F]
\end{aligned}$$

$$\begin{aligned}
& \leq q_M \beta \sum_{k=0}^{t-1} \beta^k (1+q_M)^k \|\mathbf{Z}_{t-k-1}\|_F \\
& \leq \frac{q_M \beta}{1 - \beta(1+q_M)} \left(\frac{\sigma}{\sqrt{B}} + \sqrt{\frac{1-\beta}{(1+\beta)}} \cdot \frac{\sigma}{\sqrt{B}} + G + q_G(\sigma+G) + \right. \\
& \quad \left. q_W(1+q_G)DL + (1+q_W)(1+q_G)t\eta\sqrt{r}L \right). \tag{B.17}
\end{aligned}$$

The second inequality is due to the triangle inequality. The third inequality is due to Definition B.6. The fourth inequality is due to the triangle inequality. The fifth inequality is due to $\mathbf{Z}_0 = \mathbf{M}_0$. The last inequality we used Lemma B.6 \square

C ADDITIONAL EXPERIMENTS AND DETAILS

C.1 IMITATING QUANTIZATION AND DEQUANTIZATION

We emulate floating-point quantization and dequantization by reducing the mantissa length from its original precision (52 bits for `float64` and 23 bits for `float32`) to M bits, while keeping the exponent and sign bits unchanged. This design choice is motivated by the fact that practical scaling techniques can effectively prevent overflow and underflow (Peng et al., 2023). After truncating the mantissa, we apply stochastic rounding to the nearest two representable values, and then dequantize the result back to standard `float32` or `float64`.

C.2 SYNTHETIC EXPERIMENTS

We conduct synthetic experiments on the Rosenbrock function, defined as

$$F(\mathbf{W}) = \sum_{j=1}^{n-1} \left(100\|\mathbf{W}_{j+1} - \mathbf{W}_j^2\|_F^2 + \|\mathbf{1}_m - \mathbf{W}_j\|_F^2 \right),$$

where $\mathbf{W} = [\mathbf{W}_1, \mathbf{W}_2, \dots, \mathbf{W}_d] \in \mathbb{R}^{m \times n}$ is the weight matrix. The global minimum is at $\mathbf{W}^* = [\mathbf{1}_m, \mathbf{1}_m, \dots, \mathbf{1}_m]$ with $F(\mathbf{W}^*) = 0$. We set $m = 50$, $d = 100$, and initialize $\mathbf{W}_0 \sim \mathcal{N}(\mathbf{1}_{m \times n}, 0.1^2 \mathbf{I})$. For Muon, we apply the default hyperparameters in the Newton-Schulz iteration to compute the zeroth power / orthogonalization of G (Jordan et al., 2024), using double precision.

Figure 3 shows the gradient norms of Adam with different quantization errors on the Rosenbrock function. Figure 4 shows the gradient norms of Muon with different quantization errors on the Rosenbrock function.

Figure 5 shows the function values of Adam with different quantization errors on the Rosenbrock function. Figure 6 shows the function values of Muon with different quantization errors on the Rosenbrock function. The relative quantization error is defined as $\frac{\|\mathbf{X} - Q(\mathbf{X})\|_F}{\|\mathbf{X}\|_F}$, measuring the average quantization error of \mathbf{X} , where $Q(\cdot)$ is the quantization operator.

Figure 7 shows the effect of quantizing the second moment in Adam to different mantissa lengths M , with all other components kept in FP32. As $\beta_2 \rightarrow 1$, the optimizer exhibits larger converged gradient norms and becomes more sensitive to quantization errors induced by reduced M . This phenomenon aligns with our theoretical analysis in Theorem 4.5, which highlights the amplification of quantization errors by the inverse square root of historical gradient variances in Adam when β_2 is close to 1.

C.3 CIFAR-10 EXPERIMENTS

We conduct real-data experiments on the CIFAR-10 dataset (Krizhevsky et al., 2009) using a 4-layer fully connected network (FCN). The architecture is as follows: an input layer with 3072 neurons (corresponding to $32 \times 32 \times 3$ images), followed by three hidden layers with 512, 256, and 64 neurons, respectively, and an output layer with 10 neurons for classification. ReLU activations are

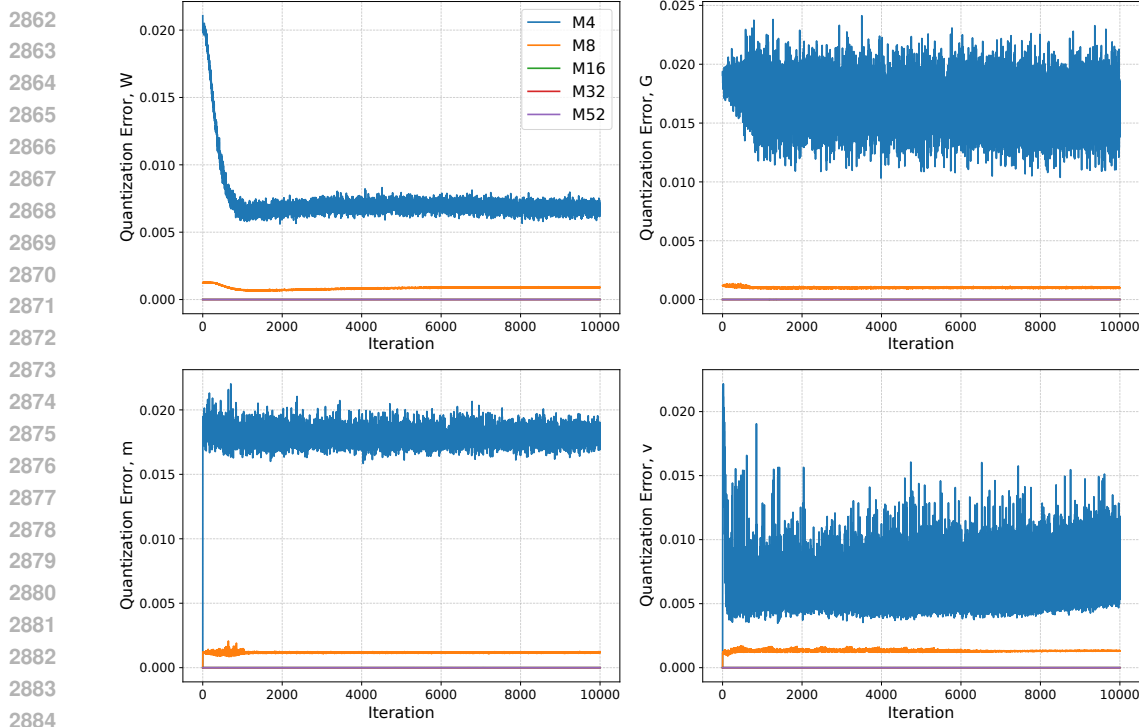


Figure 5: Rosenbrock: Adam relative quantization error of different mantissa bits (M). Weights error (top left), Gradient error (top right), First moment error (bottom left), Second moment error (bottom right). These results show that the more mantissa bits, the smaller the relative quantization error. Combining with Figure 3, we can see that the more mantissa bits, the smaller quantization error, the better convergence performance (Theorem 4.5).

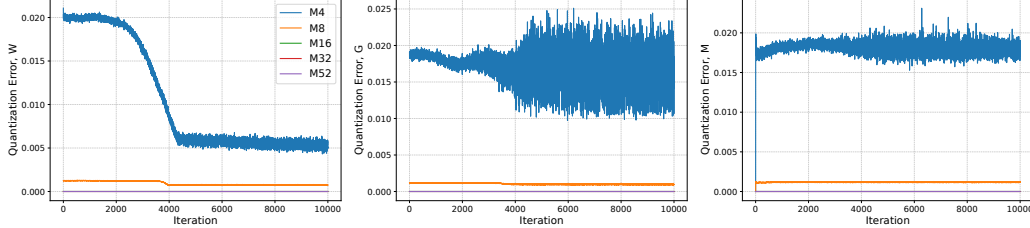


Figure 6: Rosenbrock: Muon relative quantization error of different mantissa bits (M). Weights error (left), Gradient error (middle), Momentum error (right). These results show that the more mantissa bits, the smaller the relative quantization error. Combining with Figure 4, we can see that the more mantissa bits, the smaller quantization error, the better convergence performance (Theorem 4.6).

used for all hidden layers, and the network is trained with the cross-entropy loss for 100 epochs. We evaluate both Adam and Muon under varying quantization precisions.

For Adam, we use mantissa bit-lengths $M \in \{1, 2, 3, 7, 10, 23\}$, batch size $B = 256$, learning rate $\eta = 1.5 \times 10^{-4}$, $\beta_1 = 0.95$, $\beta_2 = 0.999$, $\epsilon = 10^{-8}$, and weight decay 0.1. For Muon, vector parameters are updated using Adam, while matrix parameters are updated with Muon's orthogonalization step. We choose mantissa bit-lengths $M \in \{2, 3, 7, 10, 23\}$, batch size $B = 512$, learning rate $\eta = 0.001$, $\beta = 0.99$, weight decay 0.1, and 5 Newton–Schulz iterations, following the iteration hyperparameters in Jordan et al. (2024). The auxiliary Adam optimizer in Muon uses learning rate $\eta = 2 \times 10^{-4}$, $\beta_1 = 0.9$, $\beta_2 = 0.999$, $\epsilon = 10^{-8}$, and weight decay 0.05.

Figure 8 shows the gradient norms of Adam with different quantization errors on CIFAR-10. Figure 9 shows the gradient norms of Muon with different quantization errors on CIFAR-10. Figure 10

2916 shows the quantization errors of Adam with different precision on CIFAR-10. Figure 11 shows
 2917 the quantization errors of Muon with different precision on CIFAR-10. The relative quantization
 2918 error is defined as $\frac{\|\mathbf{X} - Q(\mathbf{X})\|_F}{\|\mathbf{X}\|_F}$, measuring the average quantization error of \mathbf{X} , where $Q(\cdot)$ is the
 2919 quantization operator.
 2920

2921 C.4 NANO GPT EXPERIMENTS 2922

2923 We evaluate the impact of quantization on training the nanoGPT model on the OpenWebText
 2924 dataset (Gokaslan et al., 2019). The model has $\sim 26.4\text{M}$ parameters, with weight tying between
 2925 the embedding and the output layer (1m_head). Its architecture includes 4 transformer layers, each
 2926 with 4 attention heads, embedding dimension 384, without dropout, and no bias terms. The dataset
 2927 contains $\sim 655.4\text{M}$ tokens, and we use a block size (context length) of 512. Training is performed
 2928 with a batch size of 32 and gradient accumulation of 4, resulting in an effective batch size of 128.
 2929 Models are trained for up to 10,000 iterations.
 2930

2931 **Optimizer and Training Settings.** We experiment with both AdamW and Muon optimizers, as
 2932 summarized below:
 2933

- 2934 • **AdamW:** learning rate 3×10^{-4} , weight decay 0.1, $\beta_1 = 0.9$, $\beta_2 = 0.95$, $\epsilon = 10^{-8}$, gradient
 2935 clipping norm 1.0. Learning rate decay is disabled.
- 2936 • **Muon:** 2D parameters in transformer blocks ($\sim 7\text{M}$) are updated with Muon’s orthogonalization-
 2937 based step (Newton-Schulz iteration), while all remaining parameters ($\sim 19\text{M}$, including embed-
 2938 dings, layer norms, and output layer) are updated with AdamW. Muon hyperparameters are: learning
 2939 rate 3×10^{-2} , $\beta = 0.95$ (with Nesterov momentum), Newton-Schulz steps 5, $\epsilon = 1 \times 10^{-7}$
 2940 for NS iteration. Auxiliary AdamW: learning rate 6×10^{-3} , $\beta_1 = 0.9$, $\beta_2 = 0.95$, $\epsilon = 10^{-8}$,
 2941 weight decay 0.01, gradient clipping norm 1.0.

2942 **Quantization.** Following the procedure in Section C, we apply mantissa truncation to weights,
 2943 gradients, and optimizer states. We vary the mantissa length $M \in \{1, 2, 10, 23\}$, keeping exponent
 2944 and sign bits in full precision.
 2945

2946 **Results.** Figures 12 and 13 show training and validation loss dynamics for nanoGPT under differ-
 2947 ent quantization precisions. We observe that:
 2948

- 2949 • Lower mantissa lengths (e.g., $M = 2$) induce slightly slower convergence and higher final
 2950 training loss, consistent with the observed gradient norm amplification in Theorem 4.5 and
 2951 Theorem 4.6.
- 2952 • Muon exhibits greater robustness to low-precision quantization compared to AdamW,
 2953 achieving lower training and validation loss at $M = 2$. This aligns with our theoretical
 2954 findings that Muon’s quantization error amplification is less sensitive than Adam’s.
- 2955 • As the mantissa length increases, both AdamW and Muon converge to almost identical
 2956 training and validation loss, indicating that higher precision mitigates quantization-induced
 2957 degradation.

2958 Overall, these results on nanoGPT extend the findings from synthetic (Rosenbrock) and CIFAR-
 2959 10 experiments to a real large-scale language modeling setting, highlighting the interplay between
 2960 quantization precision, optimizer dynamics, and convergence stability.
 2961

2962
 2963
 2964
 2965
 2966
 2967
 2968
 2969

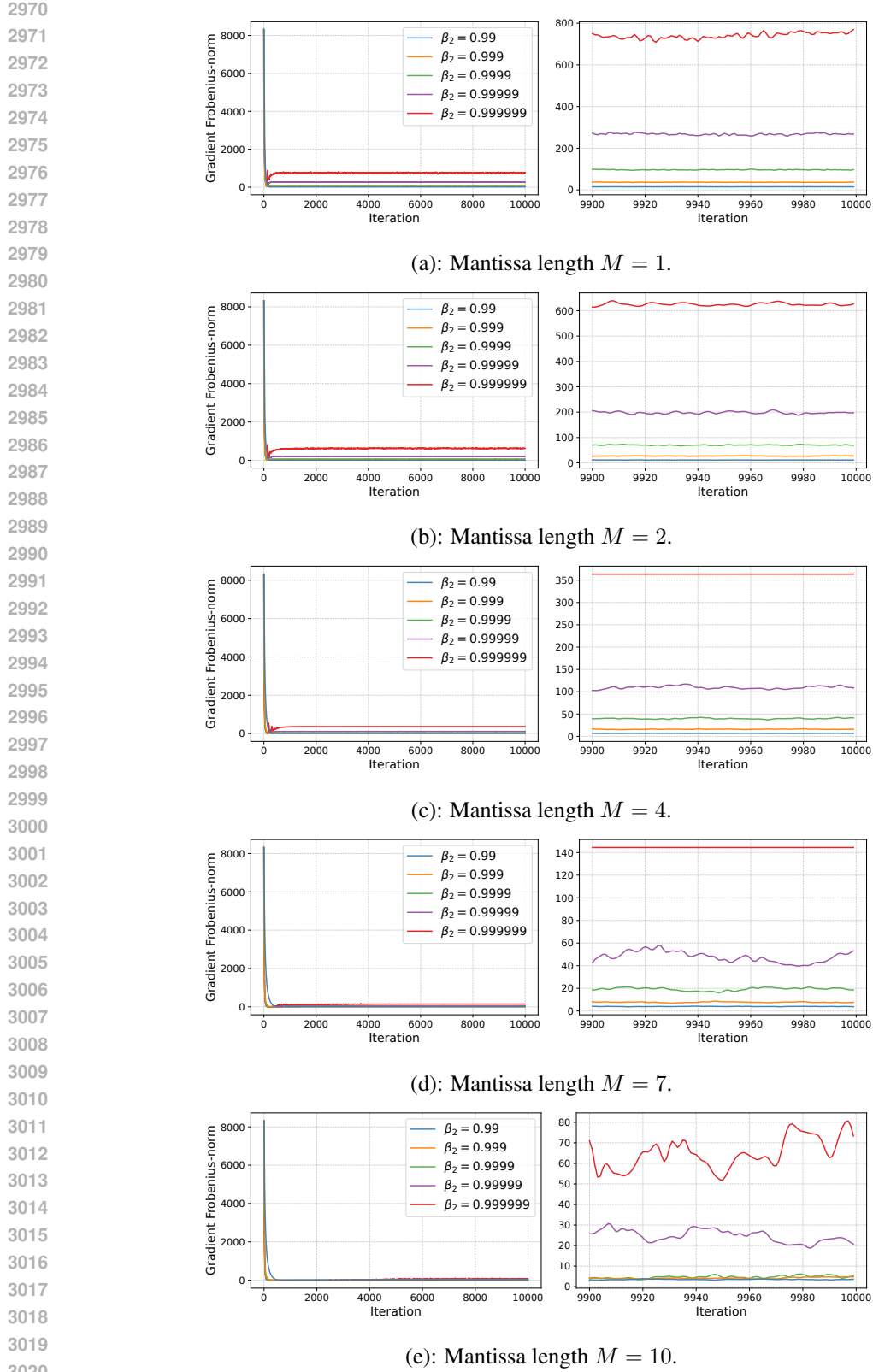


Figure 7: Rosenbrock: Effect of quantizing second moment in Adam to different mantissa lengths M , with all other components kept in FP32. As $\beta_2 \rightarrow 1$, the optimizer exhibits larger converged gradient norms and becomes more sensitive to quantization errors induced by reduced M .

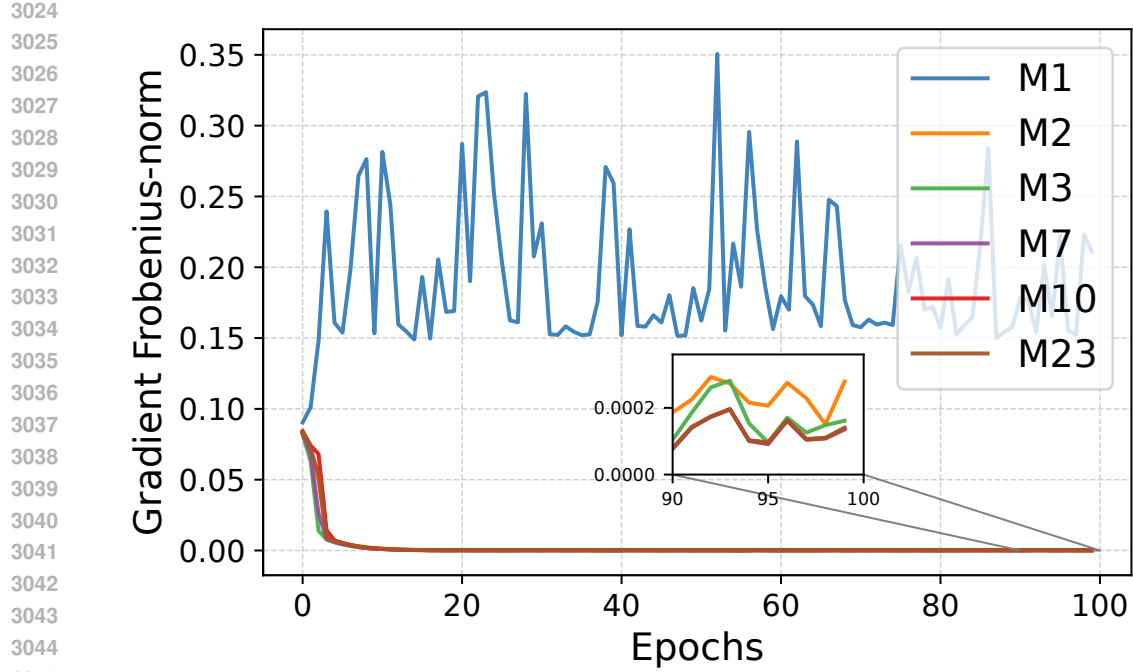


Figure 8: CIFAR-10: Adam gradient norms under different mantissa precisions M . Larger mantissa bit-lengths lead to smaller converged gradient norms. Together with Figure 10, this demonstrates that higher precision reduces quantization error and improves convergence, consistent with Theorem 4.5.

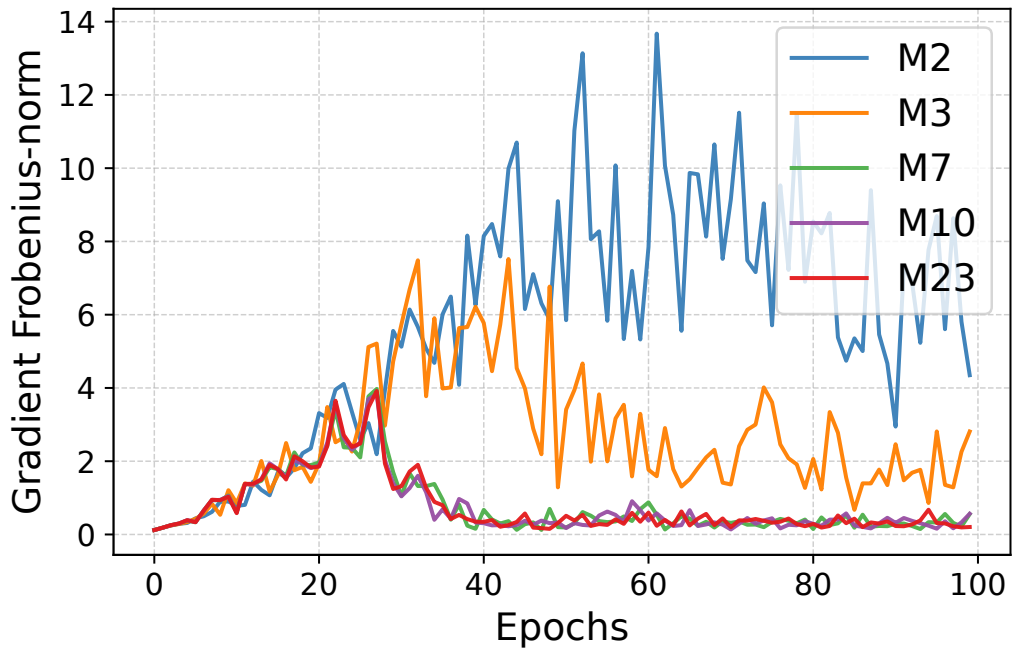


Figure 9: CIFAR-10: Muon gradient norms under different mantissa precisions M . Larger mantissa bit-lengths lead to smaller converged gradient norms. Together with Figure 11, this demonstrates that higher precision reduces quantization error and improves convergence, consistent with Theorem 4.6.

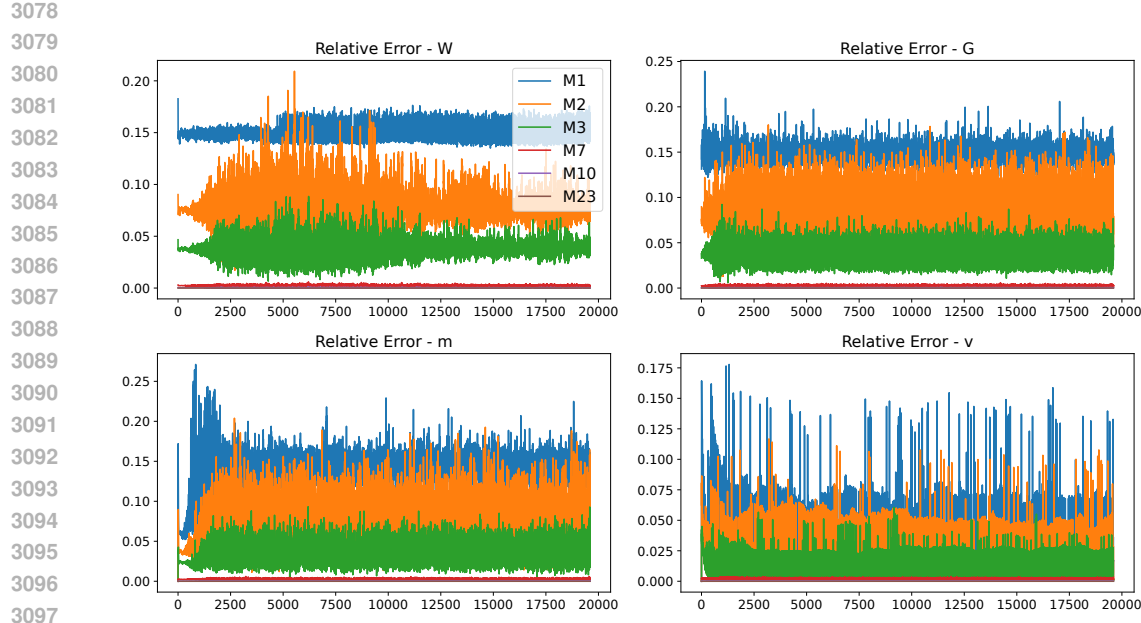


Figure 10: CIFAR-10: Adam relative quantization error of different mantissa bits (M). Weights error (top left), Gradient error (top right), First moment error (bottom left), Second moment error (bottom right). These results show that the more mantissa bits, the smaller the relative quantization error. Combining with Figure 8, we can see that the more mantissa bits, the smaller quantization error, the better convergence performance (Theorem 4.5).

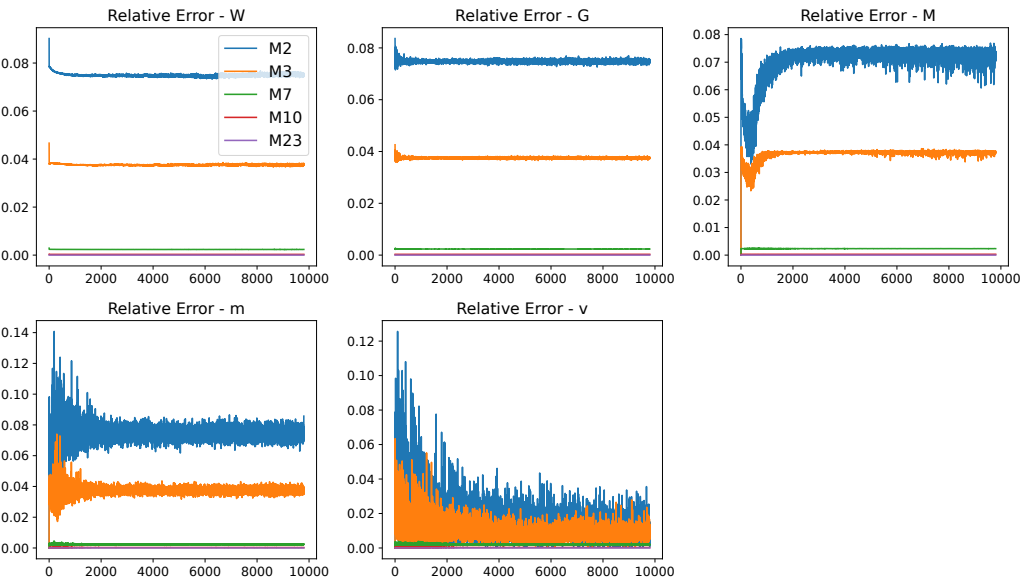


Figure 11: CIFAR-10: Muon with auxiliary Adam relative quantization error of different mantissa bits (M). Weights error (top left), Gradient error (top middle), Momentum error (top right), Auxiliary Adam first moment error (bottom left), Auxiliary Adam second moment error (bottom middle). These results show that the more mantissa bits, the smaller the relative quantization error. Combining with Figure 9, we can see that the more mantissa bits, the smaller quantization error, the better convergence performance (Theorem 4.6).

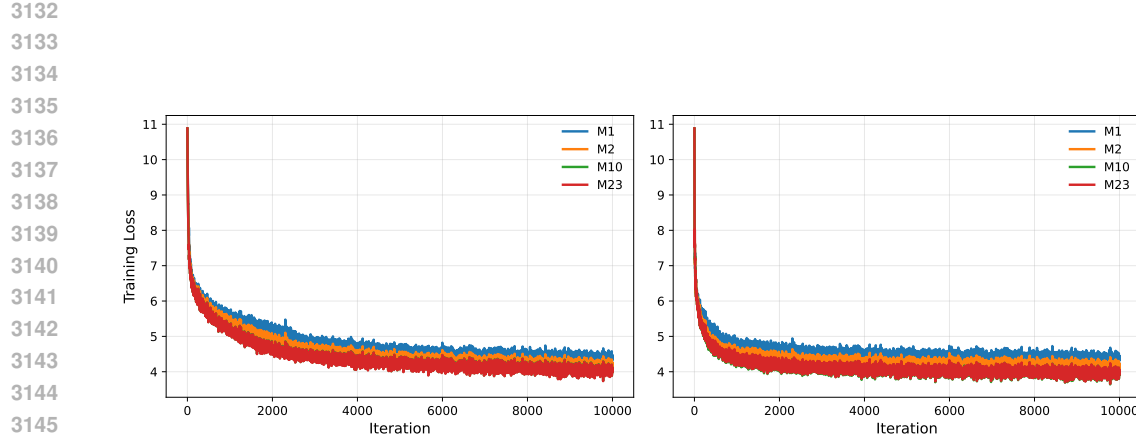


Figure 12: Training loss of nanoGPT on OpenWebText with varying mantissa lengths M . Lower M slightly increases the training loss due to amplified quantization error.

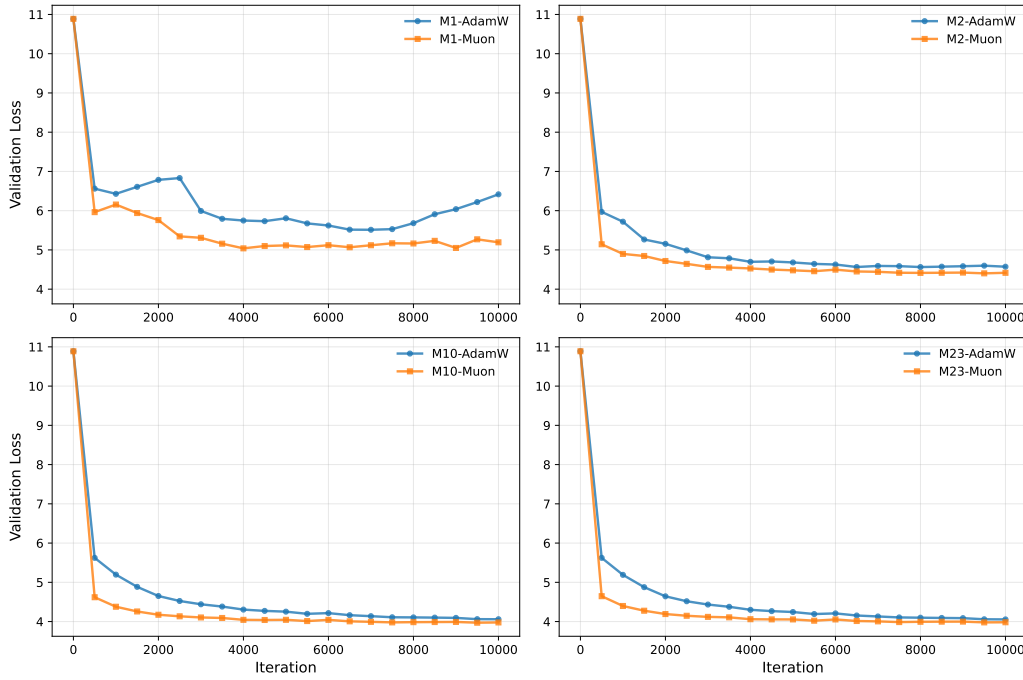


Figure 13: Validation loss of nanoGPT on OpenWebText under varying mantissa precisions M . Higher precision reduces quantization error and improves validation performance, particularly at low M . Notably, Muon exhibits greater robustness to low-precision quantization compared to AdamW, suggesting its potential advantage for low-precision training of large language models.